

**Preparation and characterization of chitosan nanoparticles
for gene delivery**

Vasco José Dias Duarte Silva

Thesis to obtain the Master of Science Degree in

Biotechnology

Examination Committee

Chairperson: Professor Luís Joaquim Pina da Fonseca

Supervisor: Professora Marília Clemente Velez Mateus

Member of the committee: Professor Gabriel António Amaro Monteiro

November 2013

Acknowledgments

This work has largely benefited from the effort and contribution of several people, to whom I wish to express my sincere gratitude.

First of all i would like to thank to my supervisor, Professor Marília Mateus who accepted me for this research thesis and helped me with her constant presence and availability to advice and share her knowledge with me, but also for guiding me through this project with endless patience, optimism and strength.

I would like to thank to all NABL group, professors and colleagues for all opinions, questions, answers and suggestions, during all meetings, which helped me to always try new approaches or improve the known ones.

To all my lab partners, who helped me day after day developing this project and also thank them for the good vibes created, which in my opinion is truly important in a work environment. Special gratitude to Salomé Magalhães, Luís Raiado, João Trabuco, Sara Pereira, Marina Monteiro, and Ricardo Pereira for their constant support and new ideas.

I would like to acknowledge all my friends that during my life, in one way or another, helped and support me with their truly friendship. A special hug to Hugo, Delgado, Duarte, Nunos, Rúben and Teresa.

My final words go to my parents Graça and Rui, my sister Cláudia, my grandmother Cremilde and to Natacha, who always supported my decisions, for believing in me and allowing me to continue my studies, for giving me hope and strength through difficult times, emotional support and most of all for their patience.

Abstract

The possibility of using gene-based therapy for treatment of both genetic and acquired diseases such as infections, degenerative disorders or cancer, has grown exponentially, mostly due to the development of several methods for delivering genes to mammalian cells (viral and non-viral vectors).

In this study, chitosan polymer was used as non-viral vector for delivery of plasmid pVAX1GFP to mammalian Chinese hamster ovary cell line, being the final goal the expression of green fluorescent protein in the nucleus of these cells.

Chitosan and plasmid DNA nanoparticles were prepared by self-assembly at amine to phosphate ratios of 5, 10, 20, 50 and 70, although complexation was not totally achieved for lower ones (N/P=5 and 10). Different molecular weight (60–220kDa) and glycol chitosans were tested, in order to determine which one provides the highest transfection efficiency.

Two lipids, a cholesterol derivate and a type of lecithin, were used to modify chitosan molecule in order to determine if their presence enhances the delivery process.

Characterization of nanoparticles size (102 to 2094nm), zeta-potential (-36 to 40mV) and polydispersion index (0.21 to 0.89) was performed in order to select the most suitable formulations for cell delivery. Also, sonication of chitosan particles and medium filtration were important processes to obtain stable and homogeneous nanoparticles, features mostly achieved in low molecular weight chitosan complexes (60-120kDa).

High transfection efficiencies were only obtained in positive control (pDNA + lipofectamine).

Keywords: gene therapy; non-viral vectors; chitosan; nanoparticles; oral delivery

Resumo

O interesse na possibilidade de utilizar a terapia génica e as vacinas de DNA para o tratamento de doenças genéticas e adquiridas, como infecções, anomalias degenerativas ou cancro, tem vindo a aumentar devido ao desenvolvimento de vários métodos para a distribuição de genes de interesse em células de mamífero.

Neste estudo, foi utilizado o polímero quitosano como vector não-viral para a distribuição do plasmídeo pVAX1GFP em células de ovário de ratinhos chineses, sendo o objectivo final a expressão da proteína verde fluorescente no núcleo destas células.

As nanopartículas de quitosano e DNA plasmídico foram preparadas por “auto-montagem” a razões amina para fosfato de 5, 10, 20, 50 e 70. A complexação não foi total para as razões mais baixas. Quitosanos de diferentes pesos moleculares (60-220kDa) e um glicol quitosano foram testados, de modo a determinar a formulação em que a eficiência de transfecção era superior.

Dois lípidos foram ainda usados para modificar a molécula de quitosano de modo a determinar se a sua presença afectaria a referida eficiência.

Caracterizou-se o diâmetro (102 até 2094nm), o potencial zeta (-36 até 40mV) e o índice de polidispersão (0.21 até 0.89) das nanopartículas, de modo a seleccionar as que mais se adequavam para a distribuição celular. A sonicação das partículas de quitosano é um processo importante para a obtenção de nanopartículas estáveis e homogéneas, características maioritariamente apresentadas pelos complexos com presença de quitosanos de baixo peso molecular (60-120kDa).

Eficiências de transfecção elevadas foram apenas obtidas nos controlos positivos dos ensaios (pDNA + lipofectamina).

Palavras-chave: terapia génica; vectores não-virais; quitosano; nanopartículas; administração oral

List of contents

Acknowledgments	ii
Abstract	iii
Resumo	iv
List of contents	v
List of figures	vii
List of tables	viii
Abbreviations.....	ix
1. Background and Objectives	1
2. Literature review	2
2.1 Gene therapy.....	2
2.2 Plasmid DNA vectors structure and design	3
2.3 Plasmid DNA pVAX1GFP	5
2.4 Methods for gene delivery	6
2.4.1 Electroporation	6
2.4.2 Calcium phosphate co-precipitation.....	7
2.4.3 Viral vectors	7
2.4.4 Non-viral vectors	8
2.5 Transfection efficiency	10
2.5.1 Manufacturing, formulation and stability barriers	10
2.5.2 Extracellular barriers	11
2.5.3 Intracellular barriers.....	12
2.6 Chitosan polymer	13
2.6.1 Chitosan molecular structure and properties.....	13
2.6.2 Molecular weight and degree of deacetylation.....	15
2.6.3 Chitosan chemical modifications	16
2.7 Formation of chitosan/pDNA nanoparticles	17
2.8 Nanoparticles characterization	21
2.9 Efficiency of cell transfection and fluorescence-activated cell sorting (FACS)	24
3. Materials and Methods.....	28
3.1. Bacterial culture and alkaline lysis	28
3.1.1. Plasmid and cell bank	28
3.1.2. Cell culture conditions	28

3.1.3.	Cell rupture – alkaline lysis.....	28
3.2.	Plasmid DNA primary purification	29
3.3.	Plasmid DNA final purification	29
3.3.1.	Hydrophobic interaction phenyl membrane chromatography	29
3.3.2.	Elution profile.....	30
3.3.3.	Concentration and diafiltration of pDNA.....	31
3.4.	Preparation of chitosan and pDNA nanoparticles.....	31
3.5.	Preparation of chitosan modified cholesterol and pDNA nanoparticles	32
3.6.	Preparation of chitosan modified lecithin and pDNA nanoparticles	33
3.7.	Size and zeta potential characterization	34
3.8.	Analytical methods	34
3.8.1.	Agarose gel electrophoresis.....	34
3.9.	Chinese hamster ovary cell culture.....	35
3.10.	<i>In vitro</i> transfection of CHO cells.....	35
3.11.	Flow cytometry analysis (FACS)	35
4.	Results and discussion	38
4.1	Preparation and characterization of chitosan particles in solution	38
4.2.	Preparation and characterization of chitosan/pDNA nanoparticles	43
4.3.	Preparation and characterization of lipids coated chitosan/pDNA nanoparticles	56
4.4.	Transfection of produced nanoparticles to animal cells.....	61
5.	Conclusion and future work.....	68
6.	References	70
7.	Appendices	74
	Appendix I - Growth of <i>E. coli</i> DH5 α	74
	Appendix II – NZYDNA Ladder III characteristics.....	75
	Appendix III – Characterization of the diameter (nm), zeta potential ZP (mV) and polydispersity index (Pdi) of chitosan particles in acetic acid solution (pH \approx 3.0).....	76
	Appendix IV - Characterization of the diameter (nm), zeta potential ZP (mV) and polydispersity index (Pdi) of chitosan/pDNA nanoparticles (pH \approx 7.3).....	79

List of figures

Figure 1 – DNA vaccination mechanism activates both cell-mediated and humoral antibody response	2
Figure 2 - Genetic elements of a plasmid DNA vaccine.....	4
Figure 3 – Plasmid DNA topological structures	4
Figure 4 – Plasmid DNA pVAX1GFP characteristic features.	5
Figure 5 – Transfection of DNA vaccine by electroporation procedure.	6
Figure 6 – Vectors used in (A) and phases of (B) gene therapy clinical trials	7
Figure 7 – Examples of Lipoplex (A) and Polyplex (B) morphologies.	9
Figure 8 - Schematic diagram showing various mechanisms where stability may be lost in colloidal systems.....	10
Figure 9 - Lipoplex-mediated transfection, endocytosis and DNA intracellular destiny.....	12
Figure 10 – Molecular structure of chitosan	13
Figure 11 - Deacetylation and hydrolysis reactions on the cationic polymer chitosan	14
Figure 12 - Production and downstream processing of plasmid DNA containing the gene of interest.....	17
Figure 13 - Hydrophobic interaction between immobilized ligands and biomolecular surface controlled predominantly by the salt concentration	18
Figure 14 – Methods for chitosan nanoparticle preparation.	20
Figure 15 - Correlation differences between small and large particles.	22
Figure 16 – Zeta-potential of a nanoparticle in solution.....	23
Figure 17 – Estimate plot of number of particles per scattering volume for different concentrations when density of 1g/cm ³ is assumed.	24
Figure 18 – Fluorescent-activated cell sorting (FACS) principle. Here, the laser beam detects the correct fluorescence and sends the charged cell droplet into the correct positive sample vial.....	25
Figure 19 - Sartobind® Phenyl Nano module for membrane hydrophobic interaction chromatography.....	29
Figure 20 – Chromatogram obtained from a hydrophobic interaction chromatography process for pDNA purification, using a Sartobind® phenyl membrane.....	30
Figure 21 – 1% agarose gel electrophoresis from the supercoiled pDNA fractions collected after HIC procedure.....	31
Figure 22 – Scheme showing cholesterol modification of chitosan oligosaccharide lactate..	33
Figure 23 – Example of dot plot (A) and histogram (B) generated by CellQuest Pro Software © (Becton Dickinson, NJ, USA).....	36
Figure 24 – Effect of sonication in diameter (nm) and zeta potential (mV) of low (LMW), medium (MMW) and high (HMW) molecular weight and glycol chitosan.	38
Figure 25 – Evaluation of diameter (A;C) and zeta potential (B;D) stability along time of different chitosan suspension preparations.....	40
Figure 26 – Evaluation of diameter (nm) and zeta potential (mV) of low (LMW), medium (MMW) and high (HMW) molecular weight and glycol chitosan where buffer (50mM acetic acid pH 3.0) was not filtered..	41
Figure 27 - Evaluation of diameter (A) and zeta potential (B) stability along time of different chitosan suspension preparations..	42

Figure 28 – 1% agarose gel of first complexation assay polyplexes.....	43
Figure 29 – Evaluation of diameter and zeta potential stability during 3 days of LMW chitosan and pDNA complexes at different N/P ratios (5, 10, 20 and 50).....	45
Figure 30 - Evaluation of diameter and zeta potential stability during 3 days of glycol chitosan (sonicated and filtered) and pDNA complexes at different N/P ratios (5, 10, 20 and 50).....	46
Figure 31 – Representation of one diameter size measurement of each polyplex tested in the first complexation assay.....	47
Figure 32 – Volume distribution of polyplexes formed in the first complexation assay..	49
Figure 33 - 1% agarose gel of second complexation assay polyplexes..	50
Figure 34 - Evaluation of diameter and zeta potential stability during 3 days of LMW chitosan and pDNA complexes at different N/P ratios (10, 20, 50 and 70).....	51
Figure 35 - Evaluation of diameter and zeta potential stability during 3 days of glycol chitosan (sonicated and filtered) and pDNA complexes at different N/P ratios (10, 20, 50 and 70).....	52
Figure 36 - Evaluation of diameter and zeta potential stability during 3 days of HMW chitosan and pDNA complexes at different N/P ratios (10, 20, 50 and 70).....	53
Figure 37 – Evaluation of the quality of LMW1, LMW2, Glycol1 (A and B) and HMW1 and HMW2 (C and D) chitosan complexes with pDNA, at different N/P ratios..	55
Figure 38 - 1% agarose gel of lipopolyplexes.....	56
Figure 39 - Evaluation of the quality of CHI/CHOL/pDNA nanoparticles at N/P ratios of 10 (A and B) and 50 (C and D);	58
Figure 40 - Evaluation of the quality of CHI/ML/pDNA nanoparticles at N/P ratio of 10 (A and B) and 50 (C and D);	60
Figure 41 – Percentage of transfected CHO cells (A) and fluorescence mean intensity (B) of selected nanoparticles.....	62
Figure 42 – Effect of incubation time (24h, 48h) on transfection percentage (A) and fluorescence mean intensity (B) of selected nanoparticles.....	63
Figure 43 – Effect of transfection time (1h, 3h) on transfection percentage (A) and fluorescence mean intensity (B) of selected nanoparticles.....	64

List of tables

Table 1 – Diameter, mean Pdi and zeta potential values of chitosan oligo lactate (control), CHI/CHOL conjugate and N/P10 and 50 complexes of conjugate and pDNA.....	57
Table 2 - Diameter, mean Pdi and zeta potential values of LMW1 CHI, ML coated chitosan (conjugate control), and N/P10 (S3) and 50 (S4) complexes of conjugate and pDNA.....	59
Table 3 - Transfection percentage and fluorescence mean intensity of selected nanoparticles transfected for 6h and incubated for 24h.	65
Table 4 - Transfection percentage and fluorescence mean intensity of selected nanoparticles transfected for 3h and incubated for 48h.	65

Abbreviations

BGH - bovine growth hormone	GI – gastrointestinal
Bp - base pair	GTP - guanosine triphosphate
CAT - chloramphenicol acetyltransferase	HIC - hydrophobic interaction chromatography
CHI - chitosan	HIV - Human immunodeficiency virus
CHI/CHOL - chitosan/cholesteryl chloroformate conjugate	HMW - high molecular weight
CHO - chinese hamster ovary	ISS - immune stimulatory sequence
CHOL - cholesteryl chloroformate	KAN - kanamycin
CMV - cytomegalovirus	LacZ - beta-galactosidase
COL - chitosan oligo lactate	LB - Luria Bertani
Da - Dalton	LMW - low molecular weight
DD - degree of deacetylation	ML - modified lecithin
DLS - dynamic light scattering	mRNA - messenger RNA
DMEM - Dulbecco's modified eagle medium	MMW - medium molecular weight
DMSO - dimethylsulfoxide	MW - molecular weight
DNA - deoxyribonucleic acid	MWD - molecular weight distribution
DOPE - dioleoylphosphatidylethanolamine	NAG - N-acetyl-D-glucosamine
DP_n - degree of polymerization	NLS - nuclear localization signal
EB - elution buffer	NMR - nuclear magnetic resonance
ECM - extracellular matrix	oc - open circular isoform
<i>E. coli</i> - <i>Escherichia coli</i>	OD - optical density
eGFP - enhanced green fluorescent protein	PAMAM - polyamidoamine
EDTA - Ethylenediamine tetraacetic acid	PBS - phosphate buffered saline
EM - electrophoretic mobility	Pdi - polydispersion index
ESF - European Science Foundation	pDNA - plasmid DNA
FACS - fluorescence activated cell sorting	PEG - polyethyleneglycol
FBS - fetal bovine serum	PEI - polyethylenimine
FDA - food and drug administration (U.S.A)	PLL - poly-L-lysine
FSC - forward scatter	sc - super coiled isoform
GAG - glycosaminoglycan	SCID – X1 - X chromosome-linked severe combined immune deficiency
gDNA - genomic DNA	SD - standard deviation
	SEC - size-exclusion chromatography
	RNA - ribonucleic acid
	SSC - side scatter
	Tris - tris(hydroxymethyl)aminomethane
	UV - ultraviolet
	ZP - zeta potential

1. Background and Objectives

Over the past decades, the interest in the possibility of using gene-based therapy for treatment of both genetic and acquired diseases such as infections, degenerative disorders or even cancer, has grown exponentially, mostly due to the development of several methods for delivering genes to mammalian cells (viral and non-viral vectors).

The principle of these therapies is based on the transfer of genetic material into a cell, tissue or organ with the aim of curing a disease or improving the clinical status of the patient, by restoring, canceling, enhancing or introducing a biochemical function.

It is then necessary to identify appropriate DNA sequences and cell types, and develop suitable carriers to get enough of the DNA into these cells nucleus in order to express the gene of interest. The use of plasmids as vectors for gene delivery is an active area of investigation due to their great potential for a safe use in prophylactic and therapeutic vaccination. Once administered, DNA vaccines activate both humoral and cellular immune responses against targeted illnesses.

The success of the development of DNA vaccines is dependent on large scale pDNA production and purification processes that must be able to meet the product standards and specifications imposed by regulatory agencies like FDA.

The use of viral and non-viral vectors is essential to deliver pDNA into mammalian cells and to overcome the several physical barriers (internalization by cell membrane, endosome entrapment, lysosome degradation and transport to the nucleus) during the plasmid trafficking from the extracellular compartments into the nucleus, that challenge the efficient plasmid delivery. Further, these structures also protect DNA from the action of degradative enzymes such as cytoplasmatic nucleases, which confers an advantage over the use of naked pDNA.

Doubts about the use of viral vectors, including immunogenicity, small DNA cargo capacity, and difficulty of large-scale production, have led to continued interest in the development of non-viral carriers (liposomes and cationic polymers).

In this study, natural linear polymer chitosan is used as non-viral vector for the delivery of plasmid pVAX1GFP to Chinese Hamster Ovary (CHO) cell line. Chitosan and pDNA nanoparticles were prepared by self-assembly at different N/P ratio (moles of glucosamine groups of chitosan per moles of pDNAs phosphate groups). Different molecular weight chitosans were tested, as well as glycol chitosan in order to determine which one provides the highest transfection efficiency. Characterization of nanoparticles diameter, zeta-potential and polydispersion index was performed in Zetasizer Nano equipment.

Previous studies showed that an optimal chitosan drug vector was not yet been defined. A fine balance between DNA protection (better with HMW chitosan) and DNA intracellular release (better with LMW chitosan) need to be achieved. Also, N/P ratio values should not be higher than 20, thus avoiding competition at cell surface^[1]. The presence of lipids in chitosan surface should also facilitate the interaction with the cell membrane, thus enhancing the delivery process^[2].

2. Literature review

2.1 Gene therapy

Over the past decades, the interest in the possibility of using gene-based therapy and DNA vaccination for treatment of both genetic and acquired diseases such as infections, degenerative disorders and cancer, has grown exponentially, mostly due to the development of several methods for delivering genes to mammalian cells (viral and non-viral vectors).

The principle of these therapies is based on the transfer of genetic material into a cell, tissue or organ with the aim of curing a disease or improving the clinical status of the patient, by restoring, canceling, enhancing or introducing a biochemical function.

Genetic or DNA vaccination is the common name for vaccination methods that induce immunity by transfecting eukaryotic host cells with DNA that encodes a therapeutic protein, instead of injecting antigens in the form of proteins or peptides. The host cells, once transfected, start producing the protein encoded by the DNA leading to an immune response against this protein (Figure 1).

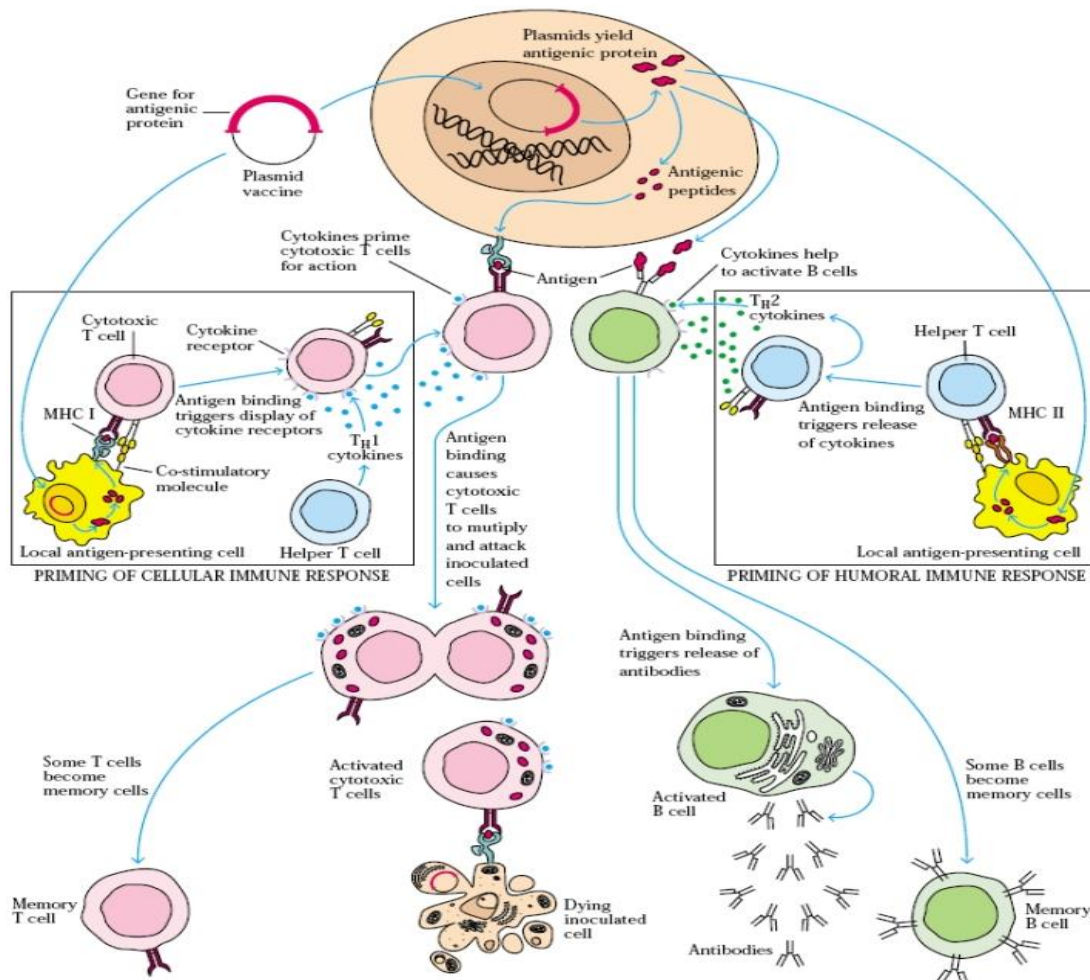


Figure 1 – DNA vaccination mechanism activates both cell-mediated and humoral antibody response (i)

(i) <http://wenliang.myweb.uga.edu/mystudy/immunology/ScienceOfImmunology/Vaccinationagainstinfectiousagents.html>

The use of plasmids as vectors is an active area of investigation due to their great potential for a safe use in prophylactic and therapeutic vaccination. Once administered, DNA vaccines activate both humoral and cellular immune responses against targeted illnesses.

In contrast to the complicated processes needed for vaccines such as attenuated viruses or subunit protein vaccines, pDNA is easy to design and construct. Moreover, it is cheap and relatively easy to manufacture and its stability at room temperature provides another advantage over attenuated viral vaccines, whose storage and global delivery are complicated by the need of keeping the vaccines at low temperatures. Also, the transfer of genes encoding therapeutic proteins gives rise to more natural sustained protein levels in vivo and decrease problems with immunotherapeutic agents being toxic at high doses and short-circulating half-lives^[3].

The success of the development of DNA vaccines is dependent on large scale pDNA production and purification processes that must be able to meet the product standards and specifications imposed by regulatory agencies like FDA.

Currently, no DNA vaccines are registered for human use. However, there are some records for veterinary use such as a prophylactic West Nile virus DNA vaccine for horses^[4] and a therapeutic DNA vaccine for melanoma in dogs^[5]. In addition, there are several ongoing human clinical trials worldwide involving DNA vaccination, mostly directed to Human Immunodeficiency Virus (HIV) and cancer, which indicates the scientific development of this field.⁽ⁱⁱ⁾

2.2 Plasmid DNA vectors structure and design

Plasmids are extrachromosomal DNA elements with a small number of copies within the host (except pUC plasmid) due to the presence of an origin of replication. These replicons have been found in species from the three representatives of the living world, namely, the domains *Archaea*, *Bacteria* and *Eukarya* and can replicate independently from the chromosome of the host strain. They also encode for multiple phenotypic functions that allow the host strain to adapt to different environments^[6].

These molecules are normally produced in large scale by cell culture of *Escherichia coli* (*E. coli*) strains such as DH5 α and there are several commercially available plasmids such as pBR322, pUC or pVAX.

Most plasmid vectors are closed circular, double-stranded DNA, whose size can be from less than 1 kilobase pairs (kbp) to more than 20 kbp and should contain two units: the plasmid propagation (bacterial backbone) that has the origin of replication and markers for prokaryotic and/or eukaryotic selection and the transcription unit which encodes the antigen under appropriate promoter control (Figure 2).

⁽ⁱⁱ⁾ <http://www.clinicaltrials.gov/>

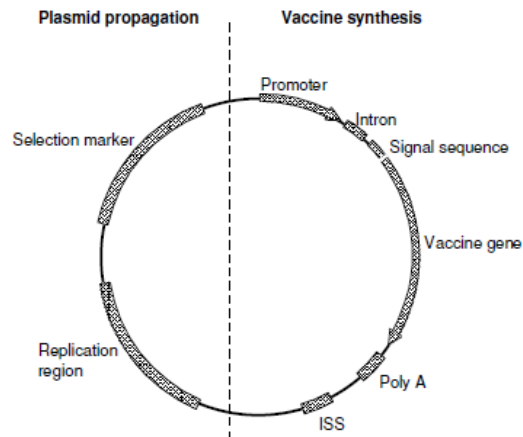


Figure 2 - Genetic elements of a plasmid DNA vaccine. Plasmid DNA vaccines consist of a unit for propagation in the microbial host and a unit that drives antigen synthesis in the eukaryotic cells. For plasmid DNA production a replication region and a selection marker are employed. The eukaryotic expression unit comprises an enhancer/promoter region, intron, signal sequence, antigen gene and a transcriptional terminator (poly A). Immune stimulatory sequences (ISS) add adjuvanticity and may be localized in both units^[7].

Plasmids, as any other DNA molecule, are formed by two linear chains of deoxyribonucleotides linked by hydrogen bonds established between purines and pyrimidines. In agreement with the Watson and Crick's model, these anti-parallel chains form a double helix in which the winding occurs in clockwise direction. In the particular case of pDNA, both molecule ends are covalently linked, that is to say, that both phosphodiester backbones remain intact, forming a closed loop. However, pDNA may acquire diverse conformations (isoforms) with different stabilities^[8] (Figure 3).

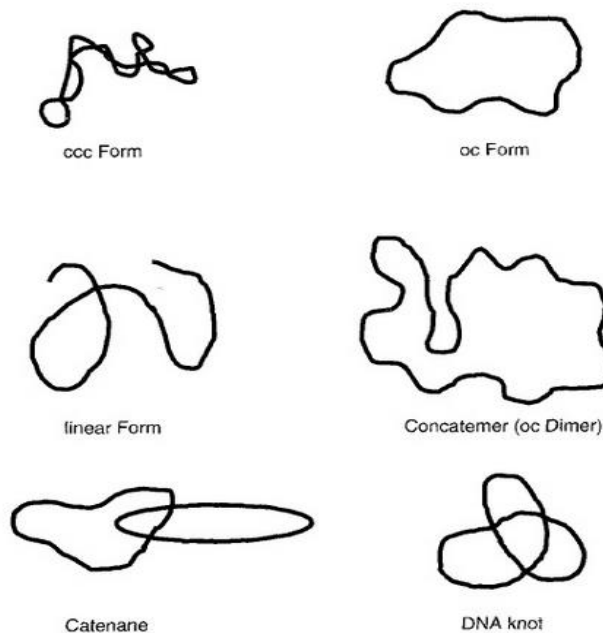


Figure 3 – Plasmid DNA topological structures^[9]

The majority of plasmids isolated from bacterial cells have covalently closed circular ccc-forms with super-coiled shape because both DNA strands are intact. Their compact structure is also due to the wounding of DNA double-strand helix around itself. The molecular coiling is lost by the presence of a mechanical stress or by the action of nucleases which break one of the DNA strands, resulting in an open circular plasmid DNA form (oc-form). This form is completely relaxed and much less compact than ccc-form. When both strands are cleaved by restriction endonucleases, linear DNA molecules are formed.

Concatemers are dimeric plasmid molecules found very often in plasmid preparations which can arise during or after replication, by homologous recombination. Catenanes can also be formed during replication if two (or more) monomeric plasmids, consisting of isolated circular double strands, are interlocked as chain links. DNA knots, which are rarely found in plasmid preparations, are single molecules where a DNA double strand is accidentally interwoven in itself^[9].

DNA molecules are generally heavy and big, with an average molecular weight of 660 Da per base pair (bp)^[9]. In order to fit into the prokaryotic cells or into the eukaryotic cell nucleus, these molecules must be condensed. Thus, super-coiling plays an important role.

Research in plasmid field has been developed in the last decades due to the apparently simple genetic organization of these elements and their easy isolation and manipulation in vitro. Moreover, since plasmids are dispensable, their manipulation does not appear, in principle, to have any adverse consequences to the host cells.

2.3 Plasmid DNA pVAX1GFP

The plasmid used in this study was the pVAX1GFP (3697bp \approx 2440kDa) obtained by modification of the commercial plasmid pVAX1LacZ (6050bp, Invitrogen), by replacement of the β -galactosidase reporter gene by the enhanced Green Fluorescent Protein (eGFP, referred to as GFP thereafter) gene^[10].

pVAX1[®] is the precursor plasmid vector and it was designed for use in the development of DNA vaccines, being consistent with the Food and Drug Administration (FDA) criteria. Its construction takes into account some important features that allow a high copy number replication in *E. coli* host cells and a high level transient expression of the protein of interest in most mammalian cells, making this plasmid a good model to be used in this work (Figure 4).

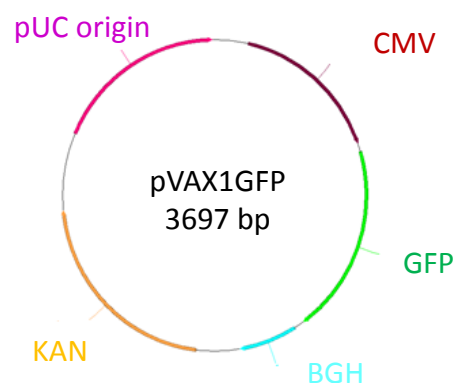


Figure 4 – Plasmid DNA pVAX1GFP characteristic features.

The Human cytomegalovirus immediate-early promoter/enhancer (CMV promoter) allows an efficient, high-level expression of the target recombinant protein; the pUC origin permits a high-copy number replication and growth in *E. coli*; the Bovine growth hormone (BGH) reverse priming site allows sequencing through the insert and the BGH polyadenylation signal (BGH polyA) is responsible for efficient transcription, termination and polyadenylation of messenger RNA (mRNA). The kanamycin-resistance gene (KAN) acts as a selection marker, preventing the growth of plasmid-free bacteria during fermentation, due to the spontaneous loss of genetically-engineered plasmids from the host cell and the decrease of growth rate plasmid-containing cells with high copy number plasmids.

2.4 Methods for gene delivery

The success of DNA vaccination, as stated in Chapter 2.1, is highly dependent on an efficient transfection process. It is then necessary to identify appropriate DNA sequences and cell types and use suitable methods to get enough DNA into these cells nucleus in order to express the gene of interest. The methods used to achieve this goal include physical treatments such as electroporation, chemical methods such as calcium phosphate precipitation, biological nanoparticles through the use of viruses as DNA vehicles and structured chemical materials such as liposomes, cationic polymers and even more organized nanoparticles.

2.4.1 Electroporation

Electroporation is a physical method in which short high-voltage pulses are applied to overcome the cell membrane barrier. The transient and reversible breakdown of the membrane is induced by the applied electric field which surpasses its capacitance and this permeable state is used to insert several molecules into cells, such as DNA, RNA, antibodies, ions or oligonucleotides (Figure 5).

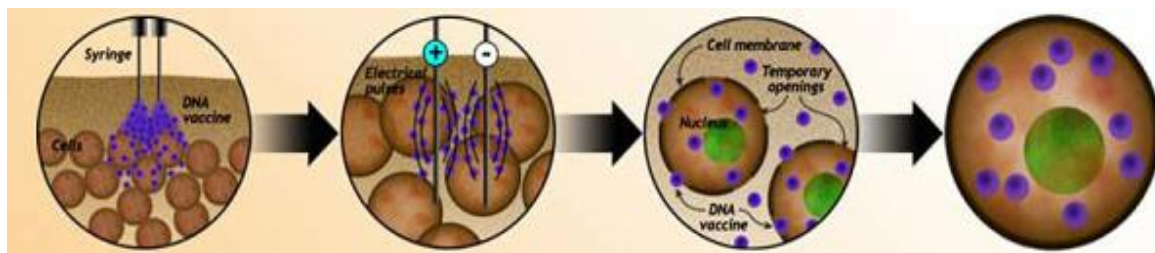


Figure 5 – Transfection of DNA vaccine by electroporation procedure. ⁽ⁱⁱⁱ⁾

This technique is effective with nearly all cells and species types, the amount of DNA required is smaller than for other methods and the procedure may be performed with intact tissue (*in vivo*). However, if the pulses are longer or more intense than adequate, some pores may become larger or fail to close after membrane discharge, causing irreversible cell damage or rupture. In addition, material transport into and out of the cell during the time of electro-permeability is relatively nonspecific, leading to an ion imbalance that could alter the cell function and cause its death^[11].

⁽ⁱⁱⁱ⁾ <http://www.vgxi.com/eng/technology/electroporation.php>

2.4.2 Calcium phosphate co-precipitation

This chemical transfection method is widely used because its components are easily available and inexpensive, the protocol is easy to use and it is effective with several types of cultured cells. The protocol involves mixing pDNA with calcium chloride and adding the mixture to a buffered phosphate solution. This controlled addition generates a precipitate with a positive net charge that is dispersed onto the cultured cells. The positive net charge allows the precipitate to interact with the negatively charged cell membrane and internalization occurs via endocytosis or phagocytosis. In addition, calcium phosphate appears to provide protection against serum and intracellular nucleases^[12].

However, this co-precipitation method is prone to variability and is not suited for *in vivo* gene transfer to whole animals. In addition, reagent consistency and size and quality of precipitate are crucial to the success of transfection. Furthermore, the pH control needs to be very precise because small changes (± 0.1) also affect the transfection efficiency.

2.4.3 Viral vectors

Viruses may be defined as small (diameter between 20 and 300nm) and infectious acellular organisms, whose genomes consist of nucleic acids (DNA and/or RNA) and which only replicate inside host cells using host metabolic machinery and ribosomes to form a pool of components that assemble into particles called virions. These protect the genome and transfer it to other cells for production of virally encoded proteins. The infection process in which functional genetic information expressed from the recombinant vectors is introduced into the target cell is called transduction.

Viral vectors cover a wide range of viral species with different types of nucleic acid composition and characteristic features related to host cell specificity, expression pattern and duration, as well as cytotoxicity.

Retroviruses are lipid-enveloped particles comprising a homodimer of linear, positive-sense, single-stranded RNA genomes of 7 to 11 kilobases. Following entry into target cells, the RNA genome is retro-transcribed into linear double stranded DNA and integrated into the cell chromatin. Adenoviruses, on the other hand, have double-stranded DNA genomes and are the most frequently used viral vectors due to their ability to engineer packaging cell lines for the generation of high-titer virus stocks and the high-level gene expression obtained in a broad range of host cells^[13].

Viral vectors are natural vehicles for heterologous gene delivery for immune responses and have been extensively studied and developed as such (Figure 6a).

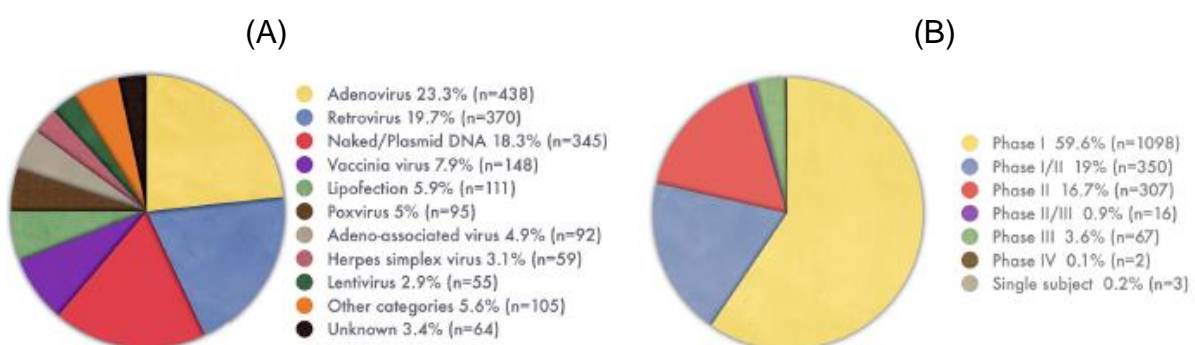


Figure 6 – Vectors used in (A) and phases of (B) gene therapy clinical trials^[14]

The first major gene therapy success was the retrovirus-based treatment of infants suffering from the X chromosome-linked severe combined immune deficiency (SCID-X1) and showed the real potential of long-term or even permanent cure of this hereditary disease^[15].

However, the application of viral vectors for clinical trials in humans requires serious consideration of safety aspects related to their use (Figure 6b), because these vehicles may provoke mutagenesis and carcinogenesis and its repeated administration induces an immune response which abolishes the transgene expression. Also, this method is technically challenging and generating recombinant viruses is time consuming. Furthermore, the cell lines to transfect must contain viral receptors in their membranes to promote interaction and internalization of the vehicle.

In contrast to viral vectors, non-viral delivery systems possess a much reduced bio-safety risk by nature. It is, therefore, not surprising that this area has been the target for intensive research and development of a multitude of vehicles.

2.4.4 Non-viral vectors

Non-viral gene delivery systems (diameters between 10 and 1000nm) have the potential to provide nucleic acid-based therapeutics that closely resembles traditional pharmaceuticals in a way that the products should be capable of being easily and repeatedly administered to the patients with little immune response. They should also be produced in large quantities with high reproducibility and low cost and be stable to storage at room temperature (non-exotic conditions).

The two main approaches in non-viral gene delivery involve the combination of nucleic acids with cationic lipids, forming structures called lipoplexes, and/or cationic polymers, resulting in stable particles called polyplexes.

Cationic lipids are used mainly in the form of liposomes, which are composed of natural phospholipids surrounding a watery interior. These compounds are widely used as gene delivery vehicles due to their similarity to cell membranes and because they may spontaneously interact with the negatively charged DNA to form a stable complex (lipoplex) that facilitates the gene transfer to cells (Figure 7a).

The formulations are generally made in combination with “helper” lipids, such as cholesterol or dioleoylphosphatidylethanolamine (DOPE). These neutral lipids are known as “helper” lipids because of their ability to increase transfection and decrease toxicity that is generally associated with cationic lipids.

Regarding the cationic polymers, the 21st century has witnessed substantial research in the field through various developments even resulting in clinical trials^{[16],[17],[18],[19]}. These polymers can be either natural or synthetic, according to their origin and may present different architectures including linear, branched or dendrimer-like ones. Widely studied cationic polymers include poly(ethyleneimine) (PEI), poly-L-lysine (PLL), gelatin and chitosan. Their properties are dependent on polymeric hydrogen bond formation and amine groups, chain flexibility, hydrophobic interactions and electrostatic forces^[20].

At physiological pH, cationic polymers can be combined with the negative phosphate groups of DNA to form a particular complex, polyplex, capable of gene transfer to target cells (Figure 7b).

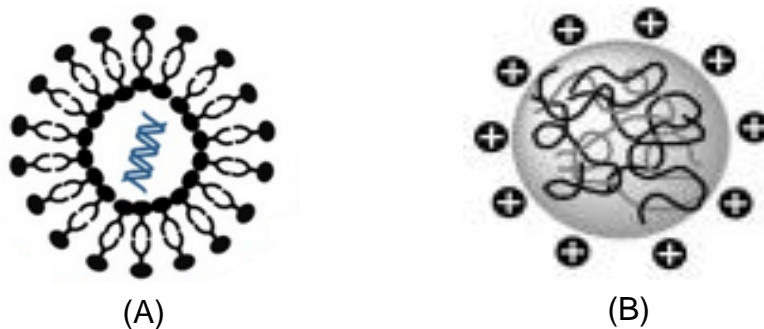


Figure 7 – Examples of Lipoplex (A) and Polyplex (B) morphologies. [21],[22]

The major advantage of cationic polymers over cationic liposomes, especially those composed of monovalent cationic lipids, is the higher efficiency of DNA condensation, resulting in a more homogeneous and smaller diameter distribution of the complex^[23], as well as low toxicity *in vitro*. A smaller diameter distribution is also more compatible with *in vivo* diffusion and with the intracellular trafficking of the DNA-complexes.

When prepared under appropriate conditions, both lipoplexes and polyplexes maintain an overall positive charge enabling them to efficiently interact and get endocytosed by the negatively charged cell membrane^[24]. This is an advantage over the use of naked DNA as a gene delivery vehicle, due to the overall negative charge conferred by DNA phosphate groups. In addition, this complexation process usually protects DNA from nucleases present in the host serum or in the cells cytoplasm.

Despite the advantages of each gene delivery vector, the process of transfection to mammalian cells must be optimised, as well as the formation conditions and stability of the referred complexes, in order to overcome the natural barriers and resist to some extreme conditions present in the host organism, with gene expression as the final goal to achieve an efficient gene delivery process.

2.5 Transfection efficiency

2.5.1 Manufacturing, formulation and stability barriers

As previously stated, cationic lipids and cationic polymers self-assemble with pDNA to form nanometer range particles that are suitable for cellular uptake and transport to nucleus, where the gene will be expressed.

However, the efficiency of this uptake is strongly dependent on the stability of the colloidal system and this stability is entirely related to manufacturing and formulation processes, as well as to the lipids/polymers properties. When applied to colloids, the term stability is one in which the particles resist flocculation or aggregation and exhibits a long shelf-life (Figure 8).

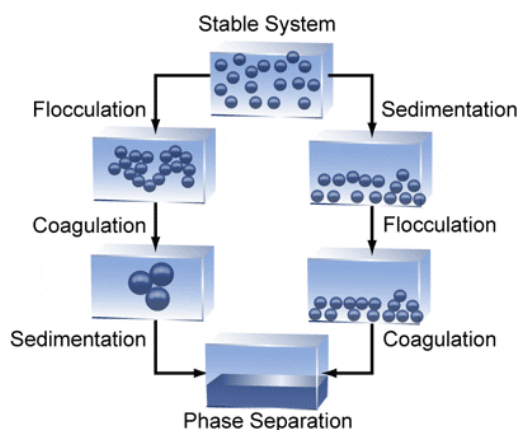


Figure 8 - Schematic diagram showing various mechanisms where stability may be lost in colloidal systems ^(iv)

In certain circumstances, the particles in a colloidal dispersion may adhere to one another and form aggregates of successively increasing size that may settle out under the influence of gravity. This is due to little or no repulsive forces of the particles when they are approaching each other. When all the particles have mutual repulsive forces, the particles in dispersion will be stable.

Although nanoparticles should be sufficiently stable to interact with the cell membrane, their stability should not be too high because DNA has to be released from the complex in order to be transported to the cell nucleus.

Positively charged particles readily aggregate as their concentration increases and are quickly precipitated above their critical flocculation concentration^[25]. The choice of an adequate buffer solution, pH and temperature to dissolve the particles is important to avoid this precipitation phenomenon. Processes like filtration, sonication or dialysis may also affect the diameter and net charge stability of the complexes.

In addition to formulation stability, storage stability will be necessary to provide a practical medicine. Lyophilization is a viable method of preparing lipoplexes^[26] and polyplexes^[27] for storage. It consists in a dehydration process by which the material is frozen and the surrounding pressure is dropped to allow the frozen water in the material to sublime.

^(iv) http://www.malvern.com/labeng/industry/colloids/colloids_stability.htm

The developments made with cationic polymers are closely linked to the broad range of properties they offer, which are essential for an efficient transfection process, such as bioavailability, biodegradability and low toxicity, which might increase the dose or repeated administration of the chitosan complexed drug.

Molecular weight (MW) and molecular weight distribution (MWD) of cationic polymers are among the factors known to dramatically affect their gene delivery performance. A previous study from Fischer and co-workers^[28] has shown that a low molecular weight (10kDa), moderately branched polyethylenimine (PEI) resulted in efficient delivery with low toxicity in comparison with commercial high molecular weight PEI. However, Godbey and colleagues^[29], using branched PEIs ranging in MW from 0.6 to 70 kDa, have determined that higher MW variants mediated significantly better *in vitro* DNA transfection, which they speculated might owe to a greater capacity for endosomal escape. Therefore, an ideal range for cationic polymer MW has not been defined yet.

Another important parameter in drug delivery issue is the size (diameter) of the delivery vehicles. The nanometer size-ranges of these systems (~10–1000 nm) offer certain distinct advantages. Due to their sub-cellular and sub-micron size, nanoparticles can penetrate deep into tissues through fine capillaries and are generally taken up efficiently by the cells. This allows efficient delivery of therapeutic agents to target sites in the body^[30]. Chitosan nanoparticles were found to interact and cross mucosal surfaces, the blood brain barrier, enhance cellular uptake, escape endolysosomal compartments, release genes continuously within the cell and provides low interaction with serum components.

The ability to prepare well-defined particles of known and uniform morphology at a high concentration is essential to the development of a pharmaceutical product.

2.5.2 Extracellular barriers

Extracellular barriers for the delivery of nucleic acids can be found from the injection to the surface of the cellular target of interest. Lipoplexes and polyplexes are colloidal suspensions of DNA (solid particles finely dispersed in a liquid) that must be stabilized to remain discrete particles in blood, which is a heterogeneous, high ionic strength suspension.

Non-viral gene delivery systems must show low toxicity, evade the adaptive immune system, minimize interactions with plasma proteins, extracellular matrices and with themselves (aggregation).

Toxicity is one of the limitations of these systems because it induces cell apoptosis mechanisms, leading to cell death and thus blocking gene expression. Several evidences show that low molecular weight preparations of polycations such as chitosan^[31] and polyethylenimine (PEI)^[28] are significantly less toxic than high molecular weight polycations both in cultured cells and in animals.

In addition, self and non-self-interactions may be avoided by creating a “brush” layer of hydrophilic polymer on the surface of lipoplexes or polyplexes, thus providing a steric stabilization to the particle without any disruption or changes in its morphology^[32].

But the major extracellular barrier is the presence of nucleases in host serum that degrades DNA. The use of vectors that encapsulate the DNA is then essential to avoid its degradation.

2.5.3 Intracellular barriers

Whichever the delivery system, there are several physiological barriers that must be overcome, to achieve the expression of the gene of interest: internalization by cell membrane, endosomal escape, cytoplasmic transport and entrance into the nucleus (Figure 9).

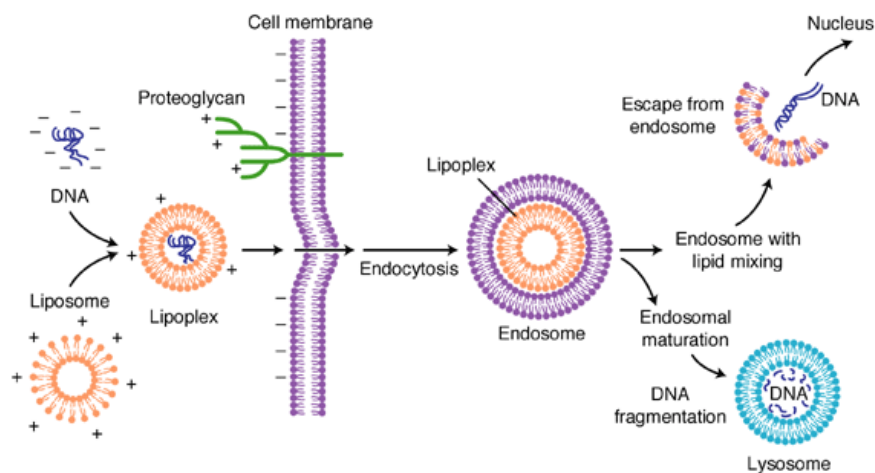


Figure 9 - Lipoplex-mediated transfection, endocytosis and DNA intracellular destiny [33]

Firstly, the complex must be internalized by the cell membrane. There are many different possible routes including receptor mediated endocytosis, pinocytosis and phagocytosis. Receptor mediated endocytosis or clathrin-dependent endocytosis is the most common method of internalization as these cells surface external ligands may attach to the delivery complex to facilitate this process^[34]. Pinocytosis is the process by which cells internalize liquids which contain suspended or soluble particles. Phagocytosis involves the ingestion of particles larger than 0.5 μm in diameter by specific host cells. It is important to note that internalization mechanisms may also be largely dependent on the cell type, the vector used and the physical-chemical parameters of the complex, which are production process dependent.

Following internalization of lipoplexes or polyplexes, endosomal entrapment and subsequent lysosomal degradation are major bottlenecks that limit the efficiency of transfection. Design of gene vectors with endosome-escape properties is considered critical for high transfection efficiency. Identification of endosomolytic or fusogenic components and their integration into non-viral gene delivery systems are major strategies being explored to facilitate endosomal escape. As examples of specific properties of interest, some polymers such as PEI and polyamidoamine (PAMAM) have innate characteristics that cause alterations to the surrounding environment. They show a “proton sponge effect” (pH-buffering effect) that provides an explanation for their endosomolytic activity. Upon PEI-based or PAMAM-based polyplex entry into acidic endosomes, the polymer behaves as a sponge that absorbs protons to protonate the polymer-containing amine groups (primary, secondary and tertiary). Accumulation of protons subsequently drives an influx of counter chloride ion into endosomes, leading to increased osmotic pressure and subsequent flow of water into the endosomal core, that eventually swells and ruptures endosomal membrane^[21]. Histidine residues were identified to enhance chitosan nanoparticles capacity to escape the endosome in HEK293 cells. These chitosan molecules were able

to complex with pDNA and crosslink nanoparticles via disulfide bridges, that breakdown in cytosol due to redox gradient between extracellular medium and inner cell^[35].

After escaping the endosome, DNA must be transported to the nucleus to be expressed. Vaughan and co-workers^[36] proposed that this transport should be mediated by dynein of the microtubules, after DNA binding. Microtubules are cytoskeletal filaments present in eukaryotic cells comprising 13 protofilaments which are polymers of alpha and beta tubulin. They are organized by the centrosome and possess a very dynamic behaviour, binding GTP for polymerization. The protofilaments are connected by the motor protein dynein, which is also responsible for the transport of various cellular components towards the nucleus, by “walking” cytoskeletal microtubules.

The nuclear envelope is the final physiological barrier hindering DNA from entering the nucleus. The nuclear envelope contains openings in the form of nuclear pore complexes, which allow free diffusion of molecules up to 50 kDa, corresponding to a hydrodynamic diameter of approximately 10 nm^[37]. These pores are too small for free diffusion of plasmids, in cells that are not undergoing mitosis. However, during mitosis the nuclear envelope is ruptured and plasmid molecules in the cytoplasm, cloned with the gene of interest, are able to access the newly-formed nuclei of daughter cells, prior to nuclear envelope restructuring. Fasbender and colleagues^[38] corroborated this hypothesis by demonstrating that non-dividing cells showed a 90% lower expression level when compared to actively dividing ones.

Conjugation of polymers with a nuclear localization signal (NLS) peptide, which is recognized by importins, may increase the nuclear localization and transfection efficiency of foreign DNA^[39].

In this project, cationic polymer chitosan is used as a vector to insert the plasmid pVAX1GFP into CHO cell lines. Formulation, characterization and stabilization tests have been performed before transfecting the referred cells.

2.6 Chitosan polymer

2.6.1 Chitosan molecular structure and properties

Chitosan is a linear, natural copolymer of β -(1-4)-linked D-glucosamine and N-acetyl-D-glucosamine (NAG) whose molecular structure comprises a linear backbone linked through glycosidic bonds. The basic amine groups of this polysaccharide are protonated and, thus, positively charged in most physiological fluids.

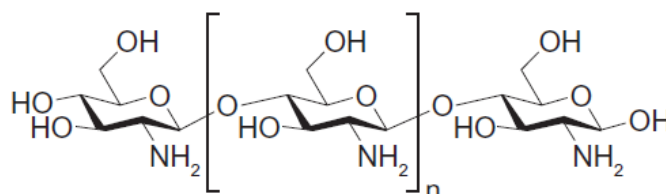


Figure 10 – Molecular structure of chitosan ^[40]

With a pKa of approximately 6.5 on the amine groups, chitosan is insoluble at neutral and alkaline pH. Affecting the number of protonable amine groups, the percentage of acetylated monomers and their distribution in the chains have a critical effect on its solubility, hydrophobicity, conformation in aqueous media and electrostatic interaction with polyanions^[41]. It is a pH-responsive polymer as its charge density strongly varies in the pH range of 5 to 7.4.

Chitosan is derived from the most abundant nitrogen-bearing organic compound found in nature, the linear polymer chitin, by alkaline^[42] or enzymatic deacetylation^[43]. Therefore, chitin and chitosan are essentially the same polymer but with arbitrarily defined degrees of deacetylation (DD), which is the percentage of the deacetylated units (glucosamine monomers) in molecule chains. Generally, if the DD is more than 40%, the term chitosan is used. Although chitin and chitosan are absent in mammals, some mammalian enzymes, such as lysozymes, can hydrolyze them (Figure 11).

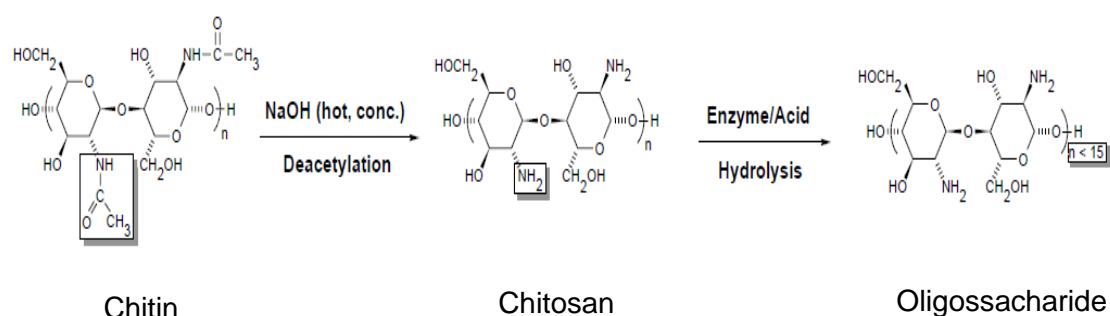


Figure 11 - Deacetylation and hydrolysis reactions on the cationic polymer chitosan (v)

This biodegradation (hydrolysis) process is dependent on several parameters. For instance, Lee *et al.*^[44] demonstrated that chitosan biodegradation declines sharply when the DD is more than 70%, while Aiba *et al.*^[45] showed that this polymer with repeated blocks of three consecutive NAG units is more susceptible to lysozymes than those with randomly distributed NAG units.

Another important property that makes this polymer a useful tool for gene delivery and tissue engineering is its biocompatibility. This is due to chitosans structure similarity with the mammalian glycosaminoglycans (GAGs), a polysaccharide present in the surface of the cells and in the extracellular matrix (ECM), conferring its high viscosities and low compressibility properties. Also, its rigidity provides structural integrity and passageways among cells, allowing for their migration^[46].

Chitosan is also a mucoadhesive polymer. Mucoadhesion is commonly defined as the attractive interaction between a mucosal surface and a pharmaceutical formulation^[47]. Mucosal membranes play important roles in protecting cellular epithelia from chemical and mechanical damage and in providing lubrication and wettability of the cell surface. Mucoadhesive drug delivery systems are attractive and flexible in formulation development due to their various possible administration routes, such as nasal, ocular, gastrointestinal (oral), vaginal and rectal. Other advantages include the increased residence time, improved drug bioavailability, reduced administration frequency, simple

(v) Chitosan – A Technologically Important Biomaterial (Aldrich®)

administration as well as the possibility of targeting particular body sites and tissues^[48]. Chitosan is also known to enhance drug absorption by re-arranging tight junction proteins^[49].

There is also relevant information regarding the immune-reactivity of chitosan. Some authors have reported its ability and of its degradation products to activate human macrophages and lymphocytes proliferation without leading to inflammatory symptoms^[50]. Additionally, other authors have found information on its role of inhibiting cytokine secretion^[51].

Another important feature is the chitosan antimicrobial activity, which enhances its potential for use as food preservatives.

Due to its properties chitosan has wide applications in medical fields besides gene delivery, such as blood anticoagulant, wound dressing, hypocholesterolemic agent and antithrombogenic system. Regarding other fields, this polymer is also used in waste-water treatment, cosmetic preparations and textiles, paper and film technologies^[52].

2.6.2 Molecular weight and degree of deacetylation

The two most important factors that determine the physicochemical properties, and consequently the specific applications of chitosan, are the degree of deacetylation (DD) and molecular weight (MW).

The DD affects the physical, chemical and biological properties of this polymer, such as the tensile strength of the films, the ability to chelate metal ions and the immunoadjuvant activity. It also affects its intrinsic pKa, leading to a change on chitosan solubility in dilute acidic solutions.

When DD is less than 40%, chitosan chains become completely insoluble in water due to the numerous H-bonds that occur among alcohol, amide and ether groups distributed on the repeating units along the polymer chains and hydrophobic interactions, due to the presence of methyl groups of the acetamide functions and to the –CH and –CH₂ groups of the glycosidic rings. When DD is higher than 40%, chitosan becomes soluble in acidic solution in a pH dependent manner^[53].

The higher is the DD of chitosan, the higher is the amount of free amino groups (-NH₂), which in turn, can become protonated to form cationic amine groups (-NH₃⁺) producing positively charged surfaces. This polycationic nature of chitosan is expected to enhance the interactions between its surface and negatively charged cells, and therefore, chitosans with a higher extent of deacetylation facilitate HEK293, HeLa and SW756 adhesion^[54].

Regarding the MW, its effect on gene delivery is noted in polyplex formation. High MW chitosans complexed with pDNA lead to stronger and more stable polyplexes that are more efficient in retaining condensed DNA upon dilution and more capable of protecting DNA from degradation by DNase and other serum components. This is due to their higher viscosity and chain length. However, stronger and more stable polyplexes have more difficulty in release DNA in cytosol to be transported to the nucleus (less than 9% release at 60h of transfection in HEK293 cells)^[55]. Low MW chitosans are more biodegradable than high MW ones and have lower binding affinity due to shorter polymer chain, thus having lower entanglement capability (more than 20% release at 60h of transfection in HEK293 cells)^[55]. Being the chain length (degree of polymerization, DP_n) proportional to the valency of the polycation, an increase in DP_n will lead to an increase in degree of aggregation, thus elevating the

nanoparticles diameter and leading to higher sedimentation levels on the cell surface^[56]. The same authors have achieved higher transfection efficacies (relative light unit/ μg luciferase protein > 1000) in HEK293 cells with chitosans having MWs between 8 and 12kDa. However, Turan and co-workers^[57] suggested that HEK293 cells can be efficiently transfected with chitosan/pDNA nanoparticles with 200-220nm and in which chitosan had a wide range of molecular weight (14-195kDa).

It is, then, necessary to achieve a fine balance between extracellular DNA protection (better with high MW) and efficient intracellular unpacking (better with low MW) to obtain a high transgene expression.

2.6.3 Chitosan chemical modifications

Due to its hydroxyl and amine functional groups, the chemical modifications of chitosan have been extensively investigated in literature in order to improve its physicochemical properties, without changing its fundamental skeleton.

The main goals of chemically modifying chitosan are to provide derivatives that are soluble at neutral and basic pH values, to control hydrophobic, cationic, and anionic properties as well as to attach various functional groups and ligands and optimize the process of drug release.

Jiang *et al.*^[58] have synthesized polyethyleneglycol (PEG) – grafted chitosan, through the reaction between methoxy PEG-nitrophenol carbonate and the referred polymer. PEG-grafted molecules effectively shielded the positively charged chitosan surface when compared to unmodified chitosans and were able to maintain complex sizes ($\approx 200\text{nm}$) in the presence of serum, in addition to affording protection to the complexed DNA against enzymatic degradation. Ultimately, this has improved the transfection efficiency *in vivo*.

Liu *et al.*^[59] also found that alkylated chitosan self-aggregate in acetic acid solution, whereas 99% deacetylated chitosan does not, due to strong electrostatic repulsion. The transfection efficiency of plasmid-encoding chloramphenicol acetyltransferase (CAT), mediated by alkylated chitosan into a mouse skeletal muscle cell line, was dependent on its hydrophobicity. Increasing the length of the alkyl side chain up to 8 carbons caused the transfection efficiency to increase. It was suggested that higher transfection efficiencies of modified chitosan were due to easier unpacking of DNA inside cells, in addition to enhancing entry into cells, facilitated by hydrophobic interactions.

The incorporation of hydrophobic units (alkyl, acyl or cholesterol) into cationic polymers enhances their adsorption to the lipophilic cell membranes and facilitates endocytosis of polyplexes. Commercial lecithin, a mixture of phospholipids in oil, is also used in complexation studies with chitosan because it is easily soluble and dispersible in aqueous solution which accelerates the formation of the desired nanoparticles.

Furthermore, the hydrophobic modification of cationic polymers has shown facilitated dissociation of polymer/DNA, enhancing the release of DNA to cytoplasm, that would otherwise remain strongly bound through ionic interactions between phosphate groups of DNA and cationic units of polymers^[60].

The chemical modification of this cationic natural polymer, without changing its main properties, could be a huge approach to enhancing the efficiency of transfection.

2.7 Formation of chitosan/pDNA nanoparticles

Chitosan and pDNA nanoparticles have recently been widely studied for its use in gene delivery processes. The optimization of the formation conditions of these nanometer range particles and their characterization are essential to achieve high quality complexes, in order to obtain high transfection efficiencies.

Thus, it is of extreme importance to use highly pure supercoiled pDNA. The production and downstream processing of pDNA containing the gene of interest is summarized in Figure 12.

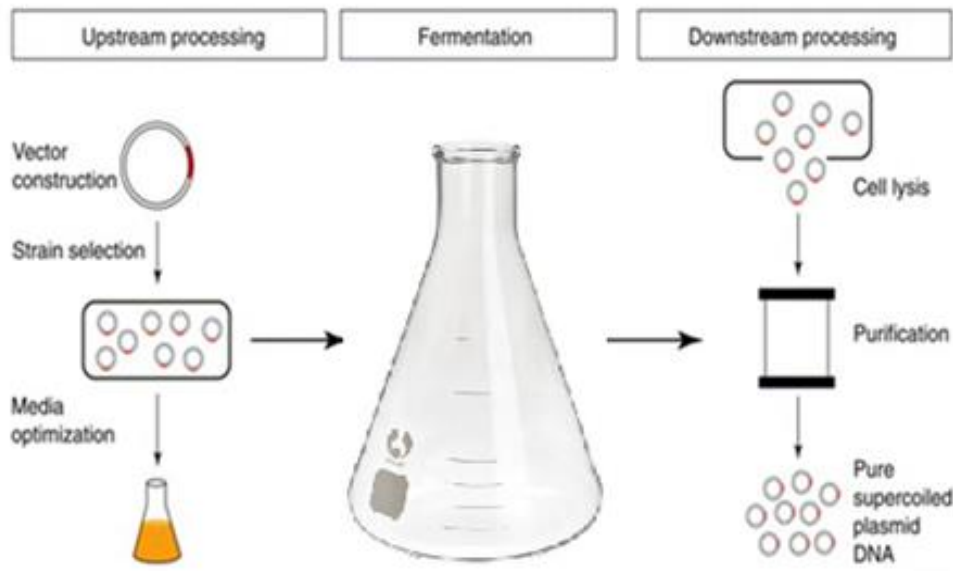


Figure 12 - Production and downstream processing of plasmid DNA containing the gene of interest. Adapted from Ferreira G.N *et al.* 2000 [61]

The main goals of the upstream and fermentation processes are the selection, design and optimization of appropriate plasmid vectors and the production of microorganism strains and growth conditions, in order to obtain large quantities of stable and supercoiled plasmid DNA.

Cell lysis is the first critical step after fermentation. In this process, all the intracellular components are released, including pDNA, RNA, proteins, gDNA and endotoxins. The recovery of large amounts of intact, supercoiled plasmid DNA is essential to obtain high overall process yields. Variations of the alkaline-lysis procedure, originally described by Birnboim and Doly^[62], have been the procedure of choice for cell disruption for plasmid recovery. The formed precipitate containing nucleic acids, proteins and cell debris is then removed by centrifugation.

Before purification of pDNA, clarification and concentration are essential steps to remove the remaining RNA and proteins in the lysate and to increase the pDNA mass fraction, respectively. The use of chaotropic salts and precipitation with PEG are the usual methods for clarification and concentration processes, respectively^[61].

Chromatography is the method of choice for the large-scale purification of supercoiled plasmid DNA, due to its scalability, reproducibility, the use of only safe chemicals and because it is sufficiently robust to withstand the abrasive cleaning conditions required for process approval and validation.

There are several chromatographic operations, although hydrophobic interaction chromatography (HIC) is the most suitable one for the initial capture, purification and concentration of supercoiled plasmid DNA. This is due to the different hydrophobic character of double-stranded pDNA and other nucleic acid impurities with high content in single strands, such as RNA and denatured gDNA, allowing their separation. The interaction between immobilized hydrophobic ligands (ex: alkyl, phenyl, aryl groups) and the non-polar regions at the biomolecular surface is significantly influenced by the presence of certain salts in the running buffer. A high salt concentration enhances the interaction while lowering this concentration weakens the referred interaction^[63].

For selective elution the salt concentration is gradually lowered and the sample components elute in order of hydrophobicity (Figure 13).

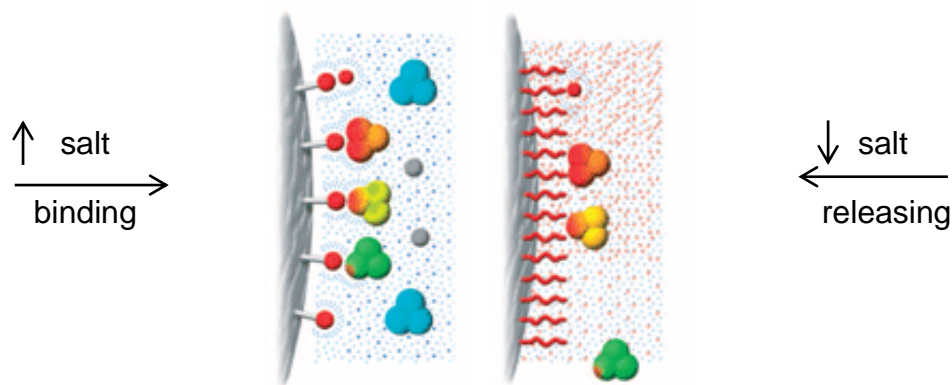


Figure 13 - Hydrophobic interaction between immobilized ligands and biomolecular surface controlled predominantly by the salt concentration (vi)

This technique also has the potential to separate native from denatured plasmid because denatured forms contain large stretches of single-stranded DNA, there is more exposure of hydrophobic bases and, consequently, the retention time is longer and the hydrophobic interaction is greater. Furthermore, HIC supports also separate endotoxins from pDNA due to their high hydrophobicity comparing to plasmids, which is translated in a longer HIC column retention.

The currently available chromatographic supports, however, continue to manifest low performances when separating these large polynucleotides, because access of these molecules to the pores of the support is hindered and absorption occurs only at the outer surface. Also, if bead size is decreased to overcome the small surface areas per column volume, low flow rates must be used to minimize pressure drops.

Membrane adsorbers with larger pore sizes are emerging as alternative to bead-based media mainly due to rapid and convective transport of solutes to the membrane surface^[64].

After purification procedures, several centrifugation or ultrafiltration/diafiltration steps are taken to desalt and concentrate the purified fractions of pDNA. The concentration of pDNA may also affect the transfection efficiency of chitosan-pDNA nanoparticles, because a higher amount of negatively

(vi) <http://www.indiamart.com/ge-healthcare-limited/products.html>

charged particles will disable the interaction between the complex and the also negatively charged cell membrane.

In order to achieve relatively stable and positively charged complexes, chitosan solution must also be stable. As stated before in Chapter 2.6.1, chitosan can only be dissolved in acidic solutions. An acetic acid solution, with a pH around 3.0 is widely used for this purpose, because aggregation and precipitation of chitosan molecules is avoided. These two phenomena would create a high density molecule, not allowing the internalization of pDNA by chitosan through electrostatic interactions.

In addition, processes like filtration and sonication can be used to enhance the “quality” of chitosan solutions. The membrane filtration of buffer solutions allows the removal of certain impurities present in those same solutions that, otherwise, could interfere in the polymer structure and properties. After dissolving chitosan powder in a buffer solution (e.g. acetic acid), sonication is a widely used process to disperse these particles in the surrounding medium. The dispersion of the particles is important to prevent precipitation phenomenon that could eventually occur.

Moreover, polymer chemical structure, namely of its functional groups, is not significantly affected by the application of moderate ultrasound energies and no new compounds are formed either. However, it has been demonstrated that if high ultrasound energies are applied, chitosan degradation is caused both by OH radicals and mechanochemical effects^[65].

Chitosan MW also affects this polymer stability in solution, namely its diameter size and zeta potential (net charge). High MW molecules should show higher diameters and zeta potential values (more positive charges) than low MW particles, due to the presence of more repeating units (n) in its structure.

The area of nanomedicine, so named in 2004 by the European Science Foundation (ESF), represents a new era in the field of drug delivery research in which nanoparticles are applied as drug delivery vehicles. These particles have several advantages such as their small size (within the nano range), their capability of encapsulating proteins, peptide drugs or nucleic acids such as pDNA, thus protecting them from enzymatic degradation for instance in the adverse gastrointestinal (GI) environment, enabling easy transport and internalization through intestinal epithelial cells, in turn improving the pharmacokinetics, bioavailability and therapeutic efficacy after administration. Another huge advantage of using nanoparticles as drug delivery vehicles is the fact that they can be administered orally, a non-invasive procedure, thus avoiding the use of needles that must be kept sterile and administered by trained personnel, which in some cases is not easy, especially in developing countries.

The use of chitosan nanoparticles in gene delivery has been widely documented with some positive and encouraging results. Aside from the advantageous properties of chitosan, previously stated in Chapter 2.6.1, this approach will allow a direct target to affected cells, mainly those present in GI tract.

Chitosan nanoparticles for oral delivery can be synthesized by a variety of methods, briefly described in Figure 14.

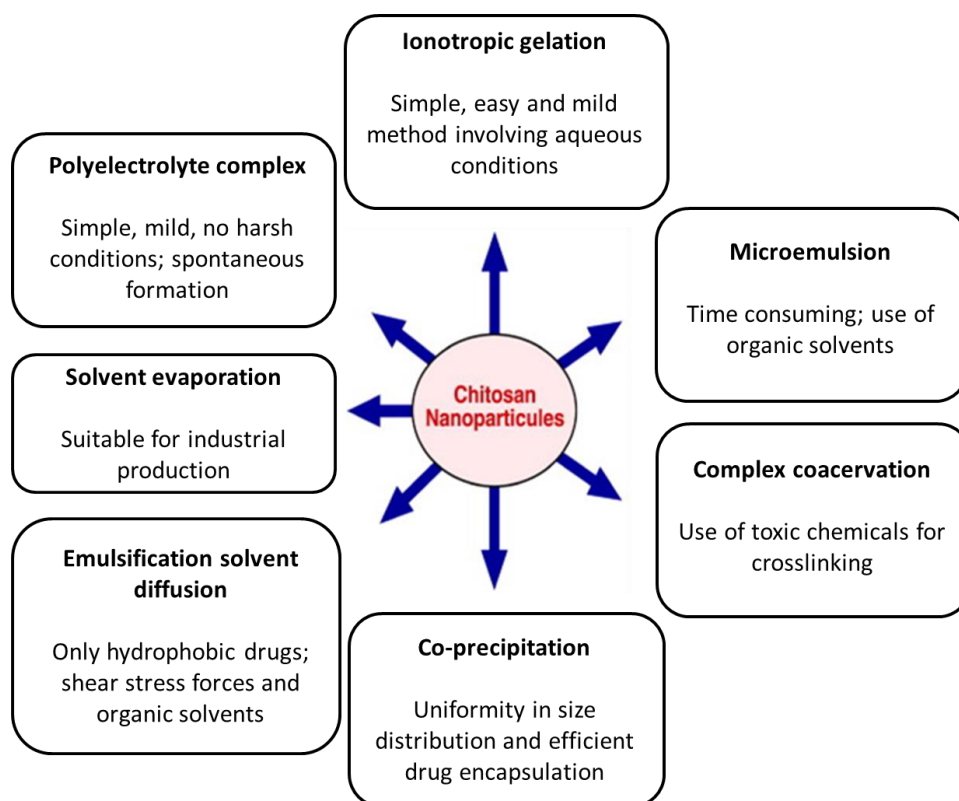


Figure 14 – Methods for chitosan nanoparticle preparation. Adapted from Mukhopadhyay et al. 2012 [66]

Most of these methods are simple and mild, which is essential to maintain the drug integrity. The self-assembled nanoparticle synthesis has proven to be more effective compared to other methods as it does not require any organic solvents. Several studies have identified particle size, encapsulation efficiency and loading contents as the key factors for achieving effective results in both *in vitro* and *in vivo* systems. In addition, different formulation parameters may be studied in order to achieve the most stable and suitable nanoparticle for transfection. These parameters include buffer type, pH of the preparation solution, the order of addition of the two solutions, cryoprotectant use, as well as the concentration of the different components and the molar ratios of the cationic and anionic solutions (N/P).

In higher N/P ratios, the amount of chitosan is superior, thus having free polycation that will compete with the positively charged polyplexes for interaction with the negatively charged cell membrane. Also, elevated N/P ratios lead to excessively stable polyplexes that release DNA more slowly and less efficiently. It is then of extremely importance to control the charge-based interaction between chitosan and DNA to achieve a successful gene delivery process. An optimal N/P ratio range between 3 and 20 was determined by Thibault and co-workers^[1].

Moreover, these particles have to be characterized, namely their diameter size and zeta potential, and stability assays must be performed in order to confirm the quality of the formulations to be delivered into target cells.

2.8 Nanoparticles characterization

Determination of nanoparticles diameter and zeta potential is achieved through dynamic light scattering (DLS) and electrophoretic mobility (EM), respectively, using equipment like the Zetasizer Nano instrument (Malvern, UK).

This instrument features pre-aligned optics and programmable measurement position plus the precise temperature control necessary for reproducible, repeatable and accurate measurements. In addition, facility is included for measurement of other key parameters such as pH and concentration.

The particle size is the diameter of the sphere that diffuses at the same speed as the particle being measured. DLS, also known as photon correlation spectroscopy, measures Brownian motion and relates this to the size of the particles. It does this by illuminating the particles with a laser and analyzing intensity fluctuations in the scattered light.

In practice, particles suspended in a liquid are never stationary. Their movement is due to the random collision with the molecules of the liquid that surrounds the particle. This movement is called Brownian motion. An important feature of Brownian motion for DLS is that small particles move quickly and large particles move slowly. The relationship between the size of a spherical particle and its speed due to Brownian motion is defined in the Stokes-Einstein equation (Eq.1),

$$d(H) = \frac{kT}{3\pi\eta D} \quad \text{Eq. 1}$$

where, $d(H)$ is the hydrodynamic diameter, D is translational diffusion coefficient which measures the velocity of the Brownian motion, k is the Boltzmann's constant, T is the absolute temperature and η is the viscosity of the solution.

An accurately known temperature is necessary for DLS because knowledge of the viscosity is required (viscosity of a liquid is related to its temperature). The temperature also needs to be stable otherwise convection currents in the sample will cause non-random movements that will ruin the correct interpretation of size^[67].

There are several factors that affect the diffusion speed of the particles. The ionic strength of the medium changes the thickness of the electric double layer called the Debye length. Thus, a low conductivity medium will produce an extended double layer of ions around the particle, reducing the diffusion speed and resulting in a larger apparent hydrodynamic diameter. Any change in the particles surface will affect the polymer conformation and will also change the apparent size by several nanometers^[67].

The best way to measure the spectrum of frequencies contained in the intensity fluctuations arising from the Brownian motion of particles is to use a device called digital auto correlator. A correlator is basically a signal comparator. It is designed to measure the degree of similarity between two signals, or one signal with itself at varying time intervals. The size distribution obtained is a plot of the relative intensity of light scattered by particles in various size classes and is, therefore, known as an intensity size distribution (Figure 15).

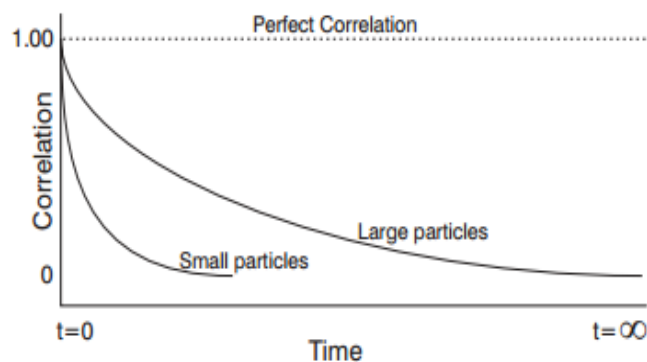


Figure 15 - Correlation differences between small and large particles. (vii)

Analysis of correlograms can give a lot of information about the sample. The time at which the correlation starts to significantly decay is an indication of the mean size of the particles in a sample. The steeper the line, the more monodisperse are the particles in sample, that is to say, the particles in a mixture have the same size, shape or mass. Conversely, the more extended the decay becomes, the greater the sample polydispersity, that is to say, the particles show inconsistent size, shape and mass distribution. Monodisperse nanoparticles provide high efficiency of transfection because more homogeneous formulations enhance their interaction with the cell membrane, as reported by Sunshine *et al.*^[68].

The other main nanoparticle parameter, the zeta potential, is a physical property which is exhibited by any particle in suspension. It can be used to optimize the formulated suspensions.

The increasing concentration of counter ions, ions of opposite charge to that of the particle, close to the surface of the particle, results from the development of a net charge at the particle surface. Thus, each particle has an electrical double layer around it (Figure 16). The liquid layer surrounding the particle consists of an inner region, the Stern layer, where the ions are strongly bound and an outer region, where they are less firmly attached. Within the diffuse layer there is a notional boundary inside which the ions and particles form a stable entity. When a particle moves, the ions will move with it. This boundary is called the surface of hydrodynamic shear or slipping plane. The potential that exists at this boundary is known as the zeta potential.

^(vii) Zetasizer Nano Series User Manual. MAN 0317 Issue 1.1 Feb . 2004 (Malvern Instruments Ltd.)

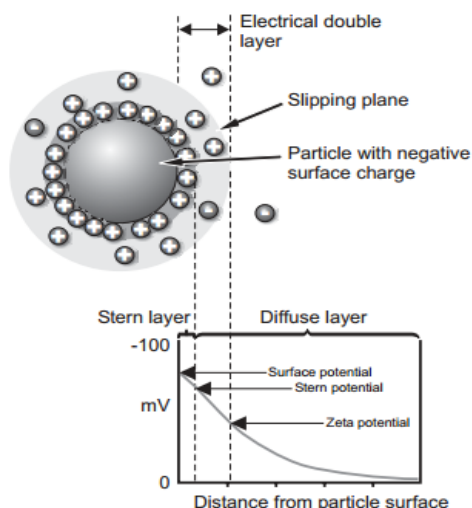


Figure 16 – Zeta-potential of a nanoparticle in solution ^(viii)

This potential is measured by EM. Charged particles suspended in the electrolyte are attracted towards the electrode of opposite charge, when an electric field is applied. Viscous forces acting on the particles tend to oppose this movement. When equilibrium between these two opposing forces is reached, the particles move with constant velocity (electrophoretic mobility). The zeta potential is then calculated through Henry's equation (Eq. 2),

$$U_e = \frac{2\varepsilon.z.f(ka)}{3\eta} \quad \text{Eq. 2}$$

where ZP is the zeta potential, U_e is the electrophoretic mobility, ε is the dielectric constant of the solution medium, η is the viscosity of the solution and $f(ka)$ is the Henry's function, which is normally equal to 1.

Regarding sample preparation, concentration is an important factor to achieve an optimal measurement. If the sample concentration is too low, there may not be enough light scattered to make a measurement, although it is unlikely to happen with Zetasizer Nano, except under extreme conditions. On the other hand, if the sample is too concentrated, light scattered by one particle will itself be scattered by another. This multiple scattering phenomenon is governed by the point at which the concentration no longer allows the sample to freely diffuse due to particle interactions^[69]. Chitosan has a concentration dependent cytotoxicity (0.2 – 2mg/mL) in most cell models^[70].

Whenever possible, the sample concentration should be selected, so that the sample can get slightly turbid.

^(viii) Zetasizer Nano Series User Manual. MAN 0317 Issue 1.1 Feb . 2004 (Malvern Instruments Ltd.)

The number of particles in the scattering volume is also important to obtain a reliable measurement. Figure 17 shows the number of particles needed per scattering volume for different concentrations when particles density of 1 g/cm³ is assumed.

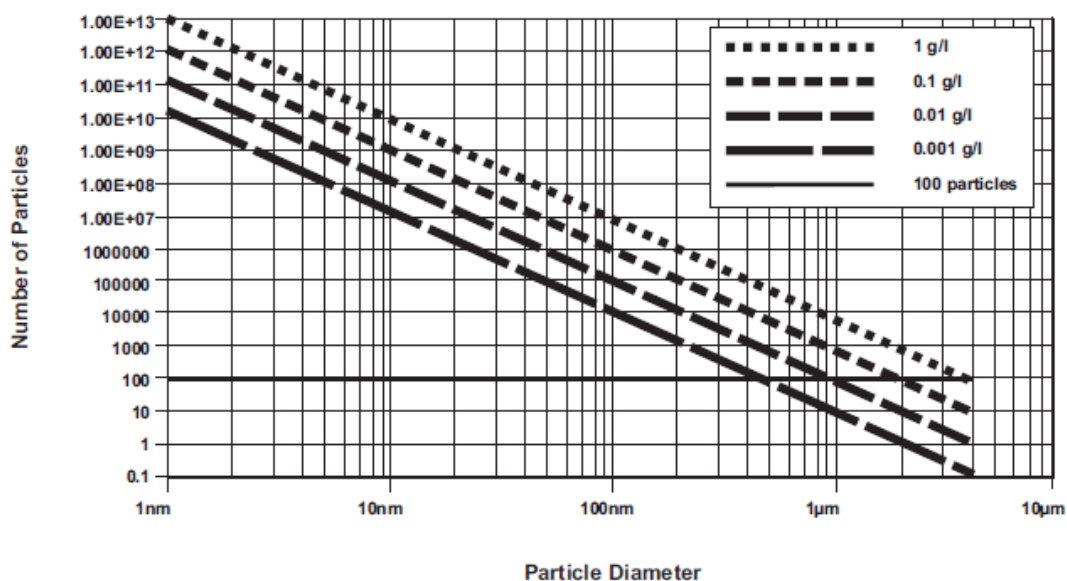


Figure 17 – Estimate plot of number of particles per scattering volume for different concentrations when density of 1g/cm³ is assumed. ^(ix)

By knowing the sample concentration used and the particle diameter (1nm to 10µm), the number of particles in the scattering volume can be determined. However, a minimum of 1000 particles should be present when the measurement is made because fluctuation of the momentary number of particles in the scattering volume will occur if the number is too small and these fluctuations will be misinterpreted by the calculation method as larger particles within the sample.

2.9 Efficiency of cell transfection and fluorescence-activated cell sorting (FACS)

Besides the parameters previously referred to in Chapter 2.5, there are other ones that can influence the efficiency of transfection process, such as the cell confluence, the time of transfection and the time of incubation of the mixture, before analyzing the samples by flow cytometry. The cell confluence is important because an elevated number of cells could cause contact inhibition and the complex may not be able to interact with the cell membrane. Thus, 100% cell confluence should be avoided.

The transfection time, which is the time-length for the complexes to be in contact with the cells, may also affect the efficiency of the process and it is particle and cell dependent. For instance, Strand and co-workers^[71] achieved transfection levels in 30-50% of the cells in HEK293 cell line, using 5µg of pDNA in pDNA-loaded chitosan nanocarriers, with 5h of contact with the cells. However, these transfection levels decreased in other more challenging cell types such as MCDK, HeLa and Calu-3^[57].

^(ix) Zetasizer Nano Series User Manual. MAN 0317 Issue 1.1 Feb . 2004 (Malvern Instruments Ltd.)

Also, transfection levels in $\approx 40\%$ of the cells in HEK293 cell line was achieved after a 24h contact of chitosan/pDNA polyplexes with the referred cells, as reported by Thibault and co-workers^[1].

The incubation time is the time of cell culture between transfection and analysis of protein expression. During this time the cell machinery will transcribe and translate the gene of interest, thus influencing the expression degree of the protein. 24h and 48h are the most used intervals in chitosan/pDNA nanoparticles delivery^{[1],[71]}.

Fluorescent proteins such as GFP have revolutionized modern biomedical and biotechnological research. The ability to transiently or stably incorporate the gene for an expressible fluorescent protein has become a critical technique for the study of gene expression, cellular and tissue development and a host of other biomedical/biotechnological phenomena.

A common and useful method to determine the degree of GFP expression in cell nucleus (percentage of transfection) is fluorescence-activated cell sorting (FACS), a specialized type of flow cytometry (Figure 18). This technique allows the sorting of heterogeneous mixture of biological cells into two or more containers, one cell at a time, based upon the specific light scattering and fluorescent characteristics of each cell. It is a useful scientific instrument as it provides fast, objective and quantitative recording of fluorescent signals from individual cells as well as physical separation of cells of particular interest.

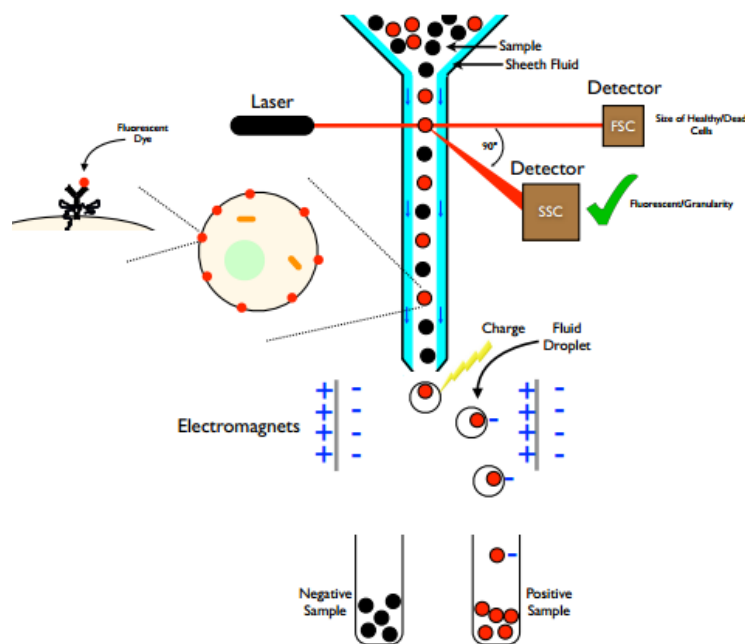


Figure 18 – Fluorescent-activated cell sorting (FACS) principle. Here, the laser beam detects the correct fluorescence and sends the charged cell droplet into the correct positive sample vial. (x)

A beam of laser light of a single wavelength is directed onto a hydrodynamically focused stream of liquid. Several detectors are aimed at the point where this stream passes through the light beam. Forward scatter (FSC) is in line with the beam and Side scatter (SSC) which is perpendicular to it and one or more fluorescence detectors. One cell at a time passes through the beam, scatters the

(x) <http://etheses.whiterose.ac.uk/2040/>

ray and fluorescent molecules inside the cell (eGFP in this study) may be excited into emitting light at a longer wavelength than the light source. This combination of scattered and fluorescent light is picked up by the detectors and, by analysing fluctuations in brightness at each detector, it is possible to derive various types of information about the chemical and physical structure of each individual cell. The cell volume is correlated with FSC and SSC depends on the inner complexity of the particles (ex: membrane roughness or shape of the nucleus). This is due to the fact that the light is scattered off of the internal components of the cell^[72].

Background auto-fluorescence of non-transfected cells must be taken into account to determine transfection efficiencies, considering the difference between the total cell population inside the gate, and the background auto-fluorescence of non-transfected cells, indicated by the green fluorescence parameter.

Commercial flow cytometry systems are usually equipped with argon-ion lasers emitting at the blue-green 488nm wavelength, allowing the efficient excitation of fluorescein and other traditional fluorochromes. However, wild type GFP could not be excited on these systems because its excitation maximum is in the long ultraviolet (UV) range, with emission in the green (approximately 510nm). The development of the enhanced green fluorescent protein (eGFP) by the Tsien laboratory via site-directed mutagenesis produced a modified GFP that was optimally excited at 488 nm while retaining or enhancing the wild type emission, expression and photostability properties^[73]. GFP is now a practical technique for flow cytometry, and is widely applied in a variety of systems.

Regarding the goal of this project, which is to determine the chitosan/pDNA nanoparticle that provides higher transfection efficiencies, FACS represents the most suitable method to analyze it, through eGFP fluorescence.

3. Materials and Methods

3.1. Bacterial culture and alkaline lysis

3.1.1. Plasmid and cell bank

The plasmid vector pVAX1GFP having 3697 bp was used^[10] for transforming *Escherichia coli* DH5 α (Invitrogen) cells from which a cell bank was produced and stored in 20% (v/v) autoclaved glycerol at - 80°C, in 1.5 mL microcentrifuge tubes. Working cell banks were prepared after growing the plasmid-containing host strain in 100-mL Erlenmeyer flasks containing 30 mL of 20g/L Luria Bertani (LB) selective medium from Sigma Aldrich (LB components: NaCl- 5 g/L; Tryptone- 10 g/L; Yeast extract- 5 g/L) with 30 μ L of 30 μ g_{kanamycin}/mL, for about 6 h at 37°C and 250 rpm in an ARALAB orbital shaker model AGITORB 200, until the cell culture reached around $\frac{3}{4}$ of the exponential phase (Optical Density at 600nm (O.D._{600nm}) \approx 3). All Erlenmeyer flasks containing the LB medium to be used in the cell pre-culture and culture were previously autoclaved at 121°C for 20 min.

3.1.2. Cell culture conditions

Pre-culture of *E. coli* DH5 α cells occurred overnight, after inoculation from the working cell bank, until the exponential growth phase was reached (Appendix I). The conditions used are the same described in 3.1.1 for gene banking. In this phase, the required volume of cells to inoculate the larger 2000 mL Erlenmeyer flask containing 250 mL LB was determined, in order to obtain an initial O.D._{600nm} of 0.2.

The cells were then transferred to 2000mL Erlenmeyer flasks at 37°C and 250 rpm with 250mL LB medium and 250 μ L of the same kanamycin stock solution and the cell culture progressed for approximately 6h before the stationary growth phase was reached (OD_{600nm} \approx 4). Cells were harvested by centrifugation at 6000 rpm for 15min at 4°C in a Sorvall RC6 centrifuge with a SLA 3000 rotor. Supernatants were discarded.

3.1.3. Cell rupture – alkaline lysis

After the cell harvesting, the resultant pellet was resuspended, using vortex, in 8mL of buffer P1 (50mM glucose, 25mM Tris-HCl, 10mM EDTA, pH 8.0). The resultant suspension was transferred to smaller centrifuge tubes (45mL) and alkaline lysis was performed by adding 8mL of P2 solution (0.2N NaOH, 1% SDS), followed by gentle mixing and the tubes were left resting for 10min at room temperature. In order to stop lysis, 8mL of P3 solution (5M potassium acetate, 6.8M glacial acetic acid) were added, followed by gentle mixing and tubes were left resting on ice for 10min. The resultant neutralised alkaline lysate was centrifuged at 13000rpm for 30min at 4°C in a Sorvall RC6 centrifuge with a SS-34 rotor, to remove cell debris and part of the gDNA and proteins. The supernatant was placed in a new tube and centrifuged again with the same settings as before, to remove the remaining

debris. The resulting pDNA-containing lysate (the final supernatant) was stored at -20°C until further processing^{[74], (xi)}.

3.2. Plasmid DNA primary purification

The precipitation of nucleic acids (pDNA, RNA and traces of gDNA) was performed by adding 16.8mL of 100% (v/v) 2-propanol to the resulting pDNA-containing lysate and, after gentle mixing, this was left at 4°C for at least 2h. Thereafter, this mixture was centrifuged under the same conditions described in section 3.1.3 and the supernatant was discharged. The pellet was washed with 2mL of 70% (v/v) ethanol and centrifuged again with the same settings as before. The supernatant was discharged and the tube was inverted on top of absorbent paper, to collect the primarily purified pDNA without any traces of ethanol. The pellet was then dissolved in 6mL of 10mM Tris-HCl pH 8.0 in a 45mL centrifuge tube by gentle mixing and later mixed with 1.44g of ammonium sulphate. The solution rested on ice, for 10min, to eliminate the remaining impurities by precipitation. The mixture was then centrifuged at 13300rpm and 4°C for 45min and the supernatant transferred to a 15mL falcon tube and stored at -20°C until further processing^{[74], (x)}.

3.3. Plasmid DNA final purification

3.3.1. Hydrophobic interaction phenyl membrane chromatography

The membrane adsorber Sartobind® Phenyl Nano units of 3mL bed volume, bearing phenyl moieties at its surface, were provided by Sartorius AG and connected to an Äkta™ Purifier 10 FPLC system from GE Healthcare (Sweden), which continuously monitored the conductivity and UV absorbance at 260 nm.



Figure 19 - Sartobind® Phenyl Nano module for membrane hydrophobic interaction chromatography. ^(xii)

Chromatographic runs were performed at a flow rate of 1 mL.min⁻¹ as described by Raiado-Pereira^[75]. Fractions were collected from the eluted peaks and then kept at -20 °C for further concentration and diafiltration steps, followed by agarose gel analysis. 1.8 M (NH₄)₂SO₄ in 10 mM Tris-HCl pH 8.0 was used as binding buffer (BB) and 10 mM Tris-HCl pH 8.0 as elution buffer (EB).

^(xi) Gomes, A.G. Plasmid DNA purification by HIC and SEC, BERG Protocols, Instituto Superior Técnico; (2008).

^(xii) <http://www.sartorius.com/en/product/product-detail/96hicp42euc11-a/>

3.3.2. Elution profile

The membrane module was used with a step elution profile. A volume of 5 mL of a pre-purified pVax1/GFP solution, obtained as described in section 3.2 ($>200\text{ng}/\mu\text{L}$), was injected into the membrane adsorber at $1\text{ mL}\cdot\text{min}^{-1}$ and allowed to flow through for 15 min, leading to the clearance of unbound solutes. Then a 20 mL long (20 min) gradient from 0 to 40 % EB was applied followed by a step change in conductivity from 40 % to 100 % EB that also runs through for 20 mL.

Membrane chromatography was therefore used to selectively elute the plasmid isoforms. Ideal chromatogram of a pDNA purification process is represented in Figure 20. This type of chromatogram was the basis to achieve purified super coiled pDNA.

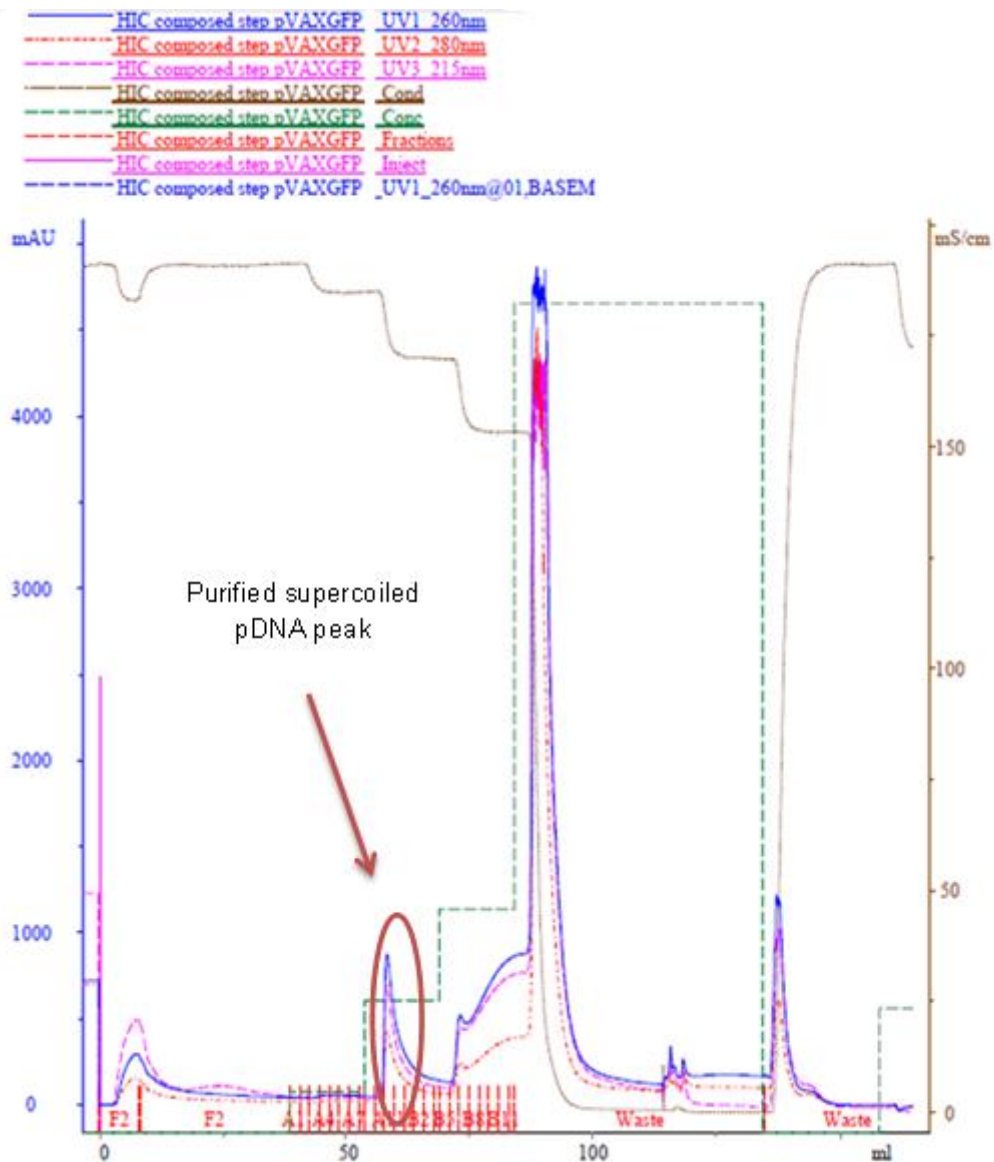


Figure 20 – Chromatogram obtained from a hydrophobic interaction chromatography process for pDNA purification, using a Sartobind® phenyl membrane. Components are eluted according to their hydrophobicity, allowing their separation. Only the fractions corresponding to purified supercoiled pDNA peak are then used for complexation assays with chitosan solutions.

3.3.3. Concentration and diafiltration of pDNA

The fractions collected from the eluted peaks ($V \approx 12\text{mL}$) were concentrated to a final volume of 0.3mL and desalted in a swing bucket rotor for 5min at 4000rpm and 4°C in a 2mL Amicon® Ultra centrifugal filters (Milipore, Ireland) bearing a 50kDa Ultracel® cellulose membrane. The diafiltration step was performed by adding 10mM Tris-HCl pH 8.0 in 5 times the volume present in the Amicon ($V \approx 1.5\text{mL}$) followed by a centrifugation step using the same settings as before^[75]. Recovery of concentrated pVax1/GFP was achieved by turning the Amicon upside down and centrifuging it again under the same conditions.

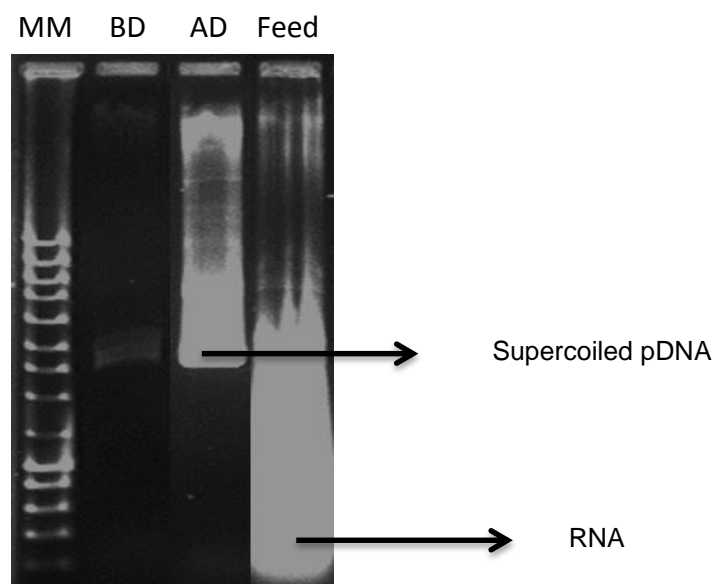


Figure 21 – 1% agarose gel electrophoresis from the supercoiled pDNA fractions collected after HIC procedure was performed during $1\text{h}30$ at 100V . MM – molecular weight marker (NZY DNA ladder III) – more information on Appendix II; BD – pDNA collected fractions (before concentration and desalting); AD – pDNA collected fractions (AD); Feed – Lysate before HIC procedure (contaminated - RNA)

After purification, the final plasmid DNA concentration ($\approx 200\text{ng}/\mu\text{L}$) was measured on NanoVuePlus equipment (General Electric Healthcare, UK). Purified pDNA ($2\mu\text{L}$) was used and the equipment was firstly equilibrated with $2\mu\text{L}$ of MiliQ H_2O . Agarose gel electrophoresis was performed, in order to assess the quality of purified pDNA (Figure 21).

3.4. Preparation of chitosan and pDNA nanoparticles

High purity chitosans with different molecular weights (low molecular weight (LMW) $60\text{--}120\text{kDa}$; medium molecular weight (MMW) $110\text{--}150\text{kDa}$; high molecular weight (HMW) $140\text{--}220\text{kDa}$) as well as high purity glycol chitosan were purchased from Sigma-Aldrich® (St. Louis, USA). 5mg of each chitosan were dissolved in 5mL filtered/non-filtered 50mM acetic acid solution with $\text{pH} \approx 3.0$, overnight at 50°C in a hybridization oven/shaker (General Electric Healthcare, UK). This acetic acid solution was prepared from a glacial acetic acid stock solution.

Before the first characterization of the suspensions in a Zetasizer Nano ZS (Malvern, UK), discussed in the following Chapter 3.5, sonication during 5min at 50W with a pulse of 5sec and 10sec between pulses with a sonifier sonoplus (Bandelin, Berlin Germany) was/was not performed.

The goal was to study the effect of both filtration and sonication in chitosan particles properties (diameter size and zeta potential) as well as on their time stability.

Self-assembly of chitosan nanoparticles with pVAX1GFP was made by simple and quick mixing of both solutions in 1.5mL test tubes, followed by 30s vortex and incubation for 30min at room temperature to stabilize the polyplexes. The final volume of the mixture in each preparation was limited to below 500µL, aiming to yield uniform nanoparticles. Different nitrogen to phosphate charge ratios (N/P ratios = 5, 10, 20, 50 and 70) were tested and the pDNA mass added was fully dependent on those ratios, as well as on pDNA concentrations in the purified and concentrated fractions. The chitosan solution mass was fixed at 100µg. N/P is expressed as the ratio of moles of the amine groups of chitosan to the phosphate ones of pDNA.

$$N(\text{amine moles}) = \frac{m \text{ chitosan (g)}}{MW \text{ glucosamine residue } \left(\frac{\text{g}}{\text{mol}}\right)} \quad \text{Eq. 3}$$

$$V_{pDNA}(\mu\text{L}) = \frac{N(\text{mol}) \cdot MW \text{ nucleotide } \left(\frac{\text{ng}}{\text{mol}}\right) \cdot N/P}{C_{pDNA} \left(\frac{\text{ng}}{\mu\text{L}}\right)} \quad \text{Eq. 4}$$

$$P(\text{phosphate moles}) = \frac{C_{pDNA} \left(\frac{\text{ng}}{\mu\text{L}}\right) \cdot V_{pDNA}(\mu\text{L})}{MW \text{ nucleotide } \left(\frac{\text{ng}}{\text{mol}}\right)} \quad \text{Eq. 5}$$

In Eq. 4, m represents the mass (g) of chitosan used in complexation procedures and MW is the molecular weight of chitosan glucosamine residues which is equal to 231 g/mol.

In Eq.5 and Eq.6, V_{pDNA} (µL) is the volume of pDNA necessary to prepare complexes at a certain N/P ratio, N is the number of amine moles in chitosan, P is the number of phosphate moles in pDNA, MW is the nucleotide molecular weight (≈330 g/mol) and C_{pDNA} (ng/µL) is the pDNA concentration used in complexation assays. Therefore, pDNA mass varied between 2µg and 28µg.

The time between complexation and characterization was also varied, in order to determine its influence on complexes diameter, zeta potential and stability in solution.

3.5. Preparation of chitosan modified cholesterol and pDNA nanoparticles

For the preparation of this nanoparticles the procedure of Maity and Jana [76] was followed.

Chitosan oligosaccharide lactate (COL) ($M_n \approx 5000$) and cholesteryl chloroformate (CHOL) (97%) were purchased from Sigma-Aldrich® (St. Louis, USA) and used as received. An amount of 60mg (0.012mM) of COL was dissolved in 2 mL of dimethylsulfoxide (DMSO) at room temperature

with gentle mixing. Then, triethylamine solution (120 μ L of triethylamine dissolved in 0.5mL of dichloromethane) was added and stirred for 30min at room temperature. Next, 17mg (\approx 0.038mM) of cholesteryl chloroformate were dissolved in 0.5mL of dichloromethane and added to it for covalent conjugation and the reaction was continued for 3 days at room temperature with gentle stirring. This reaction is represented in Figure 22.

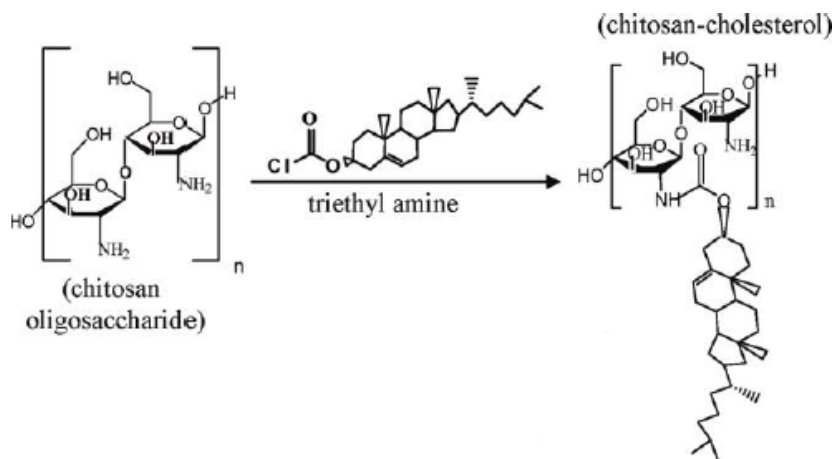


Figure 22 – Scheme showing cholesterol modification of chitosan oligosaccharide lactate [76]

The product was precipitated by centrifugation (10min, room temperature, 4000rpm) and washed with dichloromethane 4 to 5 times, with centrifugation steps (20min, room temperature, 4000rpm) between each wash step. The dried product was then dispersed in water by sonication (5min, 50W, 5s pulse, 10s between pulses) and the pH was adjusted to 3.0 with HCl 1M buffer solution. The dissolution of conjugate was obtained by placing it overnight at 50 $^{\circ}$ C in a hybridizer oven with gentle stirring. The solubilized conjugate was then placed at 4 $^{\circ}$ C until characterization and complexation with pVAX1GFP.

Complexation assays of chitosan-cholesterol conjugate (CHI/CHOL) with the referred pDNA vector were performed as previously stated in Section 3.4 for the other chitosans, except that only N/P ratios of 10 and 50 were tested, before their characterization in Zetasizer Nano equipment.

3.6. Preparation of chitosan modified lecithin and pDNA nanoparticles

The L-A-lysophosphatidylcholine type 1 powder, a modified lecithin (ML), was purchased from Sigma-Aldrich[®] (St. Louis, USA) as well as the LMW chitosan referred in Section 3.4.

Both components were separately dissolved in a previously filtered, with 0,45 μ m membrane, 50mM acetic acid solution with pH \approx 3.0, to a final concentration of 1mg/mL, overnight at 50 $^{\circ}$ C with gentle stirring in a hybridizer oven.

The reaction of positively charged chitosan with anionic ML was performed by simple mixing the two solutions in a molar mixing ratio of 4.9 chitosan molecules per ML molecule, followed by 30s vortex and overnight incubation at room temperature, to stabilize the conjugate^[77]. The complexation of LMW chitosan-ML conjugate with pVAX1GFP was performed, as previously stated in Section 3.4

for the other chitosans, except that only N/P ratios of 10 and 50 were tested, before their characterization in Zetasizer Nano equipment.

3.7. Size and zeta potential characterization

The size and zeta potential of chitosan nanoparticles and of all the formulations tested were measured in a Zetasizer Nano ZS (Malvern, UK). Particle size measurements were made in disposable cuvettes at 37°C to mimic transfection conditions, by non-invasive back scatter, with dynamic light scattering detected at an angle of 173°. One ml samples were used and 1:10 dilutions were performed (900µL buffer + 100µL sample), to avoid multiple scattering phenomenon. In chitosan suspensions the buffer used was 50mM acetic acid pH ≈ 3.0 and for complex preparations a mixture of 50mM acetic acid pH ≈ 3.0 and 10mM Tris-HCl pH ≈ 8.0 was used in the same volume ratio of chitosan per pDNA molecule (N/P ratio dependent).

The effective hydrodynamic diameter was calculated from the diffusion coefficient by the Stokes-Einstein equation (Eq.1) using the method of cumulants. In summary, the cumulants analysis gives a good description of the size that is comparable with other methods of analysis for spherical, reasonably narrow monomodal samples, i.e. with polydispersity below a value of 0.1. For samples with a slightly increased width, mean diameter and polydispersity will give values that can be used for comparative purposes.

Zeta potential measurements were also performed at 37°C using a combination of laser Doppler velocimetry and phase analysis light scattering (PALS). The measured electrophoretic mobilities were converted into zeta potential values using the Smoluchowski approximation. Zeta potential and hydrodynamic diameters are expressed as the mean standard deviation of at least two independent measurements.

After characterization of the chitosan solutions (in acetic acid buffer solution) and chitosan nanoparticles suspensions (already complexed with pDNA), both preparations were stored at 4°C, to avoid pDNA denaturation and complex dissociation.

3.8. Analytical methods

3.8.1. Agarose gel electrophoresis

Several 1% agarose gel electrophoresis were performed during this study, in order to visualize some of the results obtained. The conditions used in each electrophoresis will be given in the respective Figure caption. After electrophoresis procedure, all agarose gels were placed for 15min in contact with Ethidium Bromide and washed for 5min with MiliQ water before visualization in Eagle Eye™ II (Stratagene).

3.9. Chinese hamster ovary cell culture

In vitro expansion of CHO cells was performed in a T-75 culture flask with 10 mL of Dulbecco's Modified Eagle Medium (GIBCO High Glucose, +Pyruvate, +Glutamine, -HCO₃⁻) supplemented with 10% Fetal Bovine Serum (FBS from GIBCO, heat inactivated) and 1% penicillin and streptomycin (PenStrep from GIBCO). The cell cultures were inoculated at a concentration of 1.5×10^6 cells/mL and incubated in 5% CO₂ at 37°C. When the cells reached a confluency of about 80%, they were passed to a new T-75 flask or seeded on 24-well plates for transfection. The cells were passed by washing them in the T-75 flask with 10 mL phosphate buffer saline (PBS) and then by adding 4 mL of 0.05% trypsin-EDTA solution and incubating at 37°C for 6 min, in order to remove the adherence of the cells to the T-75 flask surface. After this incubation period, 6 mL of DMEM supplemented with 10% FBS and 1% PenStrep were added to the T-75, in order to stop the action of trypsin. Otherwise, trypsin would become toxic for the cells which would lose viability. The cells were resuspended with a 10-mL pipette to detach them and then transferred to a 15-mL falcon tube and centrifuged in a conventional bench top centrifuge (5min, 1500g, room temperature). After centrifugation, the supernatant was discarded and the cell pellet carefully washed with a small amount of PBS, to remove any traces of trypsin. Then, the cell pellet was resuspended in 10 mL DMEM supplemented with 10% FBS and 1% PenStrep and cells were counted in a hemocytometer and checked for viability using the Trypan Blue Dye (GIBCO). The volume containing the desired amount of cells was transferred either to a T-75 or to a 24-well plate and DMEM supplemented with 10% FBS and 1% PenStrep was added up to the top volume.

3.10. *In vitro* transfection of CHO cells

CHO cells were seeded 24 h prior to transfection into a 24-well tissue culture plate at a density of $\approx 10^5$ cells/mL, to obtain a confluence of 80-90% on the day of transfection. At the time of transfection, the cells were washed with 500 μ L of PBS to remove dead cells and toxins. The amount of polyplexes, which is dependent on N/P ratio tested, was added to each well. DMEM without FBS and antibiotics was added to a final volume of 500 μ L and incubated with the cells for a certain period of time (1h, 3h or 6h). After incubation, the medium was changed, the cells were washed in PBS, and 500 μ L of the complete medium (DMEM supplemented with 10% FBS and 1% PenStrep) were added to each well. The transfection experiments were performed in duplicate. Cells without contact with any kind of particles were used as negative control. Cells transfected with Lipofectamine 2000™-DNA complexes were used as positive controls of the transfection (1 μ g pDNA). The transfection efficiency was evaluated using flow cytometry analysis after 24h or 48h of transgene expression.

3.11. Flow cytometry analysis (FACS)

After 24h or 48h of transgene expression, the cells were washed with 500 μ L PBS and trypsinized for 5 min at 37°C. Afterwards, complete medium was added to stop the action of trypsin

and the cells were centrifuged in a conventional bench top centrifuge (5min, 1500g, room temperature). After centrifugation, the supernatant was discarded and the cell pellet was carefully washed with a small amount of PBS, to remove any traces of trypsin. Then, the cell pellet was resuspended in 1mL of ice-cold PBS supplemented with 4% FBS and kept on ice until analysis. The equipment used was a FACScan Scalibur (Becton-Dickinson, NJ, USA), which recorded the forward scatter (FSC), side scatter (SSC) and green fluorescence (FL1) in each run.

Data were analyzed and green fluorescence intensity corresponding to GFP expression level, histograms and dot plots (Figure 23) were generated with CellQuest Pro Software © (Becton Dickinson, NJ, USA).

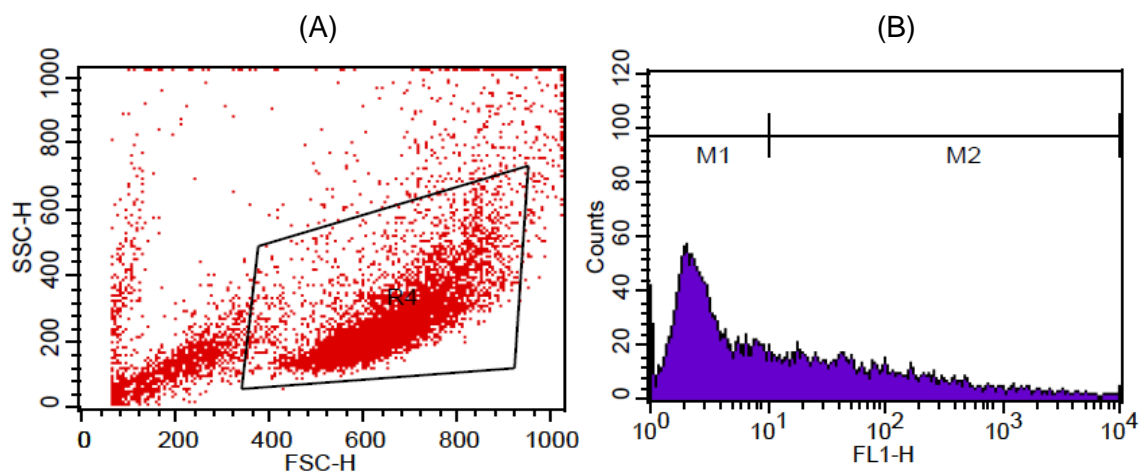


Figure 23 – Example of dot plot (A) and histogram (B) generated by CellQuest Pro Software © (Becton Dickinson, NJ, USA).

Therefore, for each sample, cells were isolated from the debris due to their characteristics of FSC versus SSC, which defined a gate that distinguished cells from any debris outside the gate. The background autofluorescence of non-transfected cells was taken into account, to determine transfection efficiencies, considering the difference between the total cell population inside the gate, and the background autofluorescence of non-transfected cells, indicated by FL1 parameter. This established the M1 and M2 parameters, corresponding to non-transfected and transfected cells with respectively^[78].

4. Results and discussion

4.1 Preparation and characterization of chitosan particles in solution

The stability of chitosan particles in suspension, namely regarding their diameter, zeta potential and polydispersity index is an important factor that has to be determined before complexation assays with the active ingredient pVAX1GFP.

Preparation of those suspensions is then crucial, to achieve such stability. The influence of sonication on chitosan particles features was studied and is represented in Figures 24 (A and B).

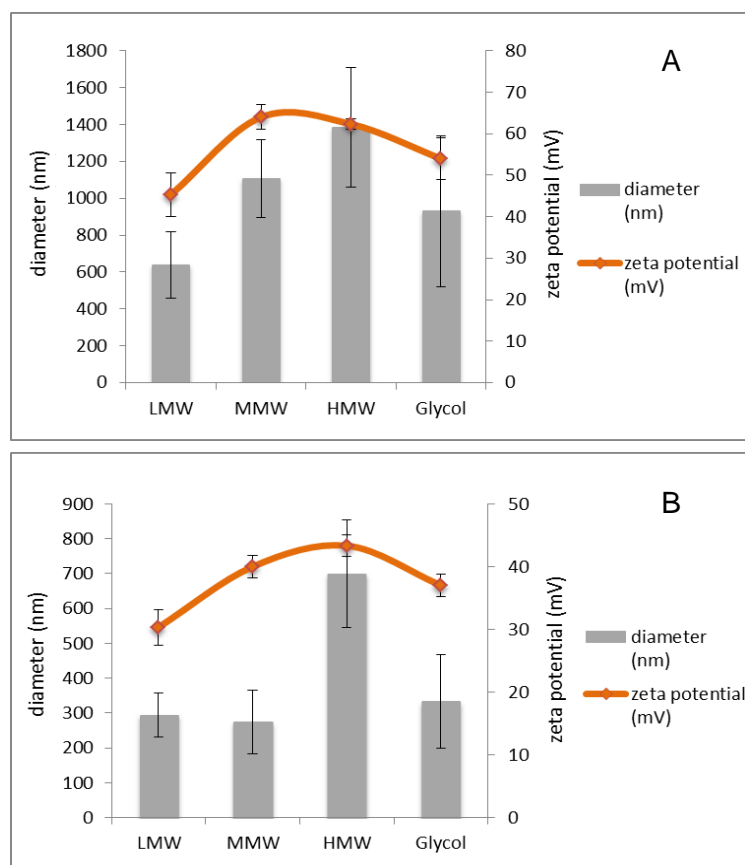


Figure 24 – Effect of sonication in diameter (nm) and zeta potential (mV) of low (LMW), medium (MMW) and high (HMW) molecular weight and glycol chitosan. A – non sonicated suspensions; B – sonicated suspensions. The values are representative of a mean of five independent measurements. All samples were 10-fold diluted in 50mM acetic acid buffer pH 3.0 before characterization.

It is visible that, after sonication (B), both diameter and zeta potential of chitosan particles in suspension decrease, when compared to non-sonicated particles (A). Non-sonicated samples show diameters in micrometres range, while sonicated particles show nanometre range diameters. This is due to shear stress, which is resultant from the application of ultrasound energy that promotes a shear on chitosan molecules, impairing aggregation, thus, avoiding the formation of larger particles. This is an important feature to enhance the transfection efficiency of the posteriorly made chitosan/pDNA complexes.

High molecular weight particles showed higher diameter and zeta potential values, before and after sonication, due to the presence of more repeated units (n) in the molecule.

A prerequisite to achieve an enhancement of the bioavailability with nanoparticles is that these must be finely dispersed in a liquid and do not aggregate. In the event of aggregation, the bioavailability decreases with intensification of aggregation and with the increase of nanoparticles diameter. This is attributed to the fact that the higher the particles volume, the smaller is their total superficial area available to adhere to the mucosal wall.

Therefore, it is necessary to prepare nanosuspensions relatively stable. The effect of sonication in diameter and zeta potential stability of chitosan particles has also been evaluated for 34 days (Figures 25 A and C) and for 14 days (Figures 25 B and D), respectively.

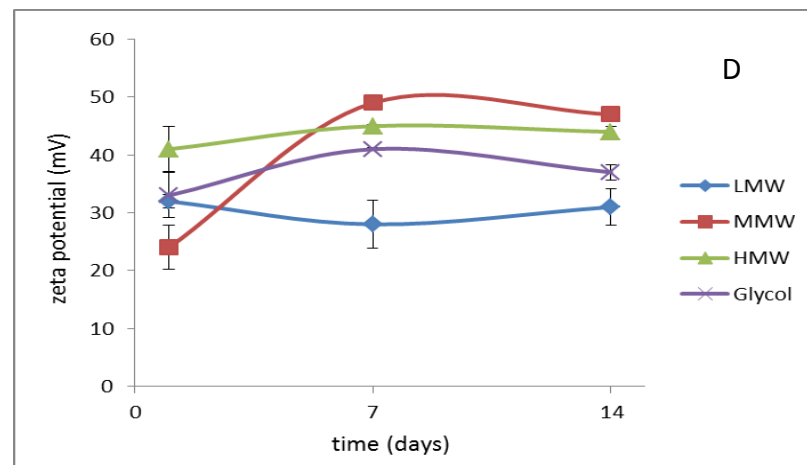
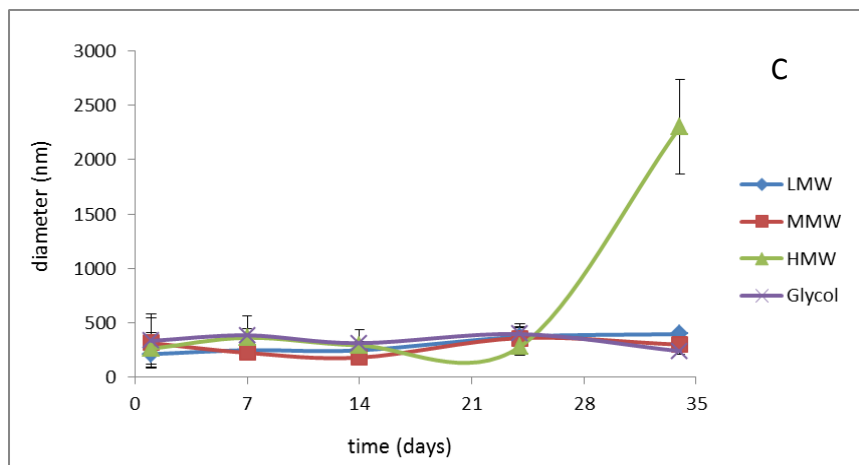
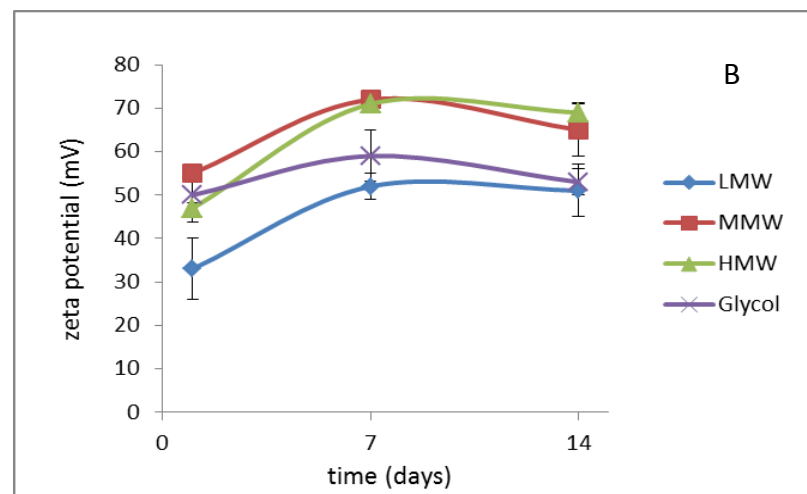
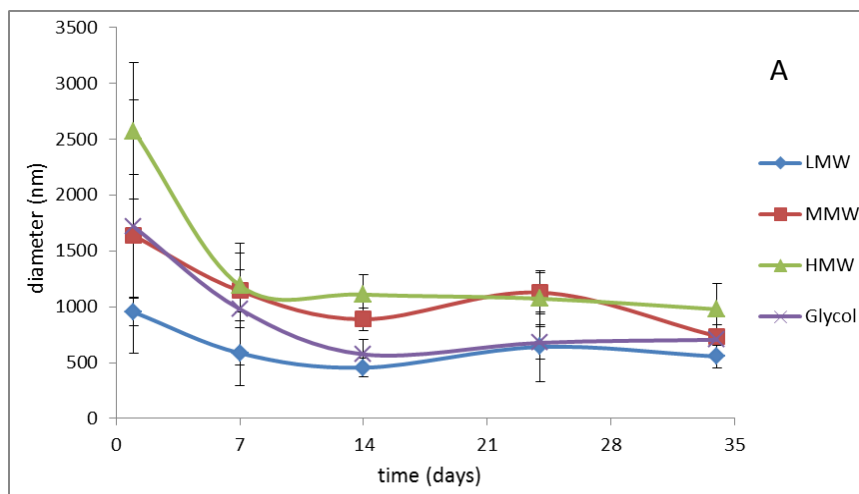


Figure 25 – Evaluation of diameter (A;C) and zeta potential (B;D) stability along time of different chitosan suspension preparations. A and B represent a non-sonicated sample, while C and D represent a sonicated sample at 50W for 5min. LMW, MMW, HMW and Glycol are, respectively, low, medium, high molecular weight and glycol chitosan. Mean values of at least two measurements. Standard deviation values are represented in Appendix III.A and III.B. All samples were 10-fold diluted in 50mM acetic acid pH 3.0 before characterization.

From analysis of Figure 25, it is notorious that sonication plays an important role in physical stability of chitosan particles in suspension. Both diameter and zeta potential values of sonicated sample (C and D) show less variation along time, when compared to those values for non-sonicated sample (A and B). The dispersion of the particles in the surrounding medium is then essential, to avoid aggregation or sedimentation phenomena.

However, the diameter of high molecular weight chitosan particles increases almost 10-fold at 34 days after preparation (Figure 25 C). The stability of these particles is affected by aggregation phenomenon that starts to occur about one month after their preparation and bioavailability of those same particles is then reduced^[79].

The effect of sonication in polydispersion index (Pdi) was also determined (Appendices III.A and III.B). The Pdi measures the heterogeneity of sizes of molecules or particles in suspensions. A higher Pdi value is indicative of the presence of other substances besides the nanoparticles or of the presence of nanoparticle aggregates, which also increase the estimated average diameter. The application of ultrasound energy seems to homogenize the chitosan particles in suspension, since Pdi values decrease when sonication is applied.

The chitosan particles concentration in the DLS cell is another important parameter for an accurate estimation of diameter and zeta potential as it may affect dynamic light scattering and electrophoretic mobility measurements. All the chitosan particles in suspension were 10-fold diluted (100µL of suspension + 900µL of 50mM acetic acid buffer pH ≈ 3.0), to avoid multiple scattering effect.

The effect of buffer filtration on chitosan particles characteristics was also tested and can be analysed by comparing Figures 24 B (filtered) and 26 (non-filtered). The chitosan suspension should not be filtered because filters can remove it by absorption as well as physical separation, except if larger sized particles such as agglomerates are present^(xiii). However, as this is a comparative analysis to determine the ideal method for preparation of chitosan nanoparticles, only buffer filtration was performed.

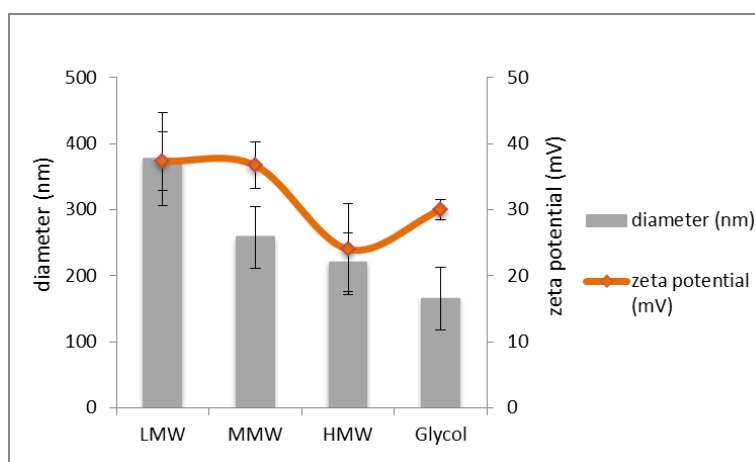


Figure 26 – Evaluation of diameter (nm) and zeta potential (mV) of low (LMW), medium (MMW) and high (HMW) molecular weight and glycol chitosan where buffer (50mM acetic acid pH 3.0) was not filtered. The values are representative of a mean of five independent measurements. All samples were 10-fold diluted before characterization.

^(xiii) Zetasizer Nano Series User Manual. MAN 0317 Issue 1.1 Feb . 2004 (Malvern Instruments Ltd.)

Insignificant diameter and zeta potential value changes were observed for LMW, MMW and Glycol chitosans, while both values decrease significantly in HMW chitosan. This might be due to dust interference during DLS and EM measurements.

Filtration process also affects the Pdi of the particles in solution, because it removes dust particles present in acetic acid buffer that could contaminate the sample, thus increasing particles diameter heterogeneity (Appendixes III.B and III.C).

The effect of buffer filtration in the stability of diameter and zeta potential of chitosan particles has also been evaluated for 34 days (Figure 27 A) and 14 days (Figure 27 B) – buffer non-filtered - and can be analysed by comparison with Figures 25 C and D, respectively – buffer filtered.

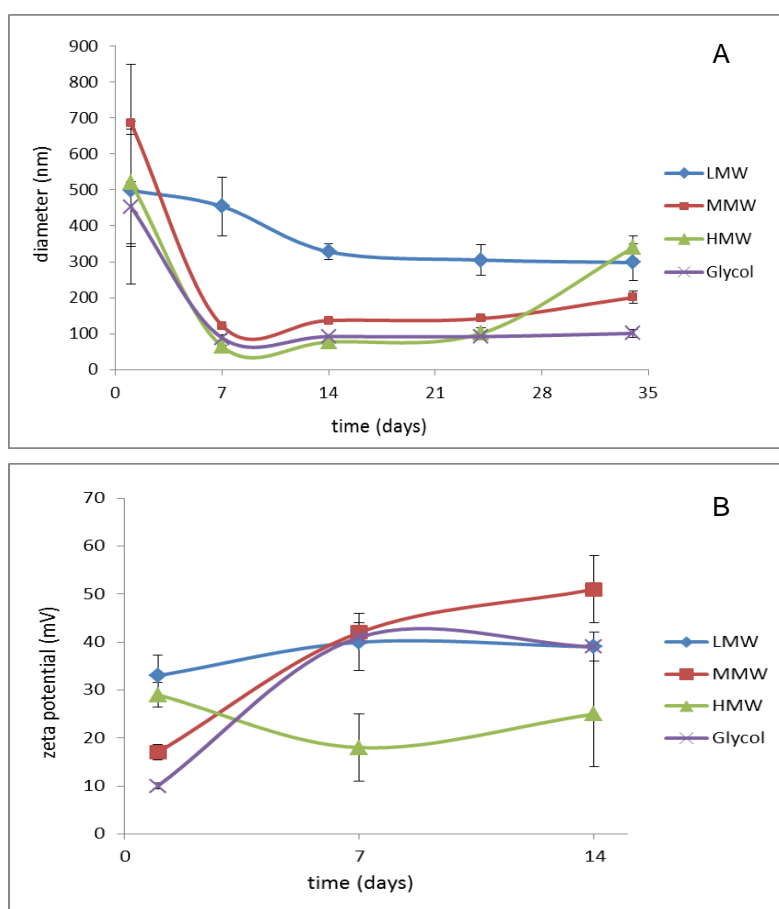


Figure 27 - Evaluation of diameter (A) and zeta potential (B) stability along time of different chitosan suspension preparations. A and B are representative of preparations in which 50mM acetic acid buffer was not filtered but the sample was sonicated and 10-fold diluted before characterization. LMW, MMW, HMW and Glycol are, respectively, low, medium, high molecular weight and glycol chitosans. Mean values of at least two measurements. Standard deviation values are represented in Appendix V.

The diameter stability of LMW, MMW and glycol chitosan particles was only obtained 14 days after their preparation, while for HMW chitosan particles this stability was not achieved as it might be noticed by diameter oscillation represented in Figure 27 A.

Stability of LMW chitosan particles in acetic acid buffer showed to be the one that is less influenced by buffer filtration process, probably due to the lower number of repeated units (n) in chitosan molecules.

Filtration of buffer solution in which the particles will be suspended is of extreme importance for their physical stability along time, because the presence of dust residues negatively affects the DLS and EM measurements.

4.2. Preparation and characterization of chitosan/pDNA nanoparticles

After testing the stability of chitosan particles in suspension, some of them were chosen to perform complexation assays with previously produced and purified pVAX1GFP plasmid.

Regarding the molecular weight, buffer filtered and sonicated LMW chitosan was the solution that showed lower diameter values and higher diameter and zeta potential time stability, important parameters to achieve an efficient transfection process. Glycol chitosan, which showed small diameters and relatively high stability along time, was also chosen to determine if this chemical modification in chitosan structure had any influence on complexation efficiency.

In the first complexation assay, chitosan particles in suspension were prepared 15 days before the assay. N/P ratios tested were 5, 10, 20 and 50 and pVAX1GFP concentration was fixed in 75ng/ μ L. This concentration was chosen after preliminary tests with different concentrations (results not shown).

To confirm if complexation of chitosan and pDNA was achieved, agarose gel electrophoresis was performed (Figure 28).

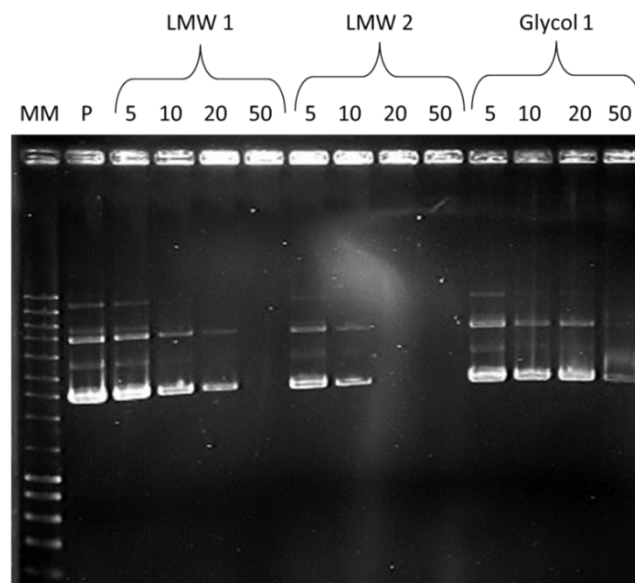


Figure 28 – 1% agarose gel of polyplexes. 2 μ L of loading buffer were added to 10 μ L of sample. Electrophoresis ran for 1h30 at 120V and ethidium bromide was used to stain the samples. MM – molecular marker NZYladderIII (6 μ L); P – pVAX1GFP (negative control); 5, 10, 20 and 50 are the N/P ratios tested; LMW1 – low molecular weight chitosan sonicated and filtered; LMW 2 – low molecular weight chitosan non-sonicated but filtered; Glycol1 – glycol chitosan sonicated and filtered.

It is notorious that complexation of pDNA with these chitosan particles, at the referred conditions, was not completely achieved, meaning that pDNA encapsulation efficiency was not total.

Regarding LMW1 complexes, N/P ratio of 50 was the only one in which pDNA was completely complexed with the chitosan particles, because no migration is observed in the gel and the intensity of light in the well is higher, when compared to other LMW1 samples and to negative control (P). This

might be due to lower pDNA volume added in complexation assay due to higher N/P ratio used. As pDNA is complexed with chitosan particles through electrostatic and hydrophobic interactions or hydrogen bonds between organic bases of nucleotide and sugar structure of polymer, it will not migrate in the gel and the light intensity, given by the intercalation of ethidium bromide in pDNA double strand and exposure to UV light, will be higher in gel wells.

These results are concordant with the ones previously reported by Yang and co-workers^[80], where higher N/P ratios give rise to higher affinities between chitosan and pDNA, since one pDNA molecule would be in contact with a higher number of chitosan molecules, than in lower N/P ratios. These particles should not promote high transfection efficiencies since DNA release in cytosol would be more difficult.

The formation of polyplexes using LMW2 chitosan particles was only totally achieved for N/P ratios of 20 and 50, meaning that sonication process can also influence complexation efficiency, as previously stated.

In glycol chitosan particles, pDNA encapsulation efficiency was relatively low for each N/P ratio tested. The presence of more OH groups in the surface of chitosan molecule seems to make the interaction between it and the previously purified pVAX1GFP more difficult.

Diameter and zeta potential stability of the referred complexes was tested and is represented in Figures 29 A and B and 30.

Regarding LMW1 complexes (Figure 29 A), all showed stable zeta potential values although the only one where this value is positive was for N/P ratio of 50. Diameter stability 3 days after complexation was achieved for N/P ratios of 5 and 50.

Also, by analysing the table present in Appendix IV.A, the number of particles present in Zetasizer measurements was higher than 1000 only for N/P ratios of 5 and 50, indicating that N/P 10 and 20 complexes were probably dissociating, which might explain the decrease in both diameters. In the same table the Pdi values which are higher than 0.35 are also represented, indicative of low homogeneous particle sizes.

It can be concluded that none of these complexes are suitable for cell interaction and internalization.

LMW2 complexes (Figure 29 B) presented different physical stability. N/P ratio of 5 was the only one which did not achieve diameter and zeta potential stability during the 3 days measurements. Also, N/P ratio of 10, 20 and 50 showed relatively homogeneous particles in size and a number of particles higher than 1000, then suitable for DLS and EM measurements (table in Appendix IV.A). These complexes are already suitable for transfection assays, although their diameters are still quite large ($\approx 500\text{nm}$ to $\approx 800\text{nm}$).

The results from stability assays of glycol chitosan at different N/P ratios are represented in Figure 30. Regarding diameter analysis, N/P 5, 20 and 50 showed relative stability in 50mM acetic acid pH 3.0 plus 10mM Tris-HCl pH 8.0 buffer, while N/P 10 complex diameter decreased daily. The number of these particles was determined to be less than 1000 (table in Appendix IV.A), probably indicating a complex dissociation, which also explains the decrease observed in diameter values.

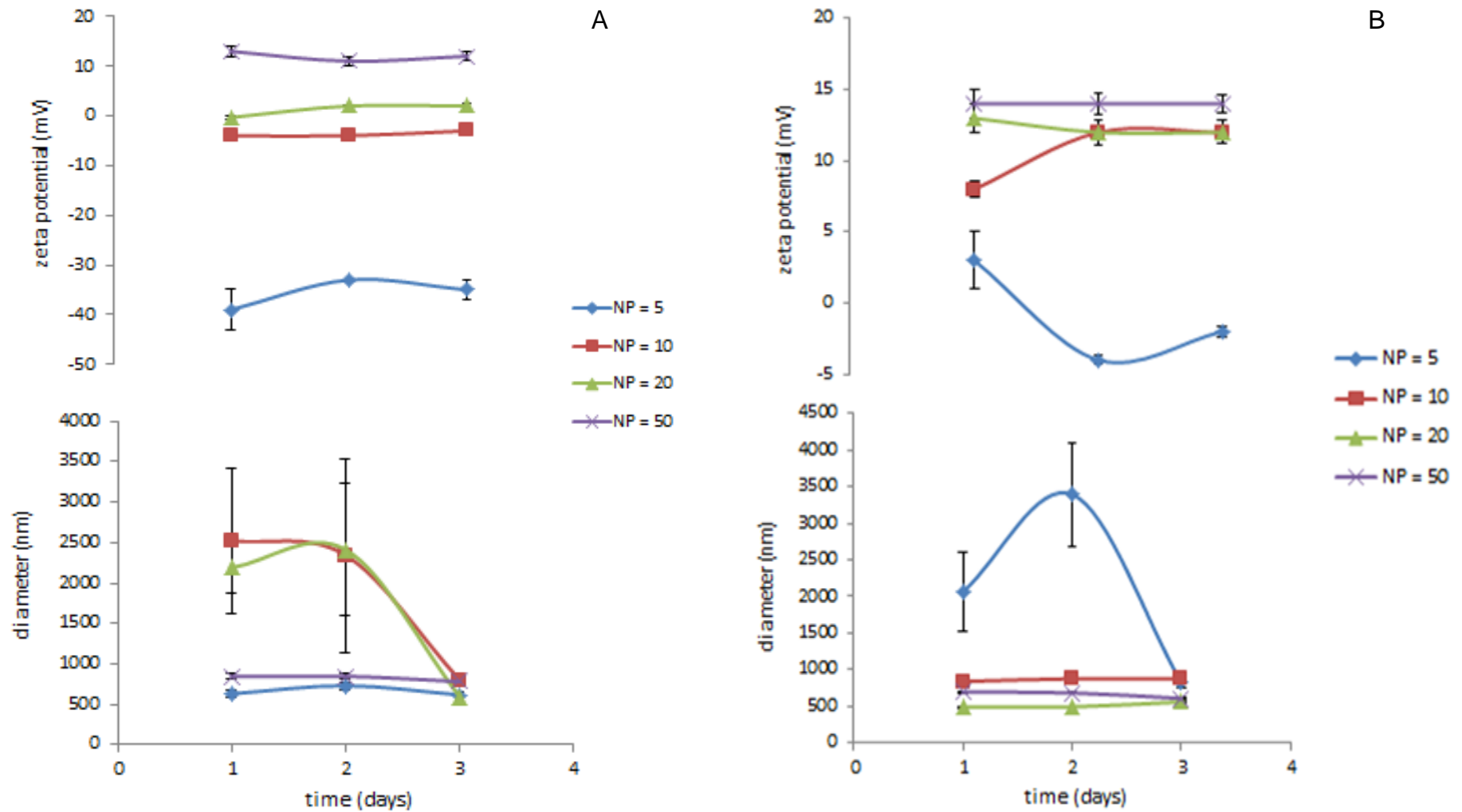


Figure 29 – Evaluation of diameter and zeta potential stability during 3 days of different chitosan and pDNA complexes at different N/P ratios (5, 10, 20 and 50). A – LMW1 chitosan (sonicated and filtered) complexes; B – LMW2 chitosan (non-sonicated and filtered) complexes. Each point is representative of a mean of at least three measurements.

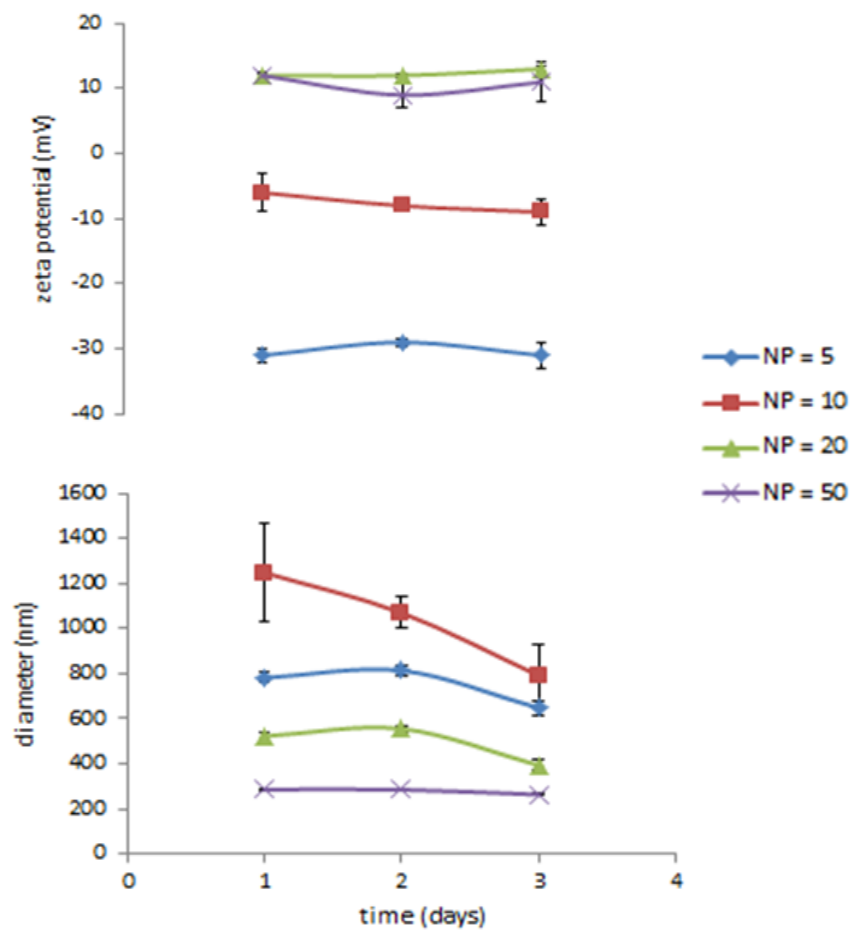


Figure 30 - Evaluation of diameter and zeta potential stability during 3 days of glycol1 chitosan (sonicated and filtered) and pDNA complexes at different N/P ratios (5, 10, 20 and 50). Each point is representative of a mean of at least three measurements.

The Pdi values (table in Appendix IV.A) of N/P 5 and 20 complexes showed to be higher than 0.35, indicative of low homogeneous particle sizes, while for N/P 50 this value is around 0.30.

Analysing the zeta potential values, stability is observed for all the tested polyplexes. However, N/P of 5 presented negative values. This might be resultant from the fact that complexation was not total (gel of Figure 28) and negative charges of pDNA stayed in particles surface, leading to negative zeta potential values of around -30mV, that will prevent interaction with the negatively charged cell membrane.

Therefore, only the N/P 50 complexes have the desirable characteristics to be used in transfection assays.

Another device that allows assessing the quality of the samples is the correlator. It measures the degree of similarity between two signals or one signal itself at varying time intervals. The size distribution obtained is a plot of the relative intensity of light scattered by the particles, arising from their Brownian motion, in various size classes and is therefore known as an intensity size distribution.

A correlator that compares the quality of all the complexes tested and previously characterized is represented in figure 31.

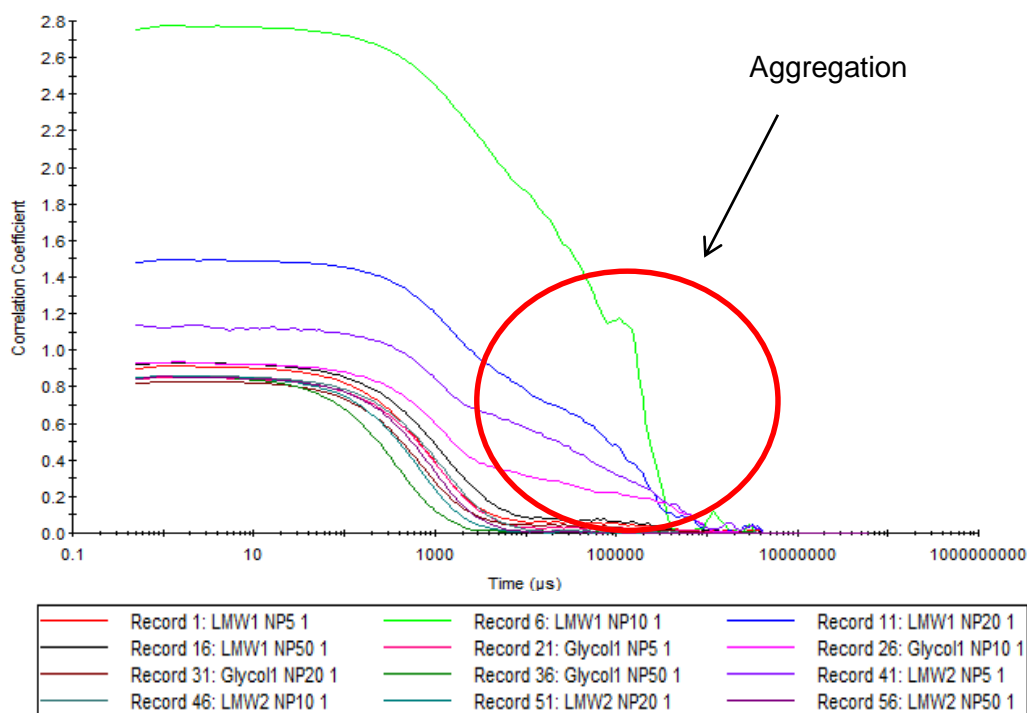


Figure 31 – Representation of one diameter size measurement of each polyplex tested in the first complexation assay.

It has been seen that particles in dispersion are in constant, random Brownian motion and that this causes the intensity of scattered light to fluctuate as a function of time. The correlator will construct the correlation function $G(\tau)$ of the scattered intensity:

$$G(\tau) = \langle I(t).I(t + \tau) \rangle \quad \text{Eq. 6}$$

where τ is the time difference (the sample time) of the correlator. For a large number of monodisperse particles in Brownian motion, the correlation function (given the symbol [G]) is an exponential decaying function of the correlator time delay τ :

$$G(\tau) = A[1 + B \exp(-2\Gamma \tau)] \quad \text{Eq. 7}$$

where A = the baseline of the correlation function, B = intercept of the correlation function.

$$\Gamma = Dq^2 \quad \text{Eq. 8}$$

where D = translational diffusion coefficient and

$$q = (4 \pi n / \lambda_0) \sin (\theta/2) \quad \text{Eq. 9}$$

where n = refractive index of dispersant, λ_0 = wavelength of the laser, θ = scattering angle. For polydisperse samples, the equation can be written as:

$$G(\tau) = A[1 + B g_1(\tau)^2] \quad \text{Eq. 10}$$

where $g_1(\tau)$ = is the sum of all the exponential decays contained in the correlation function.

Analysing the auto correlator, used to compare the quality of the polyplexes, it is notorious that are four complexes (LMW1 NP10, LMW1 NP20, LMW2 NP5 and Glycol NP10) with different behaviours from the others. These four complexes presented higher diameter values due to the formation of aggregates, which can be identified by the long tail in the end of the measurement and corroborated by the results in Figures 29 A, B and 30.

Also, these four chitosans presented the higher Pdi values that can be identified by the slope of the curves in the correlogram and confirmed by the values in table of Appendix IV.A.

It is important to refer that the diameter values represented so far are resultant from intensity cumulant analysis. If the plot of this analysis shows a substantial tail or more than one peak, then Mie theory can make use of the input parameter of sample refractive index to convert the intensity distribution to a volume distribution. This will give a more realistic view of the importance of the tail or second peak present^(xiv). The volume distribution of one measurement of each polyplex studied in the first complexation assay is represented in picture 32.

^(xiv) Dynamic Light Scattering: an introduction in 30 minutes. Malvern Instruments, UK.

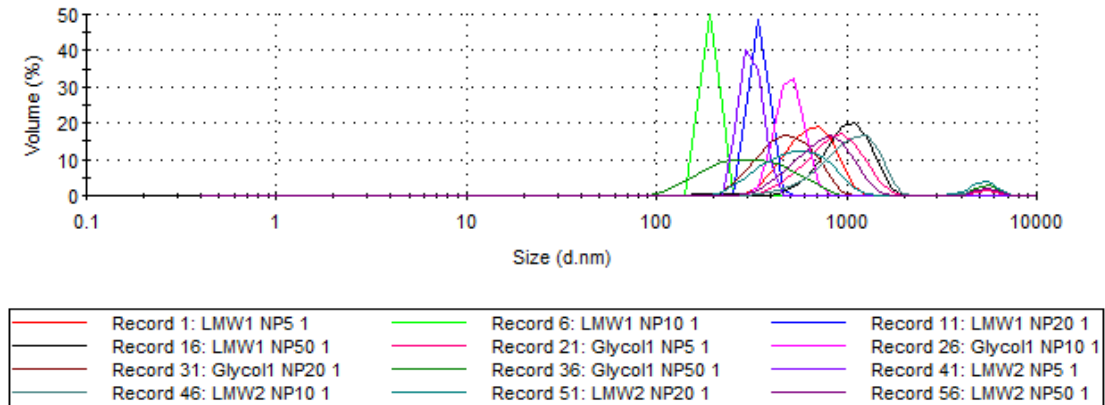


Figure 32 – Volume distribution of polyplexes formed in the first complexation assay. Identification of the peaks is represented below the graphic. Results obtained from one measurement of each polyplex.

Analysing volume distribution, the presence of two volume peaks in each polyplex measurement is visible. However, the second peak (near 10000nm) represents a small percentage of the distribution (below 10%) and, for that reason, this peak was ignored and intensity analysis was preferentially analysed.

The results of volume distribution are concordant with those obtained in correlogram analysis, since the same four complexes (LMW1 NP10, LMW1 NP20, LMW NP5 and Glycol NP10) showed different behaviour from the others, consisting with samples not suitable enough for DLS and EM measurements and consequently for transfection assays.

A second complexation test was performed with the same polyplexes, with the difference that the preparation of chitosan particles in suspension was made on the same day of this assay. The former studies were undertaken with 15-days old CHI solutions. High molecular weight (HMW) chitosans were also tested. The N/P 5 complexes, which showed inconsistent results in the first assay, were substituted by N/P 70 complexes. To confirm if complexation of chitosan and pDNA was achieved, agarose gel electrophoresis was performed (Figure 33).

Analysing the agarose gel it is notorious that the efficiency of pDNA complexation with the chitosan particles is higher than the one obtained in the first assay, since less pDNA migration is observed. However, in glycol chitosan this complexation was not 100% achieved for every N/P ratios tested, because additional OH groups in chitosan molecule probably interfere and make the interaction between pDNA and this natural cationic polymer more difficult.

Regarding HMW chitosan complexes, not tested in the first assay, the complexation efficiency with pDNA is almost total, meaning that the molecular weight of chitosan does not have much influence on this efficiency.

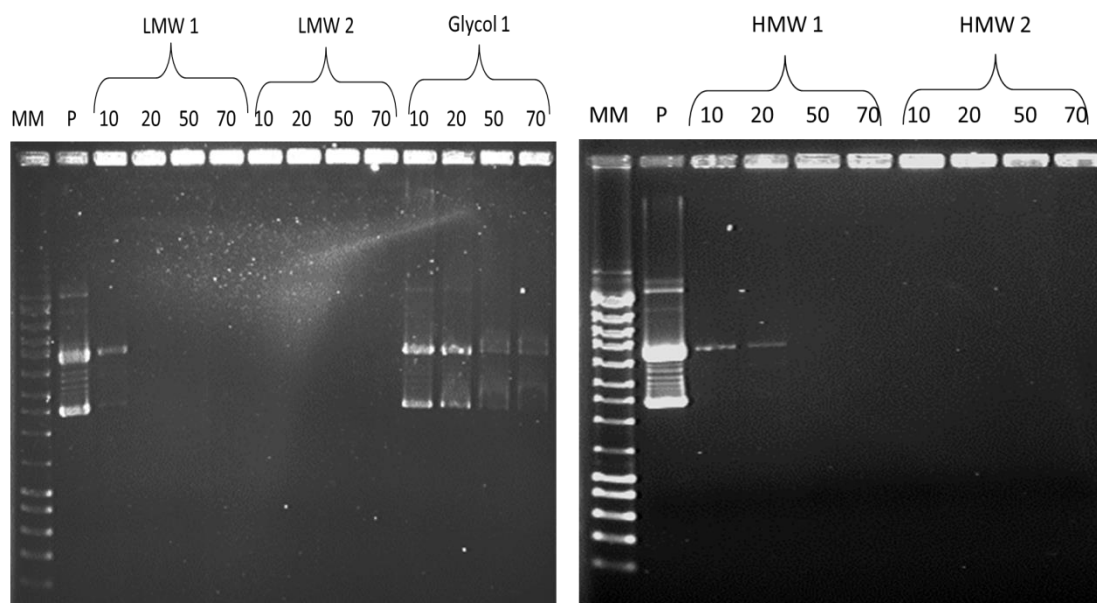


Figure 33 - 1% agarose gel of polyplexes. 2 μ L of loading buffer were added to 10 μ L of sample. Electrophoresis ran for 1h30 at 120V and ethidium bromide was used to stain the samples. MM – molecular marker NZYladderIII (6 μ L); P – pVAX1GFP (negative control); 5, 10, 20 and 50 are the N/P ratios tested; LMW1 – low molecular weight chitosan sonicated and filtered; LMW 2 – low molecular weight chitosan non-sonicated but filtered; Glycol1 – glycol chitosan sonicated and filtered; HMW1 – high molecular weight chitosan sonicated and filtered; HMW2 – high molecular weight chitosan non-sonicated but filtered.

Evaluation of the diameter and zeta potential stability of the referred complexes was tested and is represented in Figures 34 A and B (LMW1 and LMW2), 35 (Glycol) and 36 A and B (HMW1 and HMW2).

Analysing LMW1 chitosan complexes (Figure 34 A), diameter and zeta potential stability was not achieved only in N/P 50 polyplexes, which indicates that in these nanoparticles the physical stability is not linear with the N/P ratio, since N/P 10, 20 and 70 showed to be relatively stable in 50mM acetic acid pH 3.0 plus 10mM Tris-HCl pH 8.0 buffer.

It was also verified that diameter values are smaller than the ones obtained in the first complexation assay, which is an important feature for future transfection assays. These smaller values might be related with the fact that, in this second assay, chitosan particles in suspension were prepared on the same day that complexation was performed, thus decreasing the probability of aggregation or sedimentation phenomena, that interferes with particles physical stability.

N/P10 and 20 particles showed to be more homogeneous than the others since their Pdi value was less than 0.35 (table in Appendix IV.B). All the samples were suitable for DLS and EM measurements since the number of particles present was higher than 1000 (table in Appendix IV.B).

Regarding LMW2 chitosan polyplexes (Figure 34 B), the diameter values were also smaller than the ones obtained in the first complexation assay, where chitosan particles in suspension were prepared 15 days beforehand. Diameter stability was achieved in all the tested nanoparticles, although only N/P 20 and 50 showed zeta potential stability during the 3 days of measurement.

Size homogeneity was found to be higher in N/P 10 complexes due to smaller Pdi values (table in Appendix IV.B). The other particles had Pdi values higher than 0.35.

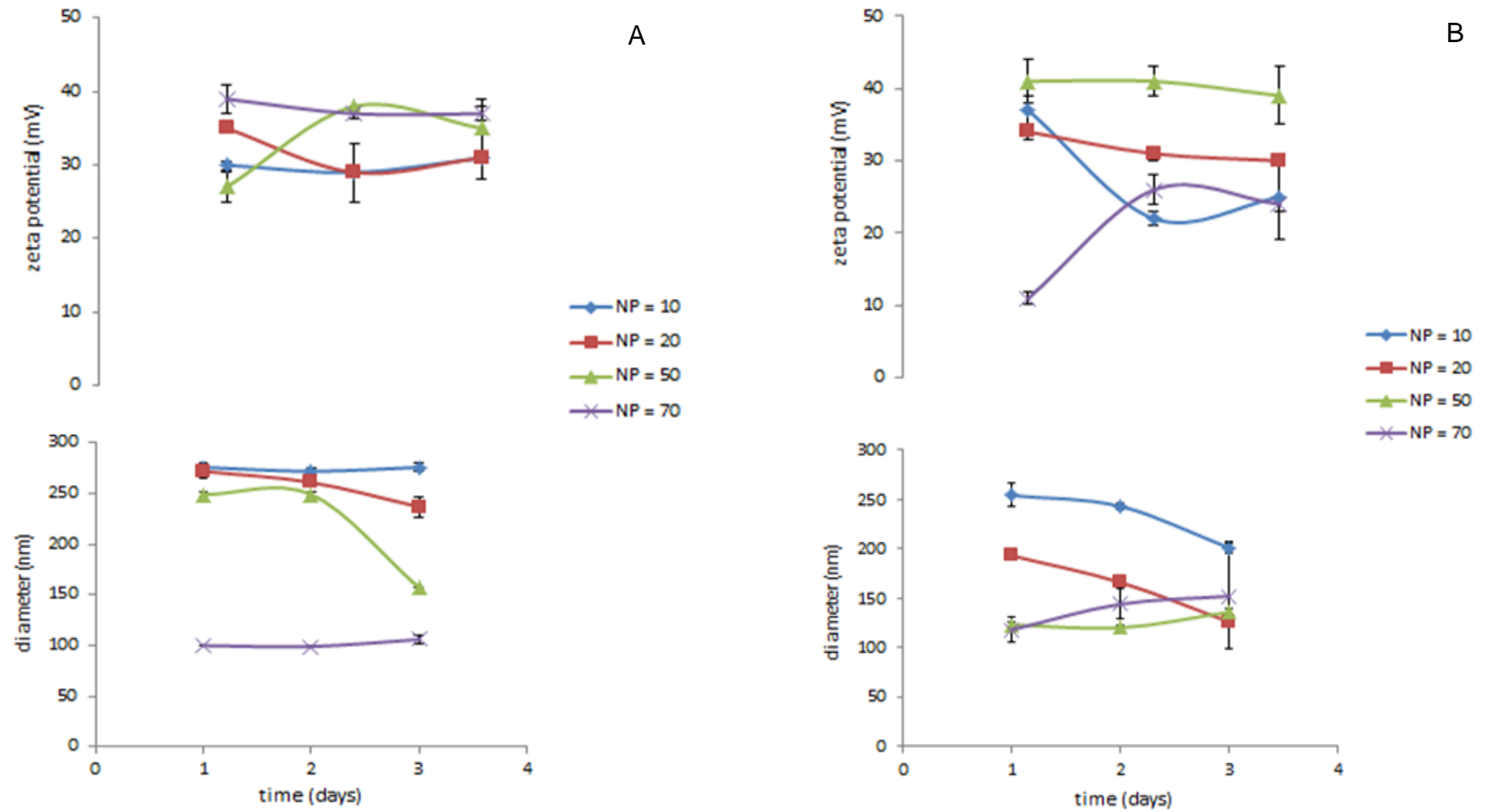


Figure 34 - Evaluation of diameter and zeta potential stability during 3 days of different chitosan and pDNA complexes at different N/P ratios (10, 20, 50 and 70). A – LMW1 chitosan (sonicated and filtered) complexes; B – LMW2 chitosan (non-sonicated and filtered) complexes. Each point is representative of a mean of at least three measurements. All samples were 10-fold diluted before characterization

All the particles were suitable for DLS and EM measurements since their number in the measured sample was higher than 1000 (table in Appendix IV.B).

The diameter and zeta potential stability of glycol chitosan complexed with pVAX1GFP is represented in Figure 35. It is visible that N/P10 nanoparticles were not stable in surrounding buffer, both in diameter and zeta potential. Also, negative values of net charge were present, meaning that pDNA encapsulation by chitosan particles was not totally achieved (see agarose gel in Figure 33) and negative pDNA molecules stayed on complex surface, resulting in the referred negative values. The number of particles present in the measured sample was lower than 1000, meaning that N/P10 complexes were not suitable for DLS and EM measurements (table in Appendix IV.B).

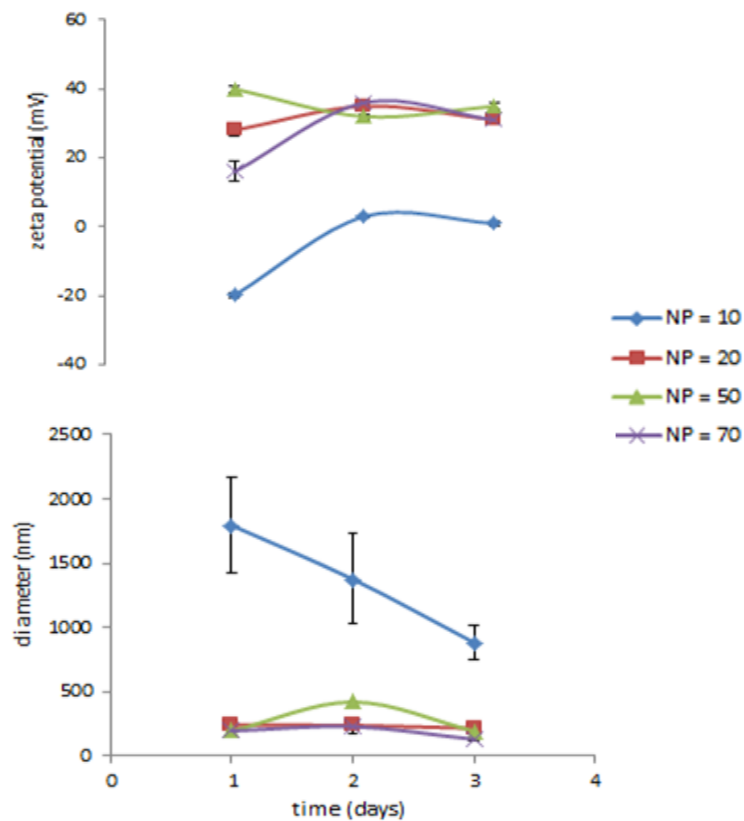


Figure 35 - Evaluation of diameter and zeta potential stability during 3 days of glycol1 chitosan (sonicated and filtered) and pDNA complexes at different N/P ratios (10, 20, 50 and 70). Each point is representative of a mean of at least three measurements. All samples were 10-fold diluted before characterization

Higher stability was obtained in N/P20 nanoparticles as well as higher homogeneity, as it might be observed by Pdi values expressed on the table of Appendix VI.

Finally, the evaluation of HMW chitosan nanoparticles physical stability is represented in Figure 36.

Regarding HMW1 chitosan complexes (Figure 36 A), N/P10 particles showed to be unstable in the surrounding media and surface charge values were nearly zero. Although these polyplexes were suitable for DLS and EM measurements (number of particles > 1000, table in Appendix IV.C), complexation with pDNA was not total and the amount of chitosan positive charges were similar to the amount of pDNA negative charges, resulting in null zeta potential values.

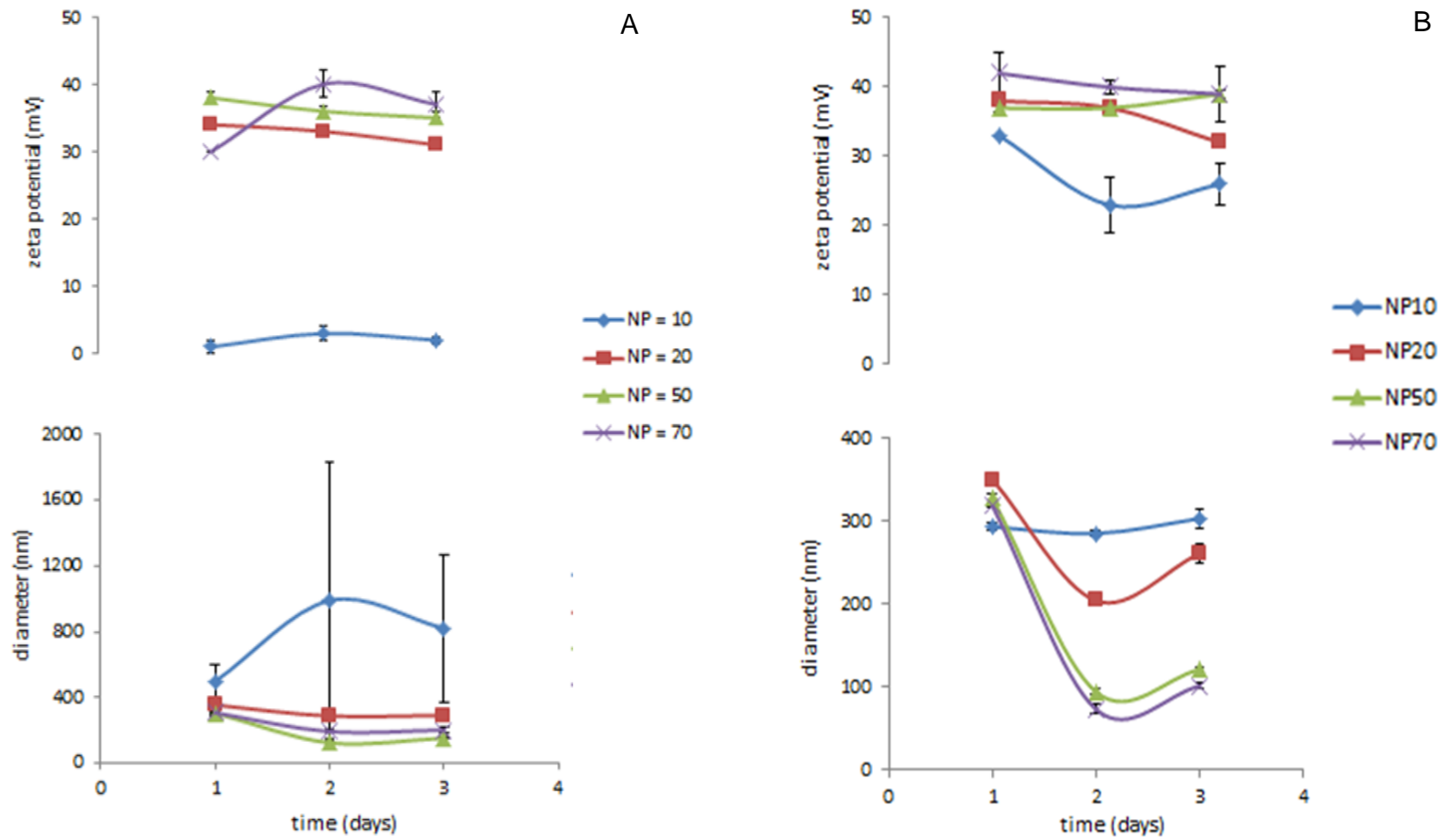


Figure 36 - Evaluation of diameter and zeta potential stability during 3 days of different chitosan and pDNA complexes at different N/P ratios (10, 20, 50 and 70). A – HMW1 chitosan (sonicated and filtered) complexes; B – HMW2 chitosan (non-sonicated and filtered) complexes. Each point is representative of a mean of at least three measurements. All samples were 10-fold diluted before characterization.

For the rest of N/P ratio nanoparticles, diameter and zeta potential stability was achieved, with relatively similar values between them (values between 200nm for N/P50 and 350nm for N/P20 nanoparticles). However, their homogeneity was different. N/P20 showed to be the more homogeneous complex (Pdi = 0.240), while N/P70 the more heterogeneous one (Pdi = 0.426), as it might be concluded by analysing the table in Appendix IV.C.

Sonication of chitosan particles before complexation assay also had an effect on polyplexes physical stability. Comparing Figures A and B (sonication vs non-sonication) it is notorious that this process influenced positively the diameter stability of N/P20, 50 and 70 and negatively the N/P10 complex in suspension. The decreasing diameter of N/P20, 50 and 70 nanoparticles (Figure 36B) might be related with the fact that in higher N/P ratios the electrostatic repulsion forces are higher than the attractive forces, avoiding condensation that would form larger particles^[80].

Complexes with N/P ratio of 10 were the most stable during this test. Also, Pdi values (table in Appendix VIII) showed that they were the more homogeneous samples, compared with other N/P ratio nanoparticles herein tested.

To confirm the results previously described, correlograms and volume distributions of all the particles were also analysed (Figures 37 A, B, C and D).

Glycol chitosan complexes with N/P ratio of 10 and HMW1 chitosan complexes with N/P ratio of 10 were the ones that had different behaviour compared to the other. Negative and null zeta potential values, respectively, were already observed for these two types of nanoparticles, corroborating the hypothesis that their use is not suitable for transfection assays.

With this study, conclusions might be reached about the preparation of chitosan particles in solution for complexation assays. Sonication and filtration processes demonstrated that their use is important to obtain stable nanoparticles, with positive net charges and diameter values around 250nm, which are important features to obtain high delivery efficiency to animal cells.

Also, the referred stability, as well as the diameter and zeta potential values, is influenced by the time in which chitosan particles in acetic acid suspension are prepared. Particles prepared on the same day of the complexation assay gave rise to more stable and homogeneous polyplexes, compared to those prepared 15 days beforehand. Furthermore, aggregation phenomenon is avoided, leading to smaller diameter nanoparticles.

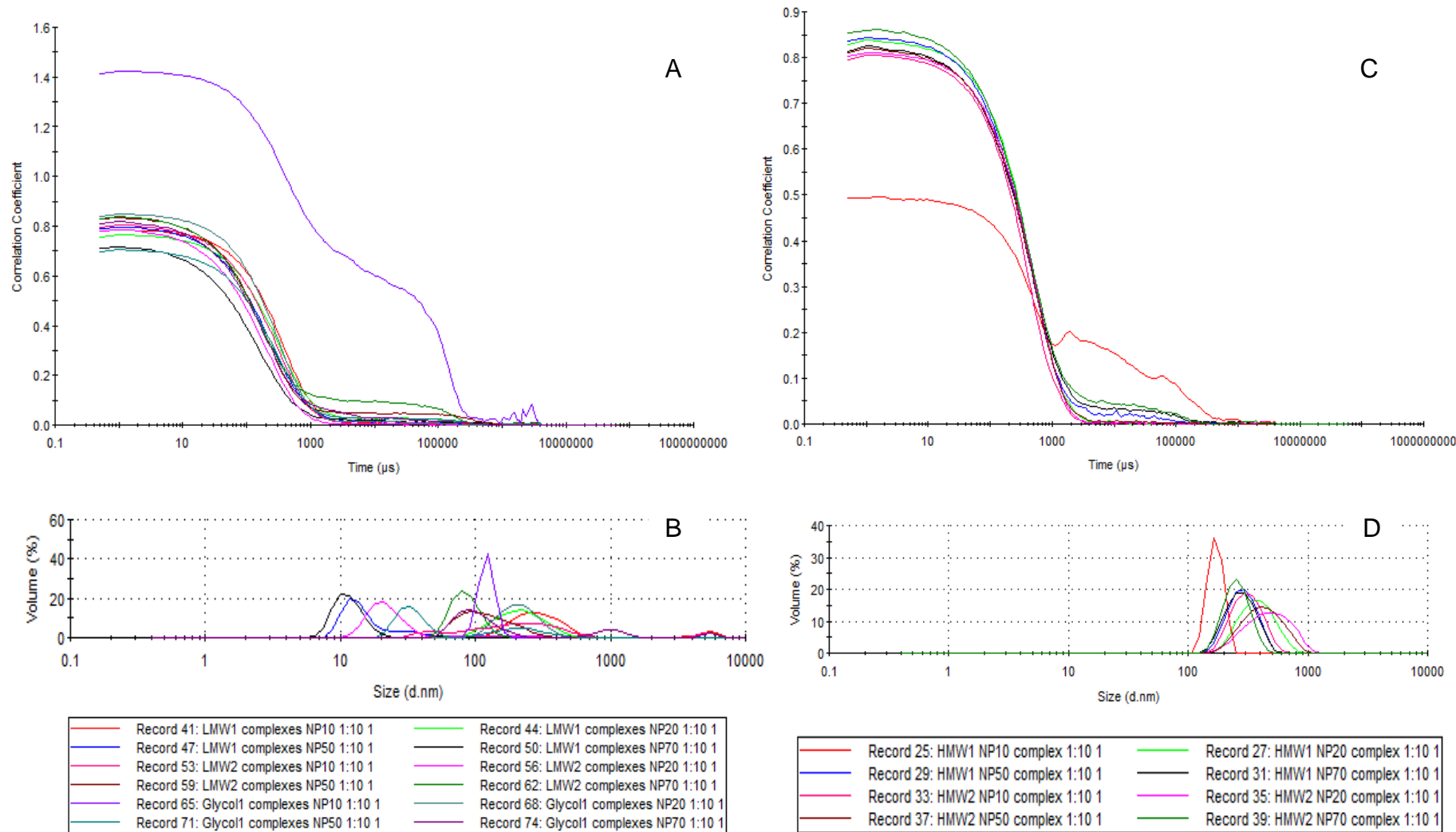


Figure 37 – Evaluation of the quality of LMW1, LMW2, Glycol1 (A and B) and HMW1 and HMW2 (C and D) chitosan complexes with pDNA, at different N/P ratios. A and C – correlogram analysis; B and D – volume distribution analysis; LMW- low molecular weight chitosan; HMW – high molecular weight chitosan; Glycol – glycol chitosan; 1 - sonication; 2 – non sonication; 50mM acetic acid pH 3.0 and 10mM Tris-HCl pH 8.0 buffer solutions were always filtered. All samples were 10-fold diluted before characterization.

4.3. Preparation and characterization of lipids coated chitosan/pDNA nanoparticles

The use of lipids, namely in the form of liposomes, has been widely investigated for use as non-viral vectors for cell delivery of therapeutic agents, pDNA included.

In this study, a cholesterol derivative (cholesteryl chloroformate, 97%) (CHOL) and a modified lecithin (ML) (L-A-lysophosphatidylcholine type I from egg yolk) were used, individually, to coat chitosan particles and determine if their presence influences the efficiency of transfection, after complexation of these conjugates with pVAX1GFP.

To confirm if complexation of these conjugates with pDNA has occurred, 1% agarose gel electrophoresis was performed (Figures 38 A and B).

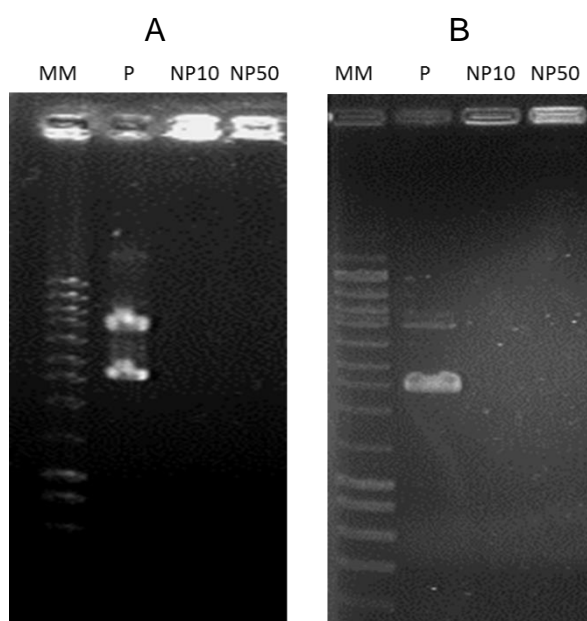


Figure 38 - 1% agarose gel of lipopolyplexes. 2 μ L of loading buffer were added to 10 μ L of sample. Electrophoresis ran for 1h30 at 120V and ethidium bromide was used to stain the samples. MM – molecular marker NZYladderIII (6 μ L); P – pVAX1GFP 75ng/ μ L (negative control); A – CHI/CHOL conjugate complexed with pDNA at N/P10 and 50 ratios; B – CHI/ML conjugate complexed with pDNA at N/P10 and 50 ratios.

Complexation was achieved for both conjugates at both N/P ratios tested, since no pDNA migration is observed in the gel, when compared to the negative control (plasmid itself).

Diameter, polydispersion index and zeta potential characterization of CHI/CHOL (chitosan/cholesterol) was performed in order to compare those values with the ones obtained after complexation of this conjugate with pDNA at N/P ratios of 10 and 50 (Table 1).

Table 1 – Diameter, mean Pdi and zeta potential values of chitosan oligo lactate (control), CHI/CHOL conjugate and N/P10 (S1) and 50 (S2) complexes of conjugate and pDNA.

Sample	T (°C)	Diameter (nm)	Mean Pdi	Zeta potential (mV)
Chitosan oligo lactate (control)	37	649 ± 29	0.80 ± 0.02	36 ± 0.1
CHI/CHOL conjugate (before complexation)	37	702 ± 51	0.57 ± 0.03	23 ± 1.5
S1 (N/P 10)	37	242 ± 15	0.29 ± 0.02	16 ± 0.7
S2 (N/P 50)	37	231 ± 48	0.28 ± 0.05	21 ± 1.7

Diameter values increased when CHI/CHOL conjugate is performed, compared to chitosan oligo lactate itself (control), since cholesterol derivative would remain at chitosan molecule surface. The electrostatic interaction between the two components resulted in a decrease of zeta potential value, since less chitosan positive charges will be available at conjugate surface.

When complexed with pVAX1GFP, electrostatic interaction of this bio-component with CHI/CHOL conjugate would promote a molecule condensation, resulting in lower diameter values for both N/P ratios tested. Zeta potential values remained positive but decreased a little when compared to the complexation precursor, since less chitosan positive charges are available after complexation.

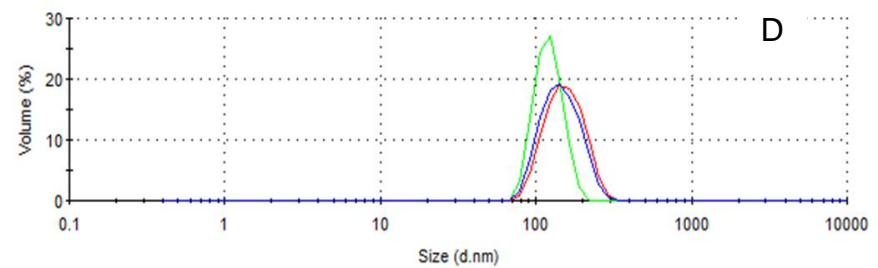
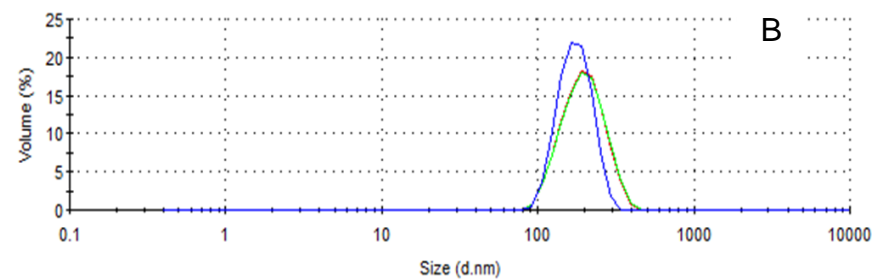
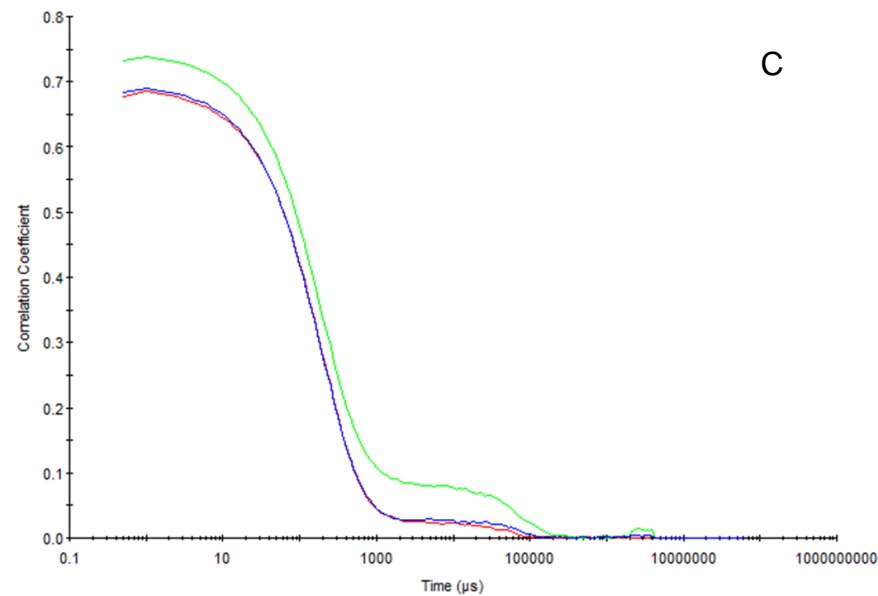
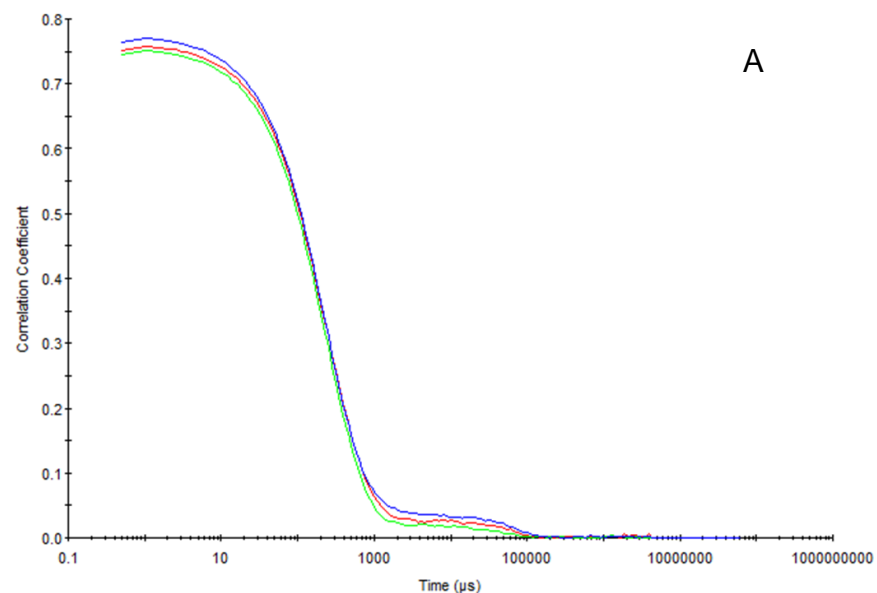
Also, more homogeneous nanoparticles were formed since their Pdi values decreased to about 0.3, meaning that complexes with pDNA are more stable than CHI/CHOL conjugate.

Results from N/P10 and N/P50 nanoparticles were relatively similar. However, higher zeta potential values were observed for N/P50 complex due to the lower content in pDNA present, compared to the other ratio tested.

To assess the quality of the formed nanoparticles, correlograms and volume distributions were also analysed (Figure 39).

Analysing the correlograms (Figures 39 A and C), the presence of some aggregates in both N/P ratios tested is notorious, especially in one of the measurements of N/P50 ratio (Figure 39 C). It is important, in future works, to use freshly prepared samples before characterization in Zetasizer equipment. Furthermore, reaction time between chitosan and cholesteryl chloroformate must be optimised, in order to enhance this formulation properties. In order to obtain more detailed information about the topology, dynamics and three-dimensional structure of CHI/CHOL conjugate, NMR spectroscopy is a powerful technique, which may also be used in future studies.

Regarding volume distributions, only one peak was obtained for each N/P ratio tested (Figures 39 B and D), meaning that the Zetasizer equipment is measuring one volume complexes, consisting with the homogeneity observed in Pdi values.



— Record 31: CHI-CHOL NP10 1:10 in Tris + acetic acid 1
— Record 32: CHI-CHOL NP10 1:10 in Tris + acetic acid 1
— Record 33: CHI-CHOL NP10 1:10 in Tris + acetic acid 1

— Record 34: CHI-CHOL NP50 1:10 in Tris + acetic acid 1
— Record 35: CHI-CHOL NP50 1:10 in Tris + acetic acid 1
— Record 36: CHI-CHOL NP50 1:10 in Tris + acetic acid 1

Figure 39 - Evaluation of the quality of CHI/CHOL/pDNA nanoparticles at N/P ratios of 10 (A and B) and 50 (C and D); A and C – correlogram analysis; B and D – volume distribution analysis; CHI – chitosan; CHOL – cholesteryl chloroformate; pDNA – plasmid DNA; 50mM acetic acid pH 3.0 and 10mM Tris-HCl pH 8.0 buffer solutions were always filtered before Zetasizer characterization

Regarding CHI/ML (chitosan/modified lecithin) conjugate, diameter, polydispersion index and zeta potential characterization was performed, in order to compare those values with the ones obtained after complexation of this conjugate with pDNA at N/P ratios of 10 and 50 (Table 2).

Table 2 – Diameter, mean Pdi and zeta potential values of LMW1 CHI, modified lecithin coated chitosan (conjugate control), and N/P10 (S3) and 50 (S4) complexes of conjugate and pDNA. LMW1 CHI – low molecular weight chitosan sonicated and buffer filtered with 0.45µm membrane

Sample	T (°C)	Diameter (nm)	Mean Pdi	Zeta potential (mV)
LMW1 CHI	37	315 ± 64	0.396 ± 0.01	34 ± 3
CHI/ML conjugate	37	2557 ± 1050	0.9 ± 0.2	32 ± 2
S3 (N/P 10)	37	378 ± 27	0.3 ± 0.047	13 ± 0.8
S4 (N/P 50)	37	458 ± 15	0.3 ± 0.045	16 ± 1.0

Diameter values highly increased when CHI/ML conjugate is formed, compared to low molecular weight chitosan itself (control), since modified lecithin would remain at chitosan molecule surface. The mean Pdi values also increase, meaning that the conjugate is less homogeneous than the control, which is corroborated by the volume distribution in which two peaks are present (results not shown). This result is probably related with the fact that not all the modified lecithin had interacted with the chitosan.

Several parameters of this reaction, such as the time of reaction and chitosan preparation, should be studied in future works. Also, to obtain more detailed information about the topology, dynamics and three-dimensional structure of CHI/ML conjugate, NMR spectroscopy is a powerful tool, which could be used in future studies.

When complexed with pVAX1GFP, electrostatic interaction of this bio-component with CHI/ML conjugate would promote a molecule condensation, resulting in lower diameter values for both N/P ratios tested. Zeta potential values remained positive but decreased a little when compared to the precursor conjugate CHI/ML, since less chitosan positive charges are available after complexation.

Also, more homogeneous nanoparticles were formed since their Pdi values decreased to about 0.3, meaning that complexes with pDNA are more stable than CHI/ML conjugate.

Results from N/P10 and N/P50 nanoparticles were relatively similar. However, higher zeta potential values were observed for N/P50 complex due to the lower content in pDNA present, compared to the other tested ratio.

To assess the quality of the formed nanoparticles, correlograms and volume distributions were also analysed (Figure 40).

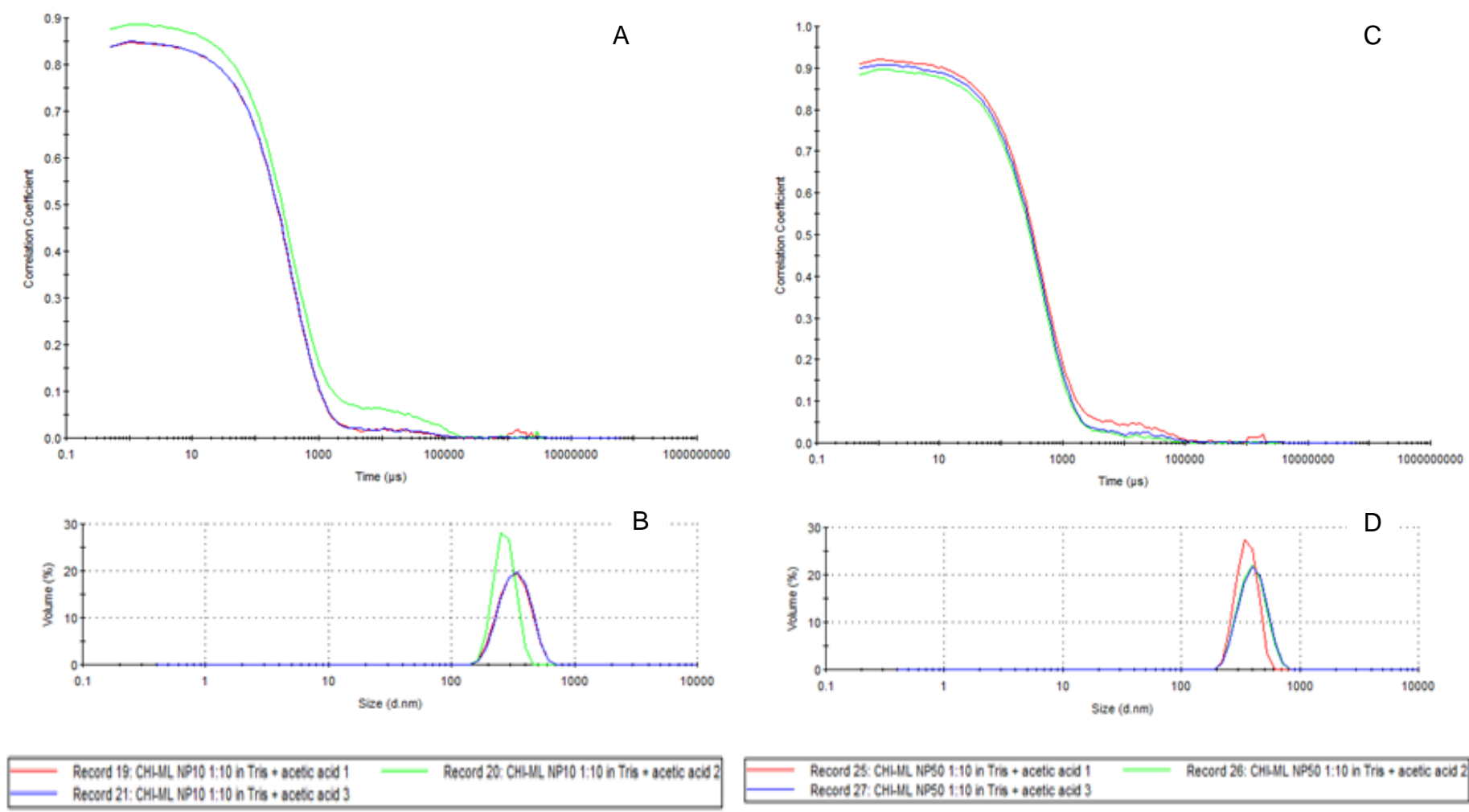


Figure 40 - Evaluation of the quality of CHI/ML/pDNA nanoparticles at N/P ratio of 10 (A and B) and 50 (C and D); A and C – correlogram analysis; B and D – volume distribution analysis; CHI – chitosan; ML – modified lecithin; pDNA – plasmid DNA; 50mM acetic acid pH 3.0 and 10mM Tris-HCl pH 8.0 buffer solutions were always filtered before Zetasizer characterization

Analysing the correlograms (Figures 40 A and C), it is verified that the tail end of the curve is relatively long, consistent with the presence of some aggregates that increase the nanoparticle's diameter. It is important, in future works, to use freshly prepared samples before characterization in Zetasizer equipment.

Regarding volume distributions, only one peak was obtained for each N/P ratio tested (Figures 40 B and D), meaning that the Zetasizer equipment is measuring one volume complexes, consistent with the homogeneity observed in Pdi values.

4.4. Transfection of produced nanoparticles to animal cells

Transfection, as previously stated in this work, is the process of introducing nucleic acids into eukaryotic cells by non-viral vectors, in this case, chitosan nanoparticles.

The selection of those nanoparticles, to be used in transfection assays, was made in order to obtain the maximum efficiency of this delivery process, i.e. high percentages of transfected CHO cells, resulting from the expression of GFP in cell nucleus.

Criteria used in this selection process include small diameter sizes (nano-range), positive net charges (zeta potential values), complex stability along the time and nanoparticles that were as homogeneous as possible (Pdi values less than 0.30). Thus, for the first experiment, sonicated LMW CHI complexed with pVAX1GFP at N/P ratio of 10 and sonicated Glycol CHI complexed with pVAX1GFP at N/P ratio of 20 were the chosen nanoparticles to be introduced into CHO cells. Negative control composed only of CHO cells, and positive control, in which pVAX1GFP was complexed with the transfection reagent Lipofectamine 2000 and then placed in contact with the referred cells, were also tested.

In this first transfection experiment, 100% cell confluence in the culture flasks was used and the duration of transfection, known as the time in which the nanoparticles are in direct contact with the cells, was limited at 1h. Also, different post transfection incubation times (24h and 48h) were studied to understand their impact on the GFP expression. The incubation time corresponds to the time between transfection and measurement of GFP fluorescence by FACS.

The transfection percentage (% of transfected cells), given by the M2 parameter and fluorescence mean intensity, given by the FL1 parameter, of the tested samples are represented in Figures 41 A and B, respectively. It is important to note that cells autofluorescence was discounted from the results obtained for positive control and chitosan/pDNA nanoparticles.

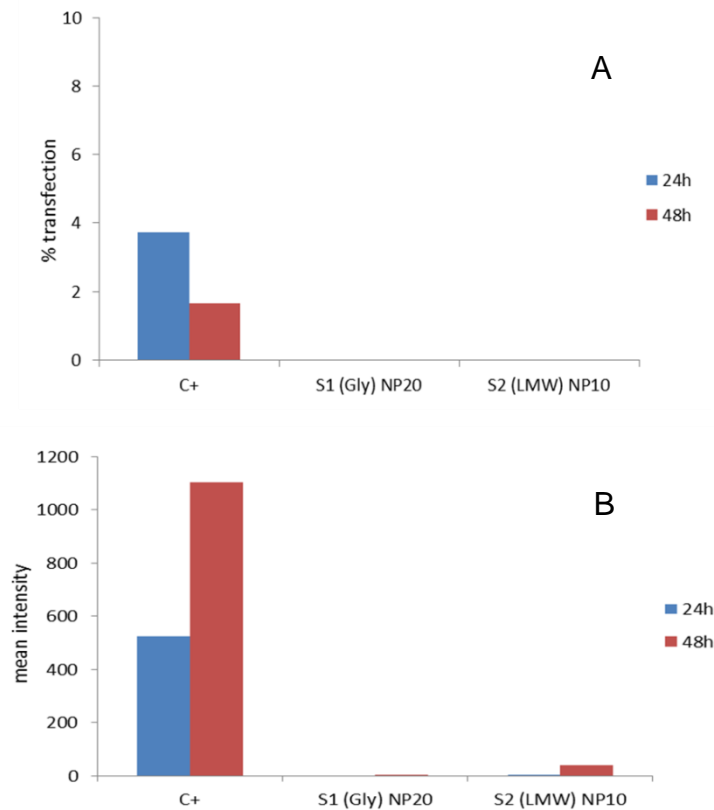


Figure 41 – Percentage of transfected CHO cells (A) and fluorescence mean intensity (B) of selected nanoparticles. C+ – positive control; S1 – sonicated glycol chitosan complexed with pVAX1GFP at N/P =20; S2 – sonicated LMW chitosan complexed with pVAX1GFP at N/P=10

Regarding the percentage of transfection, the values are extremely low even for the positive control where pDNA is complexed with the transfection reagent Lipofectamine 2000. This is an established complex with transfection normally higher than 30% when GFP is used as reporter gene^[81]. It is composed of cationic lipidic subunits that form liposomes in aqueous environments, allowing the entrapment of pharmaceutical ingredients, pDNA included. The presence of liposomes in the formulations should facilitate the interaction with the lipophilic cell membrane, enhancing their uptake.

The results obtained are probably related with the 100% cell confluency used in this first assay. Too many cells results in contact inhibition, making cells resistant to uptake of foreign DNA.

Another important parameter that was determined is the pH of the nanoparticles, which was around 7.3 for all the tested complexes. Typical set-points for pH in CHO cell culture are in the range between 6.8 and 7.4^[82]. If the nanoparticles suspensions pH values were outside this range, viability and metabolic activity of the cells, as well as recombinant protein productivity and quality would be affected.

The appearance of the cells was also verified, before and after the contact with the nanoparticles, in an optical microscope. No significant differences were observed, meaning that the tested complexes were not extremely toxic to the cells, which can cause morphological changes or even apoptosis. Elongated form was maintained and the nucleus was sometimes visible.

In the second transfection assay, in addition to the nanoparticles already tested in the first experiment, CHI/CHOL/pDNA complexes were also tested at both N/P=10 and N/P=50, in order to determine if the presence of the lipid influenced this process efficiency. Furthermore, cell confluence was set at around 80%, in order to avoid cell contact inhibition.

Incubation time analysis was performed for 1h of transfection (Figures 42 A and B) and transfection time analysis was also performed for 48h of incubation time (Figures 43 A and B).

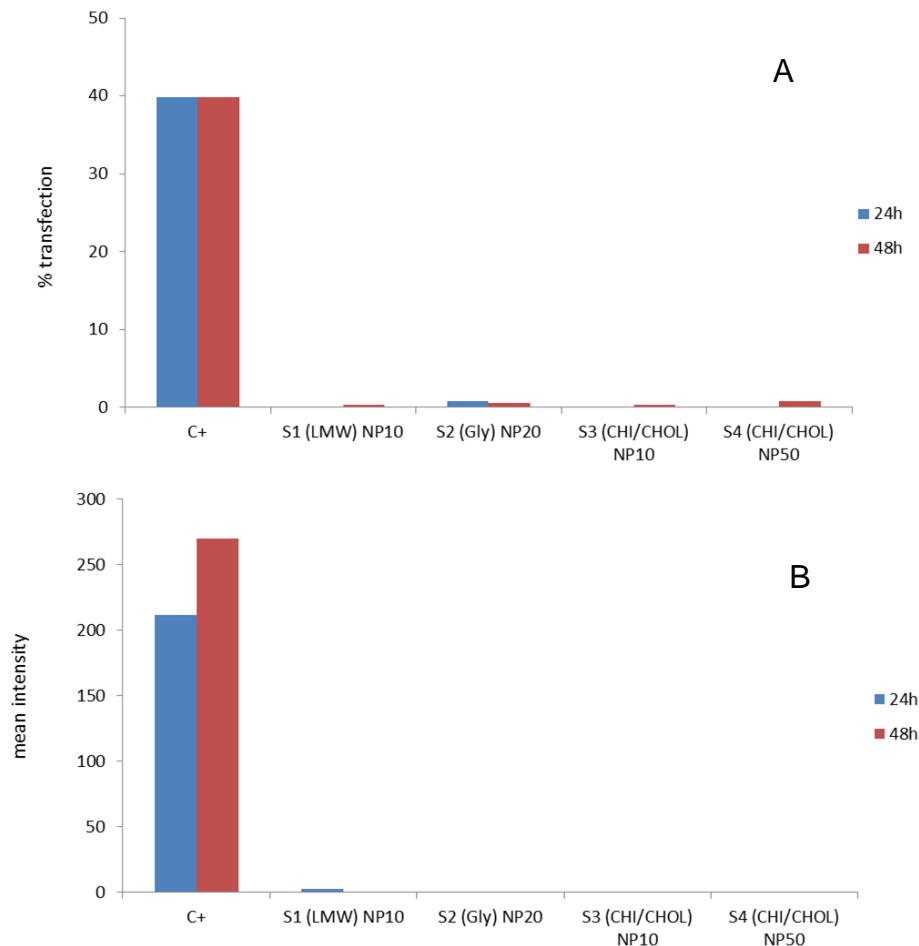


Figure 42 – Effect of incubation time (24h, 48h) on transfection percentage (A) and fluorescence mean intensity (B) of selected nanoparticles. C+ – positive control; S1 – sonicated LMW chitosan complexed with pVAX1GFP at N/P=10; S2 – sonicated glycol chitosan complexed with pVAX1GFP at N/P =20; S3 – CHI/CHOL conjugate complexed with pVAX1GFP at N/P=10; S4 – CHI/CHOL conjugate complexed with pVAX1GFP at N/P=50

It was verified that the percentage of transfected cells highly increased in positive control with Lipofectamine 2000 in both 24h and 48h of incubation ($\approx 40\%$), when compared to the values obtained with 100% cell confluence (Figure 41 A). This efficiency was relatively similar for both 24h and 48h of incubation.

However, transfection efficiency was almost null with the formulated chitosan nanoparticles. Since their pH was around 7.3 and the appearance of the cells maintained after transfection, another transfection time (3h) was studied in order to understand if the contact time between the particles and the cells had influence on this uptake process (Figures 43 A and B).

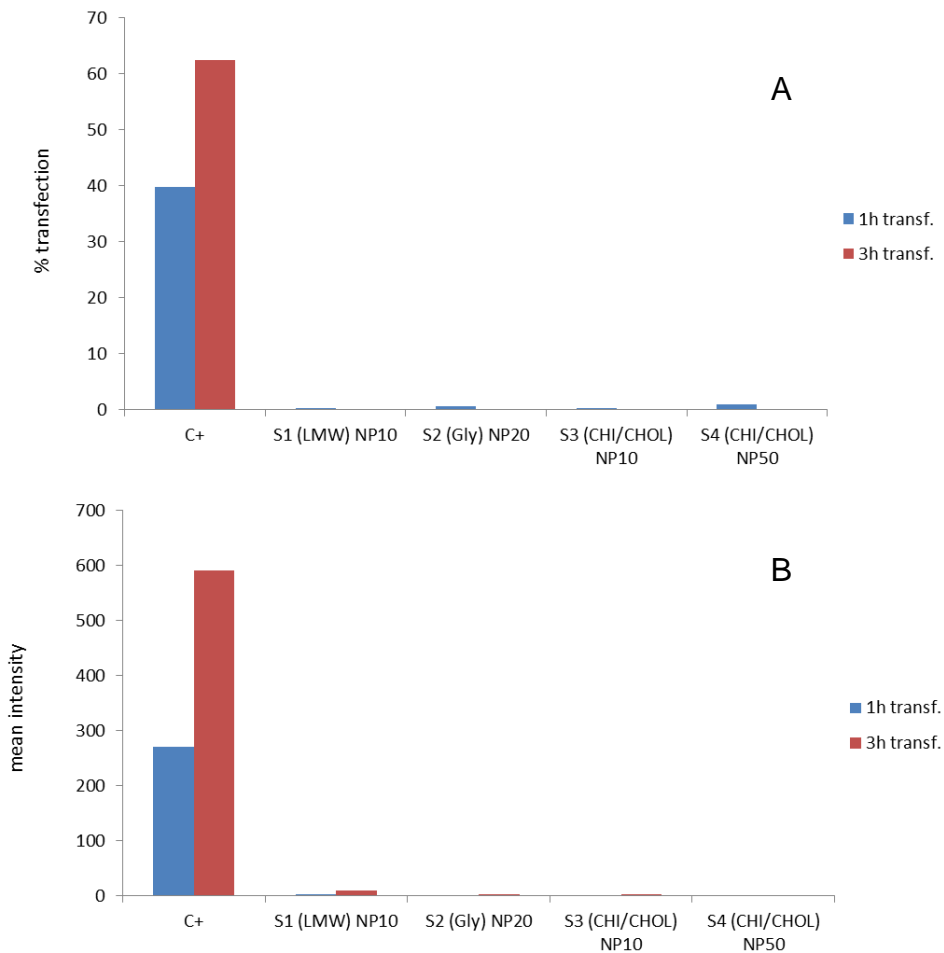


Figure 43 – Effect of transfection time (1h, 3h) on transfection percentage (A) and fluorescence mean intensity (B) of selected nanoparticles. C+ – positive control; S1 – sonicated LMW chitosan complexed with pVAX1GFP at N/P=10; S2 – sonicated glycol chitosan complexed with pVAX1GFP at N/P =20; S3 – CHI/CHOL conjugate complexed with pVAX1GFP at N/P=10; S4 – CHI/CHOL conjugate complexed with pVAX1GFP at N/P=50; incubation time = 48h

Regarding positive control, transfection increased almost 20% at 3h of transfection, meaning that the time in which the nanoparticles are in contact with the CHO cells is important for this efficiency. However, for chitosan nanoparticles this transfection time remains inappropriate, since both transfection and mean fluorescence intensity were almost inexistent. The cells didn't show significant morphological changes after transfection and pH of the nanoparticles was determined to be around 7.3.

Thus, a third assay was performed, repeating some of the assays and using other chitosan nanoparticles previously prepared. Cell confluence was maintained at 80% and two different transfection (3h, 6h) and incubation (48h, 24h, respectively) times were tested (Tables 3 and 4).

Table 3 – Transfection percentage and fluorescence mean intensity of selected nanoparticles transfected for 6h and incubated for 24h.

6h transfection (24h incubation)		
Sample	%transfection	mean intensity
C-	5.4	15.9
C+	N/A	N/A
S1 (LMW1) NP10	5.9	13.7
S2 (LMW1) NP70	2.3	13.4
S3 (Gly) NP20	N/A	N/A
S4 (LMW2) NP50	N/A	N/A
S5 (HMW1) NP50	N/A	N/A
S6 (HMW2) NP50	N/A	N/A
S7 (CHI-CHOL) NP50	N/A	N/A
S8 (CHI-ML) NP50	N/A	N/A

C- – negative control; C+ – positive control; S1 – sonicated LMW chitosan complexed with pVAX1GFP at N/P=10; S2 – sonicated LMW chitosan complexed with pVAX1GFP at N/P=70; S3 – sonicated glycol chitosan complexed with pVAX1GFP at N/P =20; S4 – non-sonicated LMW chitosan complexed with pVAX1GFP at N/P=50; S5 – sonicated HMW chitosan complexed with pVAX1GFP at N/P=50; S6 – non-sonicated HMW chitosan complexed with pVAX1GFP at N/P=50; S7 – CHI/CHOL conjugate complexed with pVAX1GFP at N/P=50; S8 – CHI/ML conjugate complexed with pVAX1GFP at N/P=50; N/A – not available

Table 4 – Transfection percentage and fluorescence mean intensity of selected nanoparticles transfected for 3h and incubated for 48h.

3h transfection (48h incubation)		
Sample	%transfection	mean intensity
C-	2.8	16.3
C+	67	825
S1 (LMW1) NP10	2.2	14.6
S2 (LMW1) NP70	3.2	14.4
S3 (Gly) NP20	2.5	14.3
S4 (LMW2) NP50	3.2	14
S5 (HMW1) NP50	N/A	N/A
S6 (HMW2) NP50	N/A	N/A
S7 (CHI-CHOL) NP50	N/A	N/A
S8 (CHI-ML) NP50	N/A	N/A

C- – negative control; C+ – positive control; S1 – sonicated LMW chitosan complexed with pVAX1GFP at N/P=10; S2 – sonicated LMW chitosan complexed with pVAX1GFP at N/P=70; S3 – sonicated glycol chitosan complexed with pVAX1GFP at N/P =20; S4 – non-sonicated LMW chitosan complexed with pVAX1GFP at N/P=50; S5 – sonicated HMW chitosan complexed with pVAX1GFP at N/P=50; S6 – non-sonicated HMW chitosan complexed with pVAX1GFP at N/P=50; S7 – CHI/CHOL conjugate complexed with pVAX1GFP at N/P=50; S8 – CHI/ML conjugate complexed with pVAX1GFP at N/P=50; N/A – not available

Regarding this last assay, the results continued to be unpromising except in positive control at 3h of transfection, where a 67% transfection was obtained. For the majority of the tested nanoparticles the results were not available, since no fluorescent signals were detected by the flow cytometer at the gate. Some kind of technical error had to be made when the cells were passed from the 24-well plate for the cytometer tubes, since their quantity was variable and almost undetectable in some of the samples tested (N/A).

More research has to be made to achieve higher transfection efficiencies, especially in the optimization of polyplex and lipopolyplex formulations and their quantity (mass) used, as well as on transfection parameters such as to test other transfection and incubation periods.

5. Conclusion and future work

The main goal of this study, which was to obtain high transfection efficiencies with chitosan nanoparticles in CHO cells, was not achieved. However, some important conclusions were made during this project regarding the preparation and characterization of the referred particles.

Sonication and buffer filtration showed to be important processes to obtain stable, homogeneous chitosan particles in solution with positive net charges and nanometer range diameters. Low molecular weight chitosan were the one that presented more regularly these important characteristics.

Self-assembly demonstrated to be an efficient complexation method for chitosan particles in solution and previously purified pVAX1GFP. Freshly prepared particles are important to avoid aggregation and sedimentation phenomena, meaning that these complexes are not stable for a long period of time, even at 4°C.

Regarding amine to phosphate ratios (N/P), no significant conclusions were made, since the quality of the polyplexes/lipopolyplexes is variable from chitosan to chitosan and from lipid to lipid.

In this study, to calculate the mass of molecules used in complexation assays, chitosans mass was fixed and pDNA mass was calculated based on the molecular mass and N/P ratio used in each formulation. For future studies, the mass of pDNA should be fixed and chitosans mass should be calculated from the MW and N/P ratio used. Most likely, the mass of pDNA per cell is a key factor on transfection efficiency.

With the “positive” results obtained for the positive control with the transfection reagent Lipofectamine 2000, it is clear that “negative” results obtained with chitosan nanoparticles are not derived from pVAX1GFP quality and stability. However, pDNA quantity used in each formulation was different. In positive control, 1µg of pDNA was used to complex with Lipofectamine 2000 while its mass on chitosan formulations varied according to N/P ratio used (from 2µg to 14µg). In future works, pDNA mass needs to be optimised in order to enhance the transfection process.

At 3h of transfection, the efficiency of this process for pDNA complexed with Lipofectamine showed to be higher than at 1h of transfection, for an incubation period of 48h. However, for chitosan polyplexes and lipopolyplexes tested no ideal periods were assessed.

Further work on creating homogenous, large-scale preparations of polyplexes and lipopolyplexes with known characteristics other than particle size distribution and zeta potential will be necessary, to enable progress in this area. Transmission electron microscopy (TEM) or scanning electron microscopy (SEM) should also be performed, in order to observe the morphology of the nanoparticles. Nuclear magnetic resonance spectroscopy (NMR) should also be taken into account to study in detail the dynamics of lipid-chitosan reactions.

Regarding the transfection conditions, 100% cell confluence should not be used in order to avoid cell to cell contact inhibition.

In a near future it should be interesting to realize a microporation assay in order to verify if these low transfection efficiencies are related with the interaction of the nanoparticles with the cell membrane or if they are being degraded inside the cell, mainly in lysosomes. Confocal microscopy

could also be helpful to understand the location of those chitosan nanoparticles inside the cell because both pDNA and chitosan would be marked with different fluorescent dyes.

6. References

1. Thibault, M. *et al.* **Excess polycation mediates efficient chitosan-based gene transfer by promoting lysosomal release of the polyplexes.** *Biomater*, 32(20); 4639-46; 2011
2. Channarong, S., Chaicumpa, W., Sinchaipanid, N., Mitrevej, A. **Development and evaluation of chitosan-coated liposomes for oral DNA vaccine: the improvement of Peyer's patch targeting using a polyplex-loaded liposomes.** *AAPS PharmSciTech*, 12(1); 192-200; 2011
3. Hallaj-Nezhadi, S. *et al.* **Preparation of chitosan-plasmid DNA nanoparticles encoding interleukin-12 and their expression in CT-26 colon carcinoma cells.** *J Pharm Pharm Sci*, 14(2); 181-95; 2011.
4. Davis, B.S. *et al.* **West Nile virus recombinant DNA vaccine protects mouse and horse from virus challenge and expresses in vitro a noninfectious recombinant antigen that can be used in enzyme-linked immunosorbent assays.** *J Virol*, 75(9); 4040-7; 2001
5. Bergman, P.J. *et al.* **Long-term survival of dogs with advanced malignant melanoma after DNA vaccination with xenogeneic human tyrosinase: a phase I trial.** *Clin Cancer Res*, 9(4); 1284-90; 2003
6. Del Solar, G., Giraldo, R., Ruiz-Echevarría, M.J., Espinosa, M., Díaz-Orejas, R. **Replication and control of circular bacterial plasmids.** *Microbiol Mol Biol Rev*, 62(2); 434-64; 1998
7. Glenting, J., Wessels, S. **Ensuring safety of DNA vaccines.** *Microb Cell Fact.*, 4; 26; 2005
8. Sinden, R.R. **DNA Structure and Function.** Acad. Press.1994
9. Scleef, M. **Plasmids for Therapy and Vaccination.** Wiley-VCH Verlag GmbH. 2001
10. Azzoni, A.R., Ribeiro, S.C., Monteiro, G.A., Prazeres, D.M.F. **The impact of polyadenylation signals on plasmid nuclease-resistance and transgene expression.** *J Gene Med*, 9(5); 392-402; 2007.
11. Kotnik, T., Kramar, P., Pucihar, G., Miklavcic, D., Tarek, M. **Cell membrane electroporation- Part 1: The phenomenon.** *Electrical Insulation Magazine, IEEE.* 28(5); 14-23; 2012
12. Loyter, A., Scangos, G., Juricek, D., Keene, D., Ruddle, F.H. **Mechanisms of DNA entry into mammalian cells. II. Phagocytosis of calcium phosphate DNA co-precipitate visualized by electron microscopy.** *Exp Cell Res*, 139(1); 223-34; 1982.
13. Bråve, A., Ljungberg, K., Wahren, B., Liu, M.A. **Vaccine Delivery Methods Using Viral Vectors.** *Molec Pharm.* 4(1); 18-32; 2006
14. Ginn, S.L., Alexander, I.E., Edelstein, M.C., Abedi, M.R., Wixon, J. **Gene therapy clinical trials worldwide to 2012 - an update.** *J Gene Med*, 15(2); 65-77; 2013.
15. Cavazzana-Calvo, M. *et al.* **Gene therapy of human severe combined immunodeficiency (SCID)-X1 disease.** *Science*, 288(5466); 669-72; 2000.
16. McLachlan, G. *et al.* **Optimizing aerosol gene delivery and expression in the ovine lung.** *Mol Ther*, 15(2); 348-54; 2007
17. Putnam, D. **Polymers for gene delivery across length scales.** *Nat Mater*, 5(6); 439-51; 2006.
18. Li, P. *et al.* **A polycationic antimicrobial and biocompatible hydrogel with microbe membrane suctioning ability.** *Nat Mater*, 10(2); 149-56; 2011
19. Shi, B., Zhang, H., Shen, Z., Bi, J., Dai, S. **Developing a chitosan supported imidazole Schiff-base for high-efficiency gene delivery.** *Polymer Chemistry*, 4(3); 840-850; 2013
20. Samal, S.K. *et al.* **Cationic polymers and their therapeutic potential.** *Chem Soc Rev*, 41(21); 7147-94; 2012
21. Liang, W., Lam, J.K.W. **Endosomal Escape Pathways for Non-Viral Nucleic Acid Delivery Systems.** *Molec Reg of Endocyt.* 2012.
22. Ke, J.H., Young, T.H. **Multilayered polyplexes with the endosomal buffering polycation in the core and the cell uptake-favorable polycation in the outer layer for enhanced gene delivery.** *Biomater*, 31(35); 9366-9372; 2010
23. Yaroslavov, A.A., Efimova, A.A., Kostenko, S.N. **Structure and properties of complexes formed by cationic polymers and anionic cholesterol-containing liposomes.** *Polym Sci Ser A*, 54(4); 264-269; 2012
24. Karmali, P.P., Chaudhuri, A. **Cationic liposomes as non-viral carriers of gene medicines: resolved issues, open questions, and future promises.** *Med Res Rev*, 27(5); 696-722; 2007

25. Pun, S.H., Davis, M.E. **Development of a Nonviral Gene Delivery Vehicle for Systemic Application.** *Bioconj Chem*, 13(3); 630-639; 2002.
26. Allison, S.D., Molina, M.C., Anchordoquy, T.J. **Stabilization of lipid/DNA complexes during the freezing step of the lyophilization process: the particle isolation hypothesis.** *Biochim Biophys Acta*, 1468(1-2); 127-38; 2000.
27. Kwok, K.Y. *et al.* **Strategies for maintaining the particle size of peptide DNA condensates following freeze-drying.** *Int J Pharm*, 203(1-2); 81-8; 2000
28. Fischer, D., Bieber, T., Li, Y., Elsasser, H.P., Kissel, T. **A novel non-viral vector for DNA delivery based on low molecular weight, branched polyethylenimine: effect of molecular weight on transfection efficiency and cytotoxicity.** *Pharm Res*, 16(8); 1273-9; 1999.
29. Godbey, W.T., Wu, K.K., Mikos, A.G. **Size matters: molecular weight affects the efficiency of poly(ethylenimine) as a gene delivery vehicle.** *J Biomed Mater Res*, 45(3); 268-75; 1999.
30. Colson, Y.L., Grinstaff, M.W. **Biologically responsive polymeric nanoparticles for drug delivery.** *Adv Mater*, 24(28); 3878-86; 2012.
31. Richardson, S.C., Kolbe, H.V., Duncan, R. **Potential of low molecular mass chitosan as a DNA delivery system: biocompatibility, body distribution and ability to complex and protect DNA.** *Int J Pharm*, 178(2); 231-43; 1999.
32. Collard, W.T., Yang Y., Kwok, K.Y., Park, Y., Rice, K.G. **Biodistribution, metabolism, and in vivo gene expression of low molecular weight glycopeptide polyethylene glycol peptide DNA co-condensates.** *J Pharm Sci*, 89(4); 499-512; 2000.
33. Parker, A.L., Newman, C., Briggs, S., Seymour, L., Sheridan, P.J. **Nonviral gene delivery: techniques and implications for molecular medicine.** *Expert Rev Mol Med*, 5(22); 1-15; 2003.
34. Wong, S.Y., Pelet, J.M., Putnam, D. **Polymer systems for gene delivery—Past, present, and future.** *Prog in Polym Sci*, 32(8–9); 799-837; 2007.
35. Chang, K.L., Higuchi, Y., Kawakami, S., Yamashita, F., Hashida, M. **Efficient gene transfection by histidine-modified chitosan through enhancement of endosomal escape.** *Bioconjug Chem*, 21(6); 1087-95; 2010
36. Vaughan, E.E., Dean, D.A. **Intracellular trafficking of plasmids during transfection is mediated by microtubules.** *Mol Ther*, 13(2); 422-8; 2006.
37. Mattaj, I.W., Englmeier, L. **Nucleocytoplasmic transport: the soluble phase.** *Annu Rev Biochem*, 67; 265-306; 1998.
38. Fasbender, A., Zabner, J., Zeiher, B.G., Welsh, M.J. **A low rate of cell proliferation and reduced DNA uptake limit cationic lipid-mediated gene transfer to primary cultures of ciliated human airway epithelia.** *Gene Ther*, 4(11); 1173-80; 1997.
39. Jeon, O., Lim, H.W., Lee, M., Song, S.J., Kim, B.S. **Poly(L-lactide-co-glycolide) nanospheres conjugated with a nuclear localization signal for delivery of plasmid DNA.** *J Drug Target*, 15(3); 190-8; 2007.
40. Wang, J.J., *et al.* **Recent advances of chitosan nanoparticles as drug carriers.** *Int J Nanomedicine*, 6; 765-74; 2011.
41. Kim, T.H., *et al.* **Chemical modification of chitosan as a gene carrier in vitro and in vivo.** *Progress in Polymer Science*, 32(7); 726-753; 2007.
42. Kurita, K., Sannan, T., Iwakura, Y. **Studies on chitin, 4. Evidence for formation of block and random copolymers of N-acetyl-D-glucosamine and D-glucosamine by hetero- and homogeneous hydrolyses.** *Die Makromolekulare Chemie*, 178(12); 3197-3202; 1977
43. Araki, Y., Ito, E. **A pathway of chitosan formation in *Mucor rouxii*. Enzymatic deacetylation of chitin.** *Eur J Biochem*, 55(1); 71-8; 1975.
44. Lee, K.Y., Ha, W.S., Park, W.H. **Blood compatibility and biodegradability of partially N-acetylated chitosan derivatives.** *Biomater*, 16(16); 1211-6; 1995.
45. Aiba, S. **Studies on chitosan: Lysozymic hydrolysis of partially N-acetylated chitosans.** *Int J Biol Macromol*, 14(4); 225-8; 1992.
46. Kangjian, W., Nianhua, D., Shiwei, X., Yichun, Y., Weihua, D. **Preparation and characterization of collagen-chitosan-chondroitin sulfate composite membranes.** *J Membr Biol*, 245(11); 707-16; 2012.
47. Shaikh, R., *et al.* **Mucoadhesive drug delivery systems.** *J Pharm Bioallied Sci*, 3(1); 89-100; 2011.

48. Andrews, G.P., Lavery, T.P., Jones, D.S. **Mucoadhesive polymeric platforms for controlled drug delivery.** *Eur J Pharm Biopharm*, 71(3); 505-18; 2009.
49. Tan, M.L., Choong, P.F., Dass, C.R. **Cancer, chitosan nanoparticles and catalytic nucleic acids.** *J Pharm Pharmacol*, 61(1); 3-12; 2009.
50. Minami, S., Suzuki, H., Okamoto, Y., Fujinaga, T., Shigemasa, Y. **Chitin and chitosan activate complement via the alternative pathway.** *Carbohydr Polym*, 36(2-3); 151-155; 1998.
51. Lin, C.W., *et al.* **The inhibition of TNF-alpha-induced E-selectin expression in endothelial cells via the JNK/NF-kappaB pathways by highly N-acetylated chitooligosaccharides.** *Biomater*, 28(7); 1355-66; 2007.
52. Dash, M., Chiellini, F., Ottenbrite, R.M., Chiellini, E. **Chitosan—A versatile semi-synthetic polymer in biomedical applications.** *Progr in Polym Sci*, 36(8); 981-1014; 2011.
53. Lamarque, G., Lucas, J.M., Viton, C., Domard, A. **Physicochemical behavior of homogeneous series of acetylated chitosans in aqueous solution: role of various structural parameters.** *Biomacromol*, 6(1); 131-42; 2005.
54. Kiang, T., *et al.*, **The effect of the degree of chitosan deacetylation on the efficiency of gene transfection.** *Biomater*, 25(22); 5293-301; 2004.
55. Yang, X., Yuan, X., Cai, D., Wang, S., Zong, L. **Low molecular weight chitosan in DNA vaccine delivery via mucosa.** *Int J Pharm*, 375(1-2); 123-32; 2009.
56. Strand, S.P., *et al.* **Molecular design of chitosan gene delivery systems with an optimized balance between polyplex stability and polyplex unpacking.** *Biomater*, 31(5); 975-87; 2010.
57. Turan, K., Nagata, K. **Chitosan-DNA nanoparticles: the effect of cell type and hydrolysis of chitosan on in vitro DNA transfection.** *Pharm Dev Technol*, 11(4); 503-12; 2006.
58. Jiang, X., *et al.* **Chitosan-g-PEG/DNA complexes deliver gene to the rat liver via intrabiliary and intraportal infusions.** *J Gene Med*, 8(4); 477-87; 2006.
59. Liu, W.G., *et al.* **N-alkylated chitosan as a potential nonviral vector for gene transfection.** *Bioconjug Chem*, 14(4); 782-9; 2003.
60. Liu, Z., Zhang, Z., Zhou, C., Jiao, Y. **Hydrophobic modifications of cationic polymers for gene delivery.** *Progr in Polym Sci*, 35(9); 1144-1162; 2010.
61. Ferreira, G.N., Monteiro, G.A., Prazeres, D.M., Cabral, J.M. **Downstream processing of plasmid DNA for gene therapy and DNA vaccine applications.** *Trends Biotechnol*, 18(9); 380-8; 2000.
62. Birnboim, H.C., Doly, J. **A rapid alkaline extraction procedure for screening recombinant plasmid DNA.** *Nucleic Acids Res*, 7(6); 1513-23; 1979
63. Bo, H., *et al.* **Using a single hydrophobic-interaction chromatography to purify pharmaceutical-grade supercoiled plasmid DNA from other isoforms.** *Pharm Biol*, 51(1); 42-8; 2013.
64. Pereira, L.R., Prazeres, D.M., Mateus, M. **Hydrophobic interaction membrane chromatography for plasmid DNA purification: Design and optimization.** *Journal of Sep Sci*, 33(9); 1175-1184; 2010.
65. Czechowska-Biskup, R., Rokita, B., Lotfy, S., Ulanski, P., Rosiak, J.M. **Degradation of chitosan and starch by 360-kHz ultrasound.** *Carbohydr Polym*, 60(2); 175-184; 2005.
66. Mukhopadhyay, P., Mishra, R., Rana, D., Kundu, P.P. **Strategies for effective oral insulin delivery with modified chitosan nanoparticles: A review.** *Progr in Polym Sci*, 37(11); 1457-1475; 2012.
67. Burchard, W., **Static and dynamic light scattering from branched polymers and biopolymers.** *Light Scattering from Polymers*; 1-124; 1983
68. Sunshine, J.C., Peng, D.Y., Green, J.J. **Uptake and transfection with polymeric nanoparticles are dependent on polymer end-group structure, but largely independent of nanoparticle physical and chemical properties.** *Mol Pharm*, 9(11); 3375-83; 2012.
69. Stepanek, P. **Static and dynamic properties of multiple light scattering.** *The Journal of Chem Phys*, 99(9); 6384-6393; 1993.
70. Garcia-Fuentes, M., Alonso, M.J. **Chitosan-based drug nanocarriers: where do we stand?** *J Control Release*, 161(2); 496-504; 2012.

71. Strand, S.P., Issa, M.M., Christensen, B.E., Vårum, K.M., Artursson, P. **Tailoring of chitosans for gene delivery: novel self-branched glycosylated chitosan oligomers with improved functional properties.** *Biomacromol*, 9(11);3268-76; 2008.
72. Rieseberg, M., Kasper, C., Reardon, K.F., Scheper, T. **Flow cytometry in biotechnology.** *Appl Microbiol Biotechnol*, 56(3-4); 350-60; 2001
73. Cubitt, A.B., *et al.* **Understanding, improving and using green fluorescent proteins.** *Trends in Biochem Scien*, 20(11); 448-455; 1995.
74. Diogo, M., Queiroz, J.O., Prazeres, D.M. **Purification of Plasmid DNA Vectors Produced in Escherichia coli for Gene Therapy and DNA Vaccination Applications.** *Microbial Processes and Products*; 165-178; 2005,
75. Raiado-Pereira, L., Prazeres, D.M., Mateus, M. **Impact of plasmid size on the purification of model plasmid DNA vaccines by phenyl membrane adsorbers.** *J Chromatogr A*, 1315; 145-51; 2013.
76. Maity, A.R., Jana, N.R. **Chitosan-Cholesterol-Based Cellular Delivery of Anionic Nanoparticles.** *The Journal of Phys Chem C*, 115(1); 137-144; 2010.
77. Chuah, A.M., Kuroiwa, T., Ichikawa, S., Kobayashi, I., Nakajima, M. **Formation of biocompatible nanoparticles via the self-assembly of chitosan and modified lecithin.** *J Food Sci*, 74(1); N1-8; 2009.
78. Carapuca, E., Azzoni, A.R., Prazeres, D.M., Monteiro, G.A., Mergulhão, F.J. **Time-course determination of plasmid content in eukaryotic and prokaryotic cells using real-time PCR.** *Mol Biotechnol*, 37(2); 120-6; 2007.
79. Shahnaz, G., *et al.* **Thiolated chitosan nanoparticles for the nasal administration of leuprolide: bioavailability and pharmacokinetic characterization.** *Int J Pharm*, 428(1-2); 164-70; 2012.
80. Yang, S.J., *et al.* **Enhancement of chitosan nanoparticle-facilitated gene transfection by ultrasound both in vitro and in vivo.** *J Biomed Mater Res B Appl Biomater*, 100(7); 1746-54; 2012.
81. Klesing, J., Chernousova, S., Epple, M. **Freeze-dried cationic calcium phosphate nanorods as versatile carriers of nucleic acids (DNA, siRNA).** *J Mat Chem*, 22(1); 199-204; 2012.
82. Zhou, H., Purdie, J., Wang, T., Ouyang, A. **pH measurement and a rational and practical pH control strategy for high throughput cell culture system.** *Biotechnol Prog*, 26(3); 872-80; 2010.

7. Appendices

Appendix I - Growth of *E. coli* DH5 α

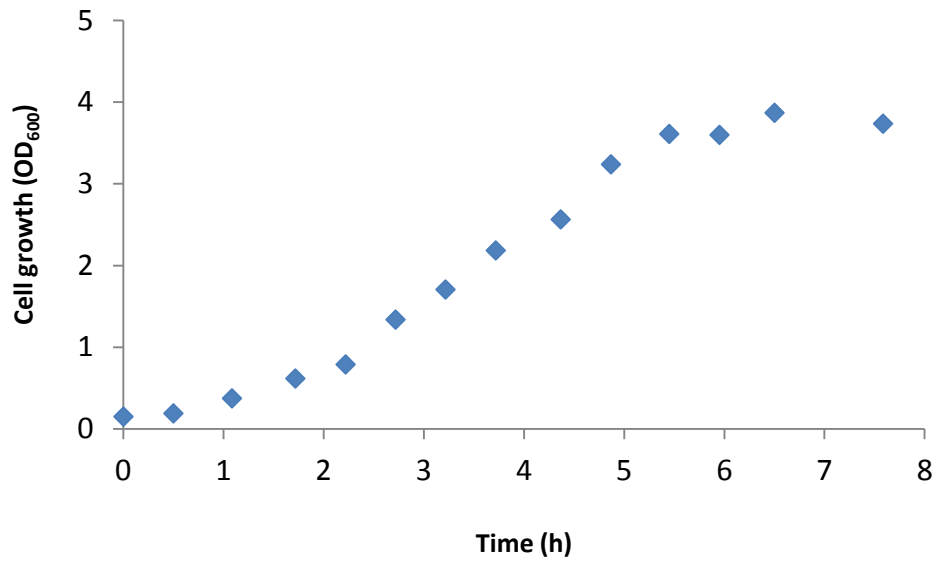
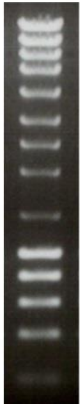


Figure I – Growth curve of *E. coli* in 250mL of LB medium at 37°C and 250rpm. Host strain: DH5 α ; Plasmid: pVAX1GFP

Appendix II – NZYDNA Ladder III characteristics

	SIZE (bp)	ng/BAND
	10000	100
	7500	75
	6000	60
	5000	50
	4000	40
	3000	30
	2500	25
	2000	20
	1400	14
	1000	100
	800	80
	600	60
	400	40
	200	20

NZYDNA Ladder III

Issue date: November 2010

1. IDENTIFICATION OF THE SUBSTANCE/PREPARATION AND OF THE COMPANY/UNDERTAKING

Identification of the substance or preparation

Catalogue references: MB04401 (200 lanes), MB04402 (500 lanes)

Product name: **NZYDNA Ladder III**

Company/undertaking identification

NZYTech, Lda., Estrada do Paço do Lumiar, Campus do Lumiar, Edifício E – R/C,

1649-038 Lisboa, Portugal, Tel. +351.213643514, Fax +351.217151168, www.nzytech.com

Emergency telephone number

INEM, Centro de Informação Anti-Venenos, Rua Infante D. Pedro, 8

1749-075 Lisboa, Portugal, Tel. +351.217950143/44/46

Outside Portugal (PT): Call your regional Poisons Information Service or call local Life Saving Service.

2. COMPOSITION/INFORMATION ON INGREDIENTS

Substance/Preparation: Preparation

Within the present knowledge of the supplier, this product does not contain any hazardous ingredients in quantities requiring reporting in this section, in accordance with EU or national regulations.

7. HANDLING AND STORAGE

Even though the above listed product is not defined as hazardous by EU, US or any other known national regulations, the material should be handled with appropriate caution and under supervision. Good manufacturing and laboratory procedures should be used. Protective gloves, safety glasses, lab coat and access to a safety shower and eyewash are recommended.

Packaging materials – recommended: Use original container.

9. PHYSICAL AND CHEMICAL PROPERTIES

Physical state: Liquid.

Colour: Blue.

16. OTHER INFORMATION

Notice to reader: The information and recommendations contained herein are to the best of our knowledge reliable. However, nothing herein is to be construed as a warranty or representation in respect of safety in use, suitability efficiency or otherwise, including freedom from patent infringements. Users should make their own tests for their particular purpose. NZYTech cannot accept any liability for any loss, damage or infringement arising from the use of the information or recommendations contained herein.

This is not an MSDS. According to EU and US regulations we are not required to supply an MSDS for a product which is not classified as hazardous.

Appendix III – Characterization of the diameter (nm), zeta potential ZP (mV) and polydispersity index (Pdi) of chitosan particles in acetic acid solution (pH ≈ 3.0).

Table III.A – Non-sonicated, 10-fold diluted chitosan particles in suspension. Acetic acid buffer was filtered with 0.45µm membrane. SD – standard deviation; days – days after suspension preparation; LMW, MMW, HMW – Low, Medium and High molecular weight chitosan; Glycol – glycol chitosan; Mean values of at least two measurements.

LMW				
days	diameter (nm)	SD	Pdi	
1	952	126	0.46	
7	585	289	0.63	
14	455	82	0.63	
24	641	308	0.68	
34	555	101	0.60	

MMW				
days	diameter (nm)	SD	Pdi	
1	1636	549	0.80	
7	1142	185	0.72	
14	888	99	0.61	
24	1128	193	0.69	
34	736	35	0.71	

HMW				
days	diameter(nm)	SD	Pdi	
1	2573	611	0.89	
7	1190	380	0.94	
14	1110	180	0.92	
24	1073	230	0.90	
34	978	231	0.89	

Glycol				
days	diameter(nm)	SD	Pdi	
1	1717	1132	0.73	
7	979	500	0.76	
14	574	137	0.67	
24	678	146	0.70	
34	705	136	0.69	

LMW			
days	ZP (mV)	SD	
1	33	7	
7	52	3	
14	51	6	

MMW			
days	ZP (mV)	SD	
1	55	0.9	
7	72	2.1	
14	65	6	

HMW			
days	ZP (mV)	SD	
1	47	1.2	
7	71	0.4	
14	69	2.3	

Glycol			
days	ZP (mV)	SD	
1	50	6.3	
7	59	5.9	
14	53	3.0	

Table III.B – Sonicated, 10-fold diluted chitosan particles in suspension. Acetic acid buffer was filtered with 0.45µm membrane. SD – standard deviation; days – days after suspension preparation; LMW, MMW, HMW – Low, Medium and High molecular weight chitosan; Glycol – glycol chitosan; Mean values of at least two measurements.

LMW			
days	size (nm)	SD	Pdi
1	211	118	0.37
7	247	67	0.36
14	246	23	0.39
24	370	79	0.42
34	395	33	0.44
MMW			
days	size (nm)	SD	Pdi
1	313	232	0.47
7	223	49	0.34
14	179	21	0.51
24	358	103	0.39
34	298	50	0.41
HMW			
days	size (nm)	SD	Pdi
1	261	143	0.44
7	361	80	0.39
14	291	38	0.49
24	279	81	0.45
34	2304	434	0.16
Glycol			
days	size (nm)	SD	Pdi
1	333	246	0.38
7	384	180	0.45
14	312	123	0.53
24	395	95	0.58
34	238	27	0.54

LMW		
days	ZP (mV)	SD
1	32	1.2
7	28	4.1
14	31	3.2
MMW		
days	ZP (mV)	SD
1	24	3.8
7	49	0.3
14	47	1.1
HMW		
days	ZP (mV)	SD
1	41	3.9
7	45	0.3
14	44	1
Glycol		
days	ZP (mV)	SD
1	33	3.9
7	41	0.3
14	37	1.3

Table III.C – Sonicated, 10-fold diluted chitosan particles in suspension. Acetic acid buffer was not filtered. SD – standard deviation; days – days after suspension preparation; LMW, MMW, HMW – Low, Medium and High molecular weight chitosan; Glycol – glycol chitosan; Mean values of at least two measurements.

LMW			
days	size (nm)	SD	Pdi
1	499	156	0.60
7	454	81	0.50
14	328	21	0.50
24	305	42	0.52
34	298	51	0.49

MMW			
days	size (nm)	SD	Pdi
1	686	162	0.71
7	122	0.85	0.30
14	137	2	0.30
24	142	7	0.28
34	201	17	0.31

HMW			
days	size (nm)	SD	Pdi
1	520	171	0.56
7	64	3	0.42
14	77	1	0.40
24	101	15	0.38
34	340	31	0.46

Glycol			
days	size (nm)	SD	Pdi
1	453	215	0.54
7	88	9	0.24
14	92	1	0.3
24	92	3	0.21
34	101	11	0.31

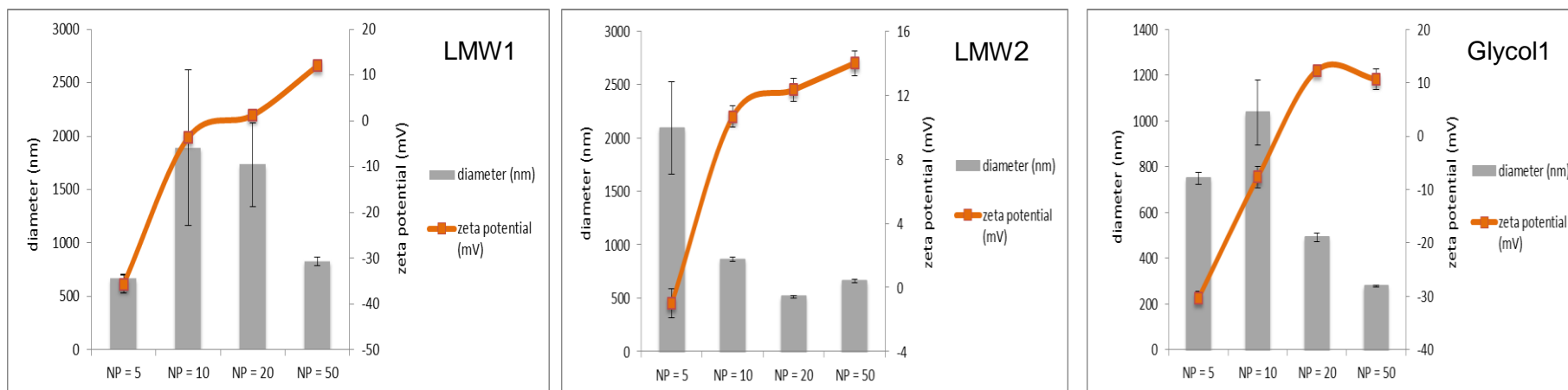
LMW		
days	ZP (mV)	SD
1	33	4.3
7	40	6
14	39	3

MMW		
days	ZP (mV)	SD
1	17	1.6
7	42	2
14	51	7

HMW		
days	ZP (mV)	SD
1	29	2.6
7	18	7
14	25	11

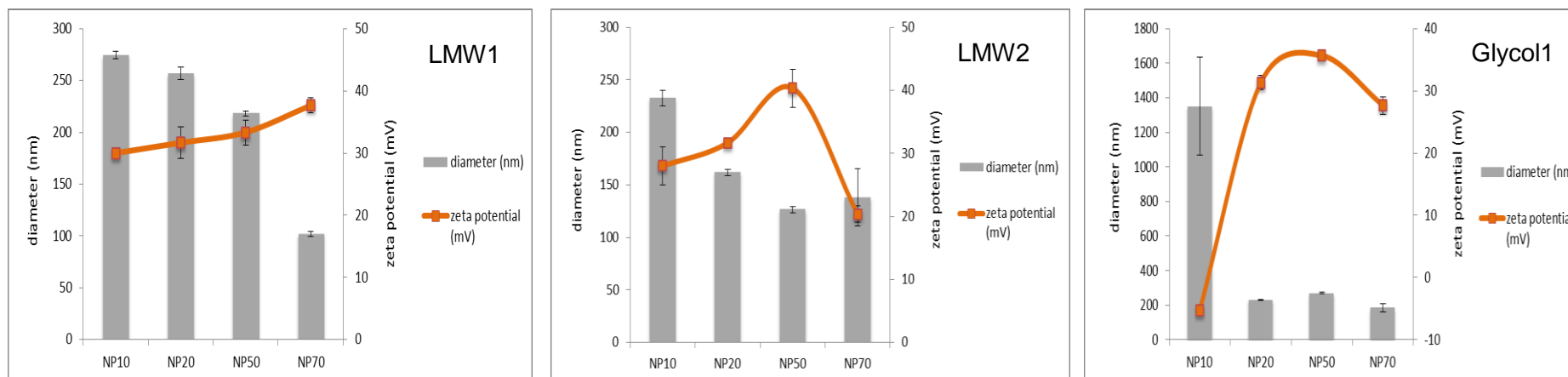
Glycol		
days	ZP (mV)	SD
1	10	0.6
7	41	1
14	39	3

Appendix IV - Characterization of the diameter (nm), zeta potential ZP (mV) and polydispersity index (Pdi) of chitosan/pDNA nanoparticles (pH ≈ 7.3).



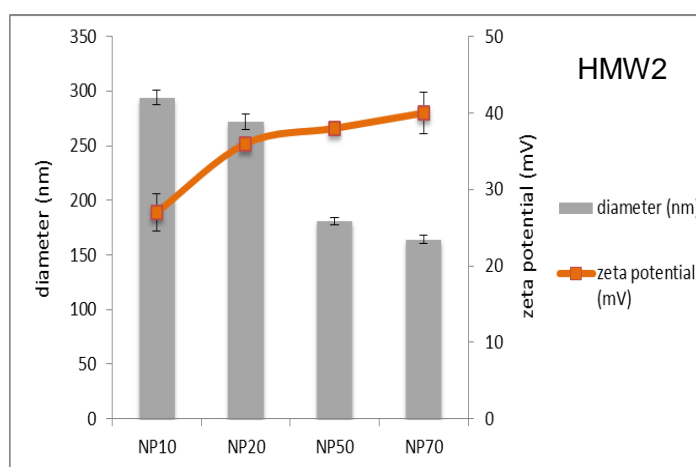
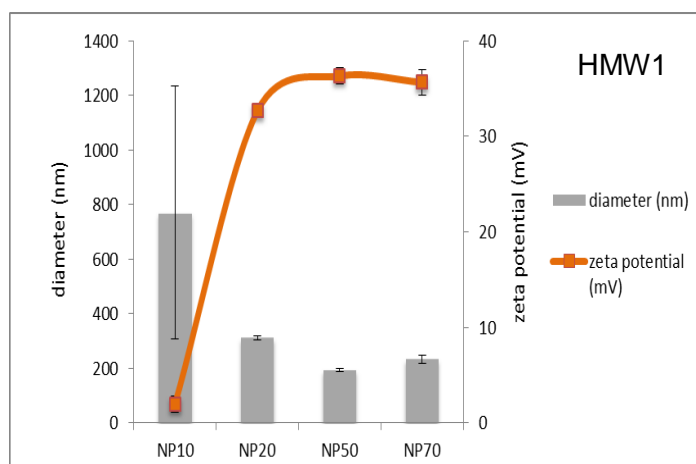
sample	N/P ratio	pdi average	SD average	number of particles
LMW1 CHI (sonicated)	NP = 5	0.383	0.048	> 1000 particulas
	NP = 10	0.825	0.086	< 1000 particulas
	NP = 20	0.848	0.078	< 1000 particulas
	NP = 50	0.520	0.045	> 1000 particulas
LMW2 CHI (non sonicated)	NP = 5	0.885	0.029	< 1000 particulas
	NP = 10	0.397	0.022	> 1000 particulas
	NP = 20	0.282	0.023	> 1000 particulas
	NP = 50	0.289	0.024	> 1000 particulas
Glycol1 CHI (sonicated)	NP = 5	0.367	0.055	> 1000 particulas
	NP = 10	0.687	0.096	< 1000 particulas
	NP = 20	0.408	0.042	> 1000 particulas
	NP = 50	0.305	0.038	> 1000 particulas

Figure IV.A – Non-fresh chitosan/pDNA nanoparticles. Preparation made 15days before characterization; buffer was filtered and samples were diluted 10-fold before characterization; SD – standard deviation; LMW1 – sonicated low molecular weight chitosan complexed with pVAX1GFP at different NP ratios; LMW2 – non-sonicated low molecular weight chitosan complexed with pVAX1GFP at different N/P ratios; Glycol1 – sonicated glycol chitosan complexed with pVAX1GFP at different N/P ratios; number of particles - nanoparticles present during zetasizer measurements for each formulation tested; Mean values of at least two measurements; in red in the table are represented the particles not suitable for DLS and EM measurements



sample	N/P ratio	pdi average	SD average	number of particles
LMW1 CHI (sonicated)	NP = 10	0.210	0.018	> 1000
	NP = 20	0.287	0.044	> 1000
	NP = 50	0.394	0.044	> 1000
	NP = 70	0.544	0.031	> 1000
LMW2 CHI (non sonicated)	NP = 10	0.287	0.018	> 1000
	NP = 20	0.44	0.020	> 1000
	NP = 50	0.397	0,042	> 1000
	NP = 70	0.354	0.117	> 1000
Glycol1 CHI (sonicated)	NP = 10	0.842	0.107	< 1000
	NP = 20	0.251	0.015	> 1000
	NP = 50	0.408	0.020	> 1000
	NP = 70	0.336	0.030	> 1000

Figure IV.B – Fresh chitosan/pDNA nanoparticles. Preparation made 1h before characterization; Buffer was filtered and samples were diluted 10-fold before characterization; SD – standard deviation; LMW1 – sonicated low molecular weight chitosan complexed with pVAX1GFP at different N/P ratios; LMW2 – non-sonicated low molecular weight chitosan complexed with pVAX1GFP at different N/P ratios; Glycol1 – sonicated glycol chitosan complexed with pVAX1GFP at different N/P ratios; number of particles – nanoparticles present during zetasizer measurements for each formulation tested; Mean values of at least two measurements; in red in the table are represented the particles not suitable for DLS and EM measurements



sample	N/P ratio	pdi average	SD average	number of particles
HMW1 CHI (sonicated)	NP = 10	0.643	0.174	> 1000
	NP = 20	0.24	0.058	> 1000
	NP = 50	0.372	0.057	> 1000
	NP = 70	0.426	0.047	> 1000
HMW2 CHI (non sonicated)	NP = 10	0.252	0.035	> 1000
	NP = 20	0.366	0.033	> 1000
	NP = 50	0.373	0.030	> 1000
	NP = 70	0.486	0.067	> 1000

Figure IV.C – Fresh chitosan/pDNA nanoparticles. preparation made 1h before characterization; buffer was filtered and samples were diluted 10-fold before characterization; SD – standard deviation; HMW1 – sonicated high molecular weight chitosan complexed with pVAX1GFP at different N/P ratios; HMW2 – non-sonicated high molecular weight chitosan complexed with pVAX1GFP at different N/P ratios; number of particles – nanoparticles present during zetasizer measurements for each formulation tested; Mean values of at least two measurements